The Role of Thioredoxin-interacting Protein in Corticosterone Induced Damage in Astrocytes

By

Sushank Acharya

A Thesis Submitted to the Faculty of Graduate Studies of

The University of Manitoba

in partial fulfillment of requirements of the degree of

Master of Science

Department of Pharmacology and Therapeutics

University of Manitoba

Winnipeg, Canada

ABSTRACT

Background: Chronic treatment with corticosterone (CORT) can induce oxidative stress and neuroinflammation. Thioredoxin-interacting protein (Txnip) inhibits antioxidant protein thioredoxin, interrupting protein thiol reduction and inducing oxidative stress. Txnip can also bind to NLRP3, facilitating NLRP3 inflammasome forming, activating caspase-1 and releasing IL-1β. Previously, our laboratory found that chronic CORT treatment increased Txnip levels in cultured mouse neurons and microglia, suggesting that CORT may upregulate Txnip, inhibiting thioredoxin activity and activating NLRP3 inflammasome, which may amplify oxidative stress and neuroinflammation.

Objective: Since astrocytes can release proinflammatory cytokines and reactive oxygen species, facilitating oxidative stress and neuroinflammatory processes. The objective of this study is to determine if CORT treatment can upregulate Txnip in astrocytes, further promoting oxidative stress and inflammation.

Methods: Primary cultured mouse astrocytes were used in the present study. Thioredoxin and Txnip protein levels were measured by immunoblotting assay. Eosin-labeled insulin was used as a substrate for measuring thioredoxin activity. Total reduced thiol level was measured using Ellman's assay. Protein sulfenylation and carbonylation were measured by dimedone conjugation and biotin-hydrazide conjugation methods respectively. NLRP3/Txnip binding was measured by co-immunoprecipitation assay. Fluorogenic Z-YVAD-AFC was used as a substrate for measuring caspase-1 activity, while IL-1β release was measured by enzyme-linked immunosorbent assay. Crispr/Cas9/Txnip sgRNA was used to knock out Txnip gene.

Results: We found that CORT treatment for 24 hours had no effect on thioredoxin levels, but increased Txnip levels. CORT-increased Txnip levels were decreased by mineralocorticoid receptor antagonist spironolactone and glucocorticoid receptor antagonist RU486. CORT treatment decreased thioredoxin activity, but had no effects on total reduced thiol levels, sulfenylated protein levels and carbonylated protein levels. However, CORT treatment increased Txnip/NLRP3 binding activity, caspase-1 activity and IL-1β release. Txnip knockout attenuated CORT-increased caspase-1 activity and IL-1β release.

Conclusion: The findings suggest that CORT treatment increases Txnip level, which could promote NLRP3 activity, activate caspase-1 and release IL-1β to facilitate neuroinflammatory process in astrocytes. However, due to enriched antioxidants in astrocytes, CORT-increased Txnip may not be sufficient to exert oxidative stress.

ACKNOWLEDGEMENT

I would like to express my sincere gratitude to my supervisor Dr. Jun-Feng Wang, for his invaluable guidance, advice, motivation and patience throughout this journey. His guidance and dedication have helped me a lot during my master's program. I am extremely grateful for his support and feedback.

I would also like to thank my advisory committee members, Dr. Eftekhar Eftekharpour and Dr. Sachin Katyal, for their knowledge and suggestions, which greatly helped my project. Without their feedback and support, this work wouldn't have been possible.

I would also like to thank all of my colleagues who helped me a lot through my Master's program. I am grateful to our research associate, Dr. Hua Tan, for helping me with the dissection of mice, helping me learn new techniques and providing technical expertise with my research design and troubleshooting. I would also like to thank Dr. Alejandra Llanes Cuesta and Azar Aghazadeh Khasraghi for sharing their knowledge while designing any experiments, helping me with troubleshooting and providing me guidance during this journey. It was a great experience to work with all of you.

I am very thankful to my parents and my brother, who supported me in every step of my graduate studies. Although I was far from home, they constantly supported and encouraged me in every step of this journey. I would also like to thank my friends and relatives, who helped me keep my spirit up and motivated me during this arduous journey. Your encouragement and friendship have made this journey more rewarding.

Last but not least, I would like to thank the Department of Pharmacology and Therapeutics, University of Manitoba and PrairieNeuro Research Centre for providing the resources and

facilities for conducting this research. This project was supported by research funding form the National Sciences and Engineering Research Council Discovery Grant.

TABLE OF CONTENTS

LIST OF FIGURES

LIST OF ABBREVIATIONS

4-HNE	4-hydroxynoneal
8-OHdG	8-hydroxy-2-deoxyguanosein
8-oxo-G	8-oxo-7,8-dihyroguanosine
ACTH	Adrenocorticotrophin
AF-1	Activating Function-1
ANOVA	Analysis of variance
AP-1	Activator protein 1
ARE	Antioxidant response element
ASC	Apoptosis-associated speck-like protein
ATP	Adenosine Triphosphate
BBB	Blood-Brain Barrier
BDNF	Brain-derived Neurotrophic Factor
bFGF	Basic fibroblast growth factor
BSA	Bovine serum albumin
CARD	Caspase activation and recruitment domain
Cas9	CRISPR-associated protein 9
CAT	Catalase
cGRE	Composite Glucocorticoid Response Element
CNS	Central Nervous System
CORT	Corticosterone
CREB	cAMP response element biding prte
CRH	Corticotrophin releasing hormone

CRISPR	Clustered Regularly Interspaced short Palindromic Repeat
CUS	Chronic Unpredictable Stress
Cx43	Connexin 43
Cys	Cysteine
DAMP	Danger-associated molecular pattern
DBD	DNA binding Domain
DMEM	Dulbecco's Modified Eagle's Medium
DTNB	2,2'-dinitro-5,5'-dithiobenzoic acid
DTT	Dithiothreitol
EDTA	Ethylene diamine tetracetic acid
EGTA	Ethylene glycol-bis(2-aminoethyl)tetraacetic acid
ELISA	Enzyme-linked immunosorbent assay
ER	Endoplasmic Reticulum
ETC	Electron Transport chain
FAD	Flavin Adenine Dinucleotide
FBS	Fetal Bovine Serum
FJB	Fluoro-Jade B
FKBP	FK506- binding immunophilins
FOXO	Forkhead box class O
GABA	Gamma-Aminobutyric acid
GC	Glucocorticoid
GCL	Glutamate-cysteine ligase
GDNF	Glial derived Neurotrophic Factor

GFAP	Glial fibrillary acid protein
GFRα1	GDNF- family receptor α1
GLUT1	Glucose transporter 1
GPx	Glutathione peroxidase
GR	Glucocorticoid Receptor
GRE	Glucocorticoid Response Element
GSH	Glutathione
GSS	Glutathione synthetase
GSSG	Oxidized glutathione
HEPES	4-(2-hydroxyethyl)-1-piperazineethanesulfonic acid
HPA axis	Hypothalamus-pituitary-adrenal axis
HRP	Horse-radish peroxidase
Hsp90	Heat shock protein 90
IAM	Iodoacetamide
Iba1	Ionized Calcium-binding adaptor molecule 1
IL-1β	Interlukin-1β
Kir 4.1	Inward rectifying K^+ 4.1 channel
LBD	Ligand binding Domain
LDH	Lactate dehydrogenase
LPS	Lipopolysaccharide
LRR	Leucine-rich repeat domain
MANF	Mesencephalic astrocyte-derived Neurotrophic Factor
MAP3K	Mitogen-activated protein kinase kinase kinase

MDA	Malondialdehyde
MES	Morphlino-ethanesulfonate
MR	Mineralocorticoid Receptor
NACHT	Nucleotide-binding and oligomerization domain
NADH	Nicotinamide Adenine Dinucleotide
NADPH	Nicotinamide Adenine Dinucleotide Phosphate
NEM	N-ethylmaleimide
NF-κB	Nuclear factor kappa B
nGRE	Negative Glucocorticoid Response Element
NLRP	NOD-like receptor family pyrin domain containing protein
NLS	Nuclear Localization Sequence
NOX	NADPH oxidase
Nrf2	Nuclear factor-erythroid factor-2 related factor 2
NTD	Amino-terminal Domain
PAMP	Pathogen associated molecular pattern
PBS	Phosphate-buffer saline
Prx	Peroxiredoxin
PVDF	Polyvinylidene Fluoride
PYD	N-terminal Pyrin Domain
ROS	Reactive Oxygen Species
s.c.	subcutaneous
SDS	Sodium dodecyl sulfate
SEM	Standard error of mean

-SH	Thiol
-SO_2H	Sulfinic acid
-SO_3H	Sulfonic acid
SOD	Superoxide dismutase
-SOH	Sulfenic acid
TCA cycle	Tricarboxylic acid cycle
TGFβ	Transforming growth factor β
TLR	Toll-like Receptor
TNB	2-nitro-5-thiobenzoic acid
TNFα	Tumor Necrosis Factor α
TRAF	Tumor necrosis factor receptor-associated factor
TrkB	Tyrosine kinase B
TrxR	Thioredoxin Reductase
TUNEL	Terminal deoxynucleotidyl transferase dUTP nick end labeling
UCP	Uncoupling protein

CHAPTER 1. INTRODUCTION

1.1 Glucocorticoid

1.1.1 Stress and hypothalamus- pituitary- adrenal axis

Glucocorticoid hormones are responsible for various physiological processes such as stress response, immunosuppression, growth, development, homeostasis, and metabolism [1]. As shown in Figure 1, the central regulation of glucocorticoid production is controlled by the parvocellular nucleus (PVN) of the hypothalamus, which secretes corticotrophin-releasing hormone (CRH) into the hypothalamic-pituitary portal circulation. CRH acts on CRH receptors in corticotrophin cells of the anterior pituitary gland to release adrenocorticotrophic hormone (ACTH) into the systemic circulation. Finally, ACTH stimulates the adrenal cortex to release glucocorticoids [2, 3]. This hypothalamus-pituitary-adrenal (HPA) axis is under the negative feedback control of circulating glucocorticoid. Acute physiological stress causes activation of the HPA axis, which stimulates the release of glucocorticoid from the adrenal cortex to regulate glucose and energy utilization, as well as immune function in response to stress. However, chronic stress causes overactivation of the HPA axis, damages neurons and impairs neuroplasticity, which is a significant risk factor for neuropsychiatric disorders [4].

1.1.2. Glucocorticoid receptors: structure and function

Glucocorticoids can target both mineralocorticoid receptors (MR) and glucocorticoid receptors (GR). These receptors belong to the class of nuclear receptors [5]. The affinity of glucocorticoid for GR is ten-fold lower than MR. In basal physiological conditions, glucocorticoid activates higher affinity MR. MR plays an essential role in maintaining electrolyte and fluid homeostasis and blood pressure. However, under stress conditions, the high level of glucocorticoid activates GR. GR plays a vital role in regulating stress responses, the immune system, and lipid

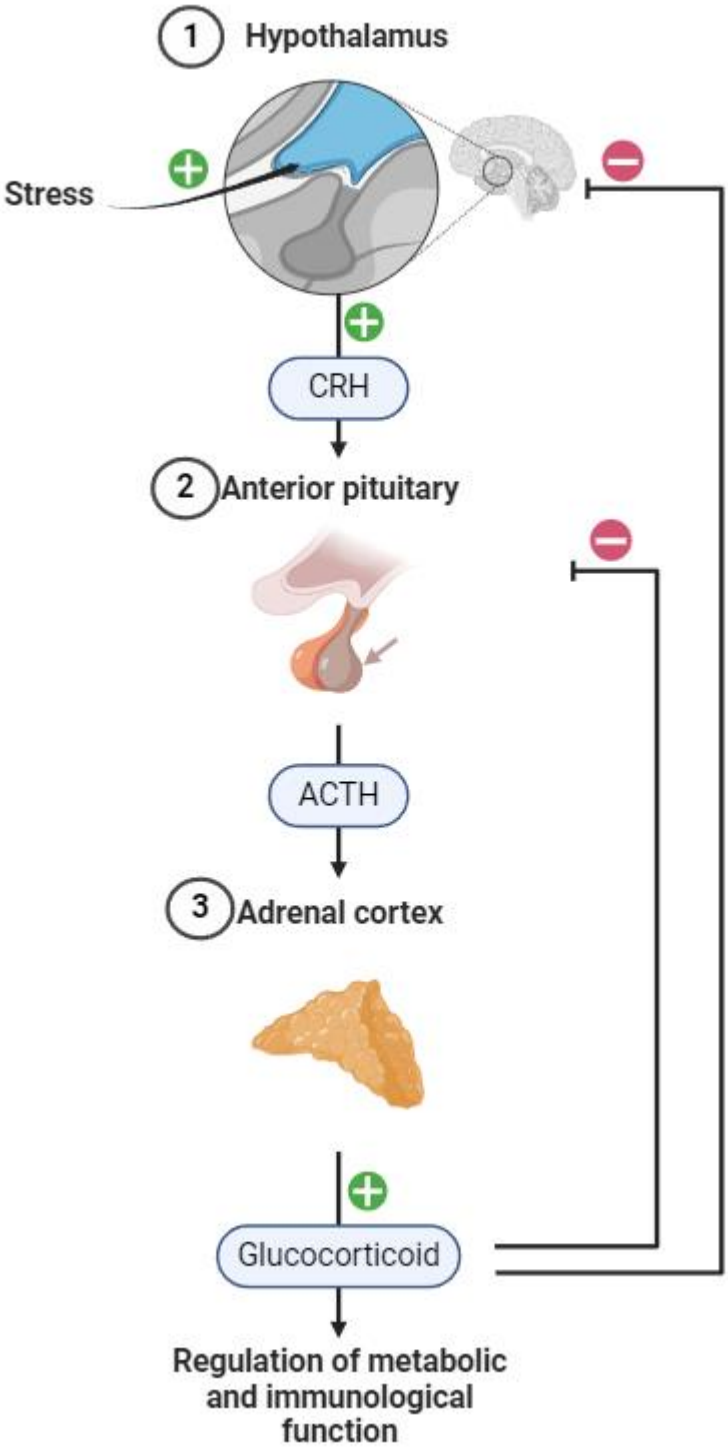

Figure 1. Hypothalamic-pituitary-adrenal axis. Stress activates the hypothalamus to release corticotrophin-releasing hormone (CRH) which stimulates the anterior pituitary to secrete adrenocorticotrophin hormone (ACTH). ACTH stimulates the adrenal cortex to release glucocorticoids which regulate metabolic and immunological function. (Created using BioRender.com)

and carbohydrate metabolism [6]. In the brain, both GR and MR have been shown to play an important role in the regulation of stress responses as well as learning and memory [7, 8].

Glucocorticoid receptor (GR) is encoded by the gene with 9 exons, which is located in chromosome 5 [9]. GR has four domains: amino-terminal domain (NTD), DNA binding domain (DBD), hinge region and carboxy-terminal ligand binding domain (LBD). The NTD contains activating function-1 (AF-1) region from 77 to 262 amino acid sequences. AF-1 region interacts with various coactivators, basal transcription factors and chromatin modulators to mediate gene activation. DBD contains two zinc finger motifs. The first zinc motif in DBD is responsible for the recognition of glucocorticoid response element (GRE), while the second zinc motif is responsible for the homodimerization of the receptor. The hinge region is a flexible loop between DBD and LBD that provides flexibility for the receptors to interact with multiple GREs. LBD consists of a second activating function-2 (AF-2) region from 526 to 556 AA, which is responsible for ligand-dependent interaction. In absence of ligand, AF-2 has inactive conformation which favors the interaction with co-repressors. Upon binding of ligand, the conformational change in the AF-2 favors binding of coactivators. [1, 3, 9-11].

GR has three major isoforms, including GRα, GRβ, and GRγ. GRα is predominantly an active isoform and responsible for most of the biological effects of GC [12]. GRα and GRβ isoforms are nearly similar in sequence from the amino acid terminus to amino acid 727. However, GRα has an additional 50 amino acids, while GRβ has an additional non-homologous 15 amino acids. Only GRα can bind to glucocorticoids, and activation of GRα can induce GRE-driven gene expression. GRβ acts as an inhibitor of GRα transcriptional activity and increased expression of GRβ is associated with glucocorticoid-resistance. GRγ has an arginine between two zinc finger motifs of DBD in the receptor. It was found that GR agonist dexamethasone can bind to both GRα

and GRγ and activate GRα- and GRγ -regulated transcription. However, GRγ-regulated transcriptional activity is approximately 50% of GRα-regulated transcriptional activity [13].

At an inactive state, GR exists mainly in the cytoplasm in the form of multiple protein complexes [14]. GR heterocomplex consists of GR, heat shock protein 90 (hsp90) dimer, FK506-binding immunophilin (either FKBP51 or FKBP52), and p23. Hsp90 is responsible for cytoplasmic localization of GR and masks both nuclear localization sequences (NLS) in the unbound state [15-17]. The immunophilins are bound to a common site in hsp90 through tetratricopeptide repeat (TPR) [15, 18]. As shown in Figure 2, once a ligand binds to the GR heterocomplex, the receptor undergoes phosphorylation at Ser211 by p38 mitogen-activated protein kinase and conformational changes, resulting in dissociation from chaperone proteins, activation or unmasking of the NLS, and translocation to the nucleus [17]. In nucleus, GR-GC complex can homodimerize or heterodimerize to interact with various binding sites and regulate expression of multiple genes through glucocorticoid response element (GRE), composite GRE (cGRE), negative GRE (nGRE) and tethering mechanism.

GRE consists of inverted repeats of two hexameric half-sites separated by 3 bp (consensus GRE sequences: GGTACAnnnTGTTCT). One monomer GR binds first to 5'-half site and then another monomer GR binds at 3'-half site, resulting in formation of dimer. The 3-bp between two half-sites is essential for binding two GRs to the GRE. GRs bind to GRE and then increases GRE-driven gene expression [19, 20]. In the case of composite GRE, GR can bind to DNA along with other transcription factors like octamer-binding transcription factor Oct1, cAMP response element binding protein (CREB), activator protein-1 (AP-1), Ets1 and others, either increasing or decreasing the expression of the genes, which depends on the bound interacting transcription factor. For example, AP-1 transcription factor is formed by either c-Jun homodimer or c-Jun/c-Fos

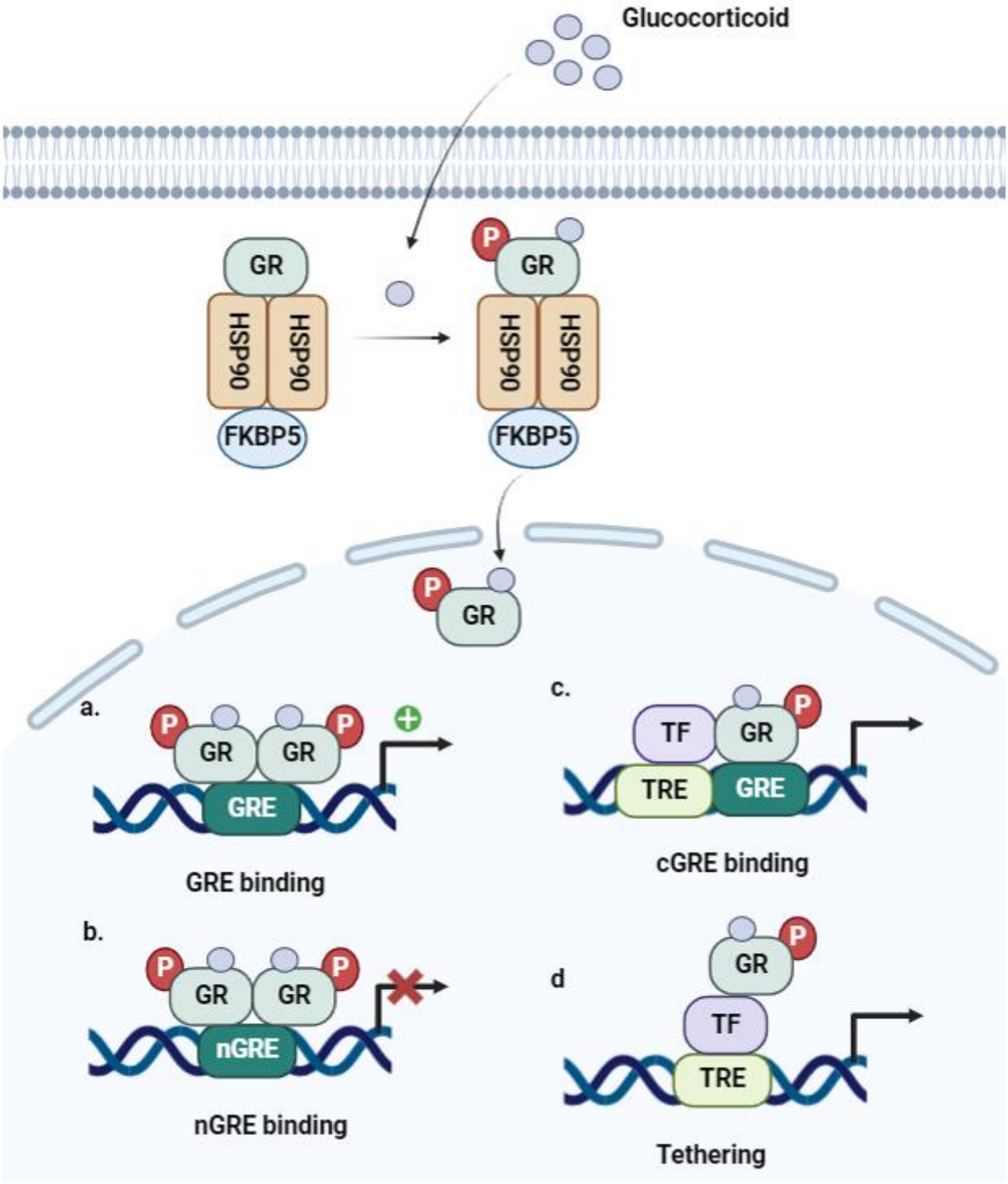

Figure 2. Mechanism of glucocorticoid receptor signaling. Once glucocorticoid binds to the glucocorticoid receptor (GR), it phosphorylates at Ser211, dissociates from chaperone molecuels, and translocates to the nucleus. In the nucleus, it regulates gene expression by GRE binding (a), nGRE binding (b), cGRE binding (c), and tethering (d). GRE- Glucocorticoid response element, cGRE- composite GRE, nGRE- negative GRE, TF- Transcription Factor TRE- Transcription factor Response Element (Created using BioRender.com)

heterodimer. If GR is bound to cGRE along with c-Jun/c-Jun homodimer, cGRE increases the expression of downstream gene. However, if GR is bound to cGRE along with c-Jun/c-Fos heterodimer, cGRE decreases the expression of downstream genes [21, 22]. Furthermore, GR can bind to nGRE, which inhibits the expression of a gene by recruitment of a co-repressor on the binding of GR. The consensus sequence of nGRE is CTCC$(n)_{0\text{-}2}$GGAGA [23]. For example, the binding of GRs to nGREs decreases the expression of pro-inflammatory genes such as C1qb and C3 genes [24], insulin receptor gene and bcl-2 gene [25, 26]. In the tethering mechanism, GR doesn't directly bind to the DNA but interacts with DNA-bound transcription factors through protein-protein interaction and regulates transcription factor activity [19]. For example, GR can bind to the RelA subunit of transcription factor NF-κB and repress transcription of genes regulated by NF-κB [27].

1.2 Chronic stress, glucocorticoid and neuronal damage

Chronic stress and chronic or excessive CORT treatment can induce neuronal damage. Chronic restraint stress in rats for 4 weeks resulted in a decrease in hippocampal volume and reduced total dendritic length of dentate granule cells [28]. Chronic restraint stress was also found to decrease the number of apical branch points and dendritic length in rat CA3 pyramidal neurons [29]. These findings suggest that chronic stress can induce neuronal damage. It was also reported that the subcutaneous CORT pellet implantation in rats for 21 days decreased volume in the dentate gyrus, CA1 and CA3 subregions of the hippocampus [30]. The CORT administration (40 mg/ml/kg, s.c.) for 21 days in rats decreased dendritic spine density and total dendritic length in the CA1 subregion of the hippocampus [31] and the total number of dendritic branch points and dendritic apical length in CA3 pyramid neurons of the hippocampus [31]. The administration of CORT for 21 days also showed increased number of shrunken, small and irregular shaped

pyramidal cells in CA1 and CA3 region of rat hippocampus [31, 32]. This evidence suggests that chronic stress and chronic CORT treatment promote dendritic atrophy in the hippocampus.

Chronic stress or chronic CORT treatment can induce neuronal death. H&E staining produces deep blue color in nuclei with hematoxylin, while pink color is produced in the cytoplasm and extracellular matrix by eosin. This provides contrast in the nucleus and cytoplasm for morphological assessment. It has been found using H&E staining that rats exposed to restraint stress 6 hours daily for 21 days revealed an increased number of cells that showed nuclear chromatin fragmentation and cell consolidation in hippocampal CA1 and CA3 regions and amygdala basolateral region [33]. Transmission electron microscopy of the hippocampal slices from restraint rats also showed neuronal cells with chromatin aggregation and nuclear deformation [34]. Treatment with CORT at 200 μM for 4 days was found to increase the number of condensed nuclei in primary cultured rat cerebrocortical neurons [35]. Terminal deoxynucleotidyl transferase dUTP nick end labeling (TUNEL) is a marker for fragmented DNA. Treatment with CORT at 100 μM for 24 hrs increased TUNEL staining in primary cultured mouse hippocampal neurons [36]. Fluoro-Jade B (FJB) is an anionic fluorescein derivative which is used to stain degenerating neurons. It has been found that restraint stress 6 hours daily for 21 days increased FJB-positive neurons in rat hippocampus and amygdala [33, 34]. Oral administration with CORT (20 mg/kg) for 21 days increased the number of FJB-positive cells in the dentate gyrus of mouse hippocampus [37]. Treatment with CORT at 100 μM was found to reduce cell viability in primary mouse hippocampal neurons [38]. These findings together suggest that chronic stress or chronic and excessive CORT treatment can cause apoptosis and neurodegeneration, resulting in neuronal damage.

1.2.1 Chronic stress, chronic CORT treatment and oxidative stress

Oxidative stress and neuroinflammation show an important role in chronic stress-induced and chronic or excessive CORT treatment-induced neuronal damage.

1.2.1.1 Oxidative stress:

Oxidative stress occurs due to excess production of reactive oxygen species (ROS) and/or deficiency of cellular antioxidant defense [39]. Hydroxyl radical (•OH), superoxide radical ($O_2^{\bullet-}$), and hydrogen peroxide (H_2O_2) are major ROS in biological system. Mitochondria is the major source of ROS in cells. Besides mitochondria, ROS are also produced by various oxidases, such as NADPH oxidase and xanthine oxidase. ROS are reactive molecules that can oxidize DNA, lipids, and proteins and promote cell damage. ROS can cause oxidative DNA damage, which can introduce mutations or genetic instability. DNA oxidation promotes errors in transcription and translation. In addition, ROS can interact with lipids to form lipid peroxides, which affect the integrity of the membrane and can affect cellular functions. The end products of lipid peroxidation like malondialdehyde (MDA) or 4-hydroxynoneal (HNE), can interact with the protein, forming MDA-protein adducts or 4HNE-protein adducts and impairing protein function [40]. Protein oxidation is ROS-induced covalent modification of proteins and might lead to loss of protein biochemical function. The cysteine residue is highly polarizable and nucleophilic due to the high electronegativity of the sulphur atom. As shown in Figure 3, on exposure to H_2O_2, the thiol group (-SH) in cysteine is oxidized to sulfenic acid (-SOH). The conversion of -SH to -SOH is a reversible mode of oxidation. It is an unstable and reactive functional group. The electrophilic sulfur atom in the -SOH group reacts with -SH in another cysteine residue to form a stable disulfide bond (-S-S-). However, under excessive oxidative stress, the sulfenic acid can be further oxidized to irreversible sulfinic acid ($-SO_2H$) and sulfonic acid ($-SO_3H$) [41, 42]. Cysteine oxidative

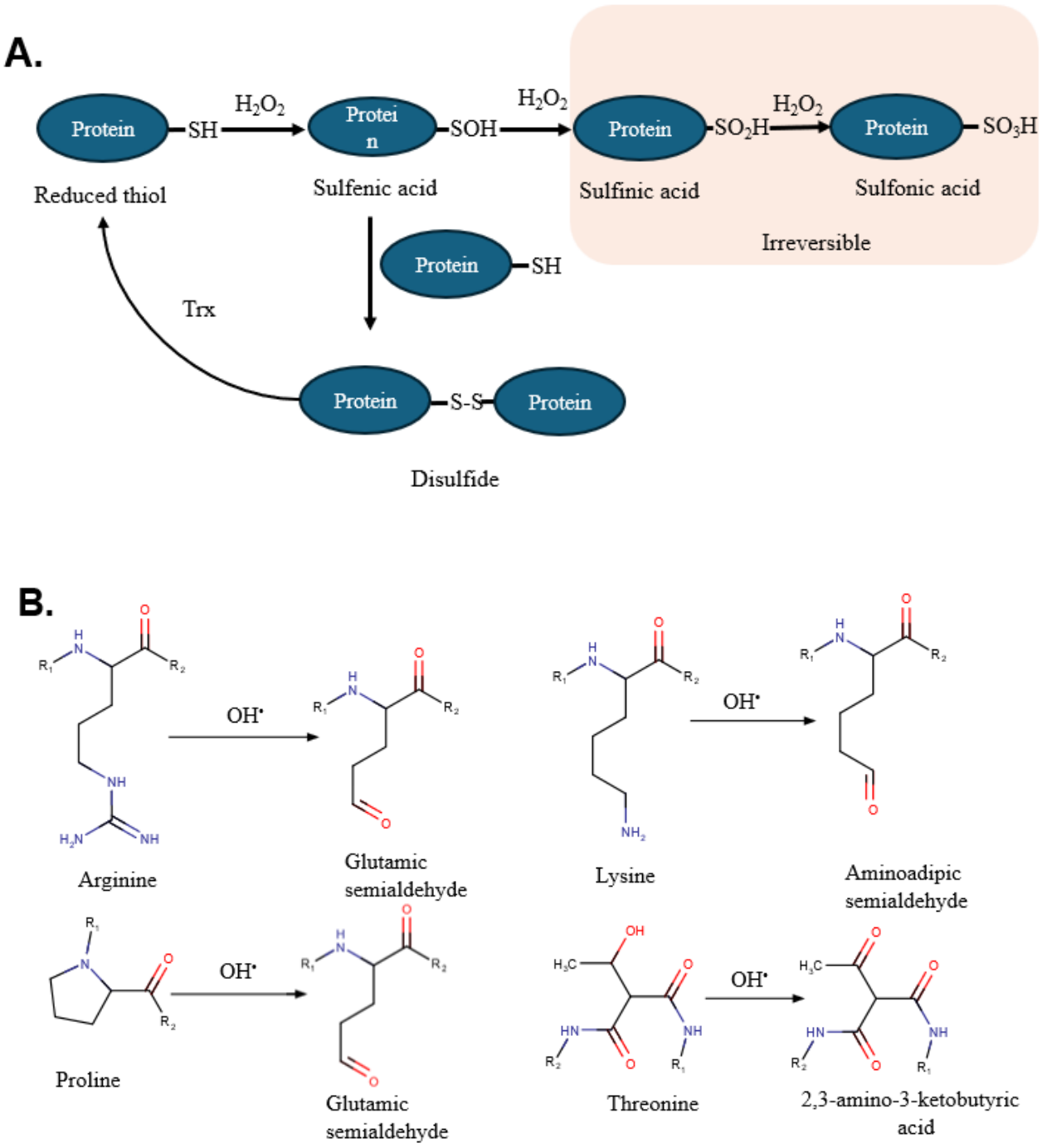

Figure 3. Oxidation of various amino acid residues A) Sulfenylation, sulfinylation, sulfonylation and disulfidation of cysteine residue by H_2O_2 B) Carbonylation of arginine, lysine, proline and threonine by $OH^{\bullet}$ radical (Marvin was used to create chemical structures, Marvin 24.1.2,2024, ChemAxon (www.chemaxon.com))

modification can alter protein activity, protein interaction and cell redox status, resulting in cell damage. $HO^{\bullet}$ radical can react with amino acids of protein side-chain like lysine, proline, threonine, and arginine residues to yield carbonyl derivatives, causing protein carbonylation. Protein carbonylation is an irreversible post-translational modification. Reactive $HO^{\bullet}$ radical is generated by H_2O_2 reacting with the oxidized form of a transition metal like Fe^{3+} or Cu^{2+} through the Fenton reaction. Besides this, end products of lipid peroxidation 4-HNE and MDA can form adducts with protein cysteine, lysine, or histidine residues and add a carbonyl group to the proteins, leading to carbonylation. Protein carbonylation causes changes in protein conformation, resulting in loss of protein function [43].

ROS can be neutralized by endogenous antioxidant system. Antioxidants consist of enzymatic antioxidants like glutathione peroxidase (GPx), superoxidase dismutase (SOD), peroxiredoxin (Prx), catalase (CAT), and non-enzymatic antioxidants like ubiquinol, urate, ascorbate, tocopherol, glutathione and carotenoids. The antioxidant acts either by preventing the formation of reactive species or by catalyzing the conversion of ROS into a more stable product and less reactive species that don't damage cells [44]. SOD is a metal-containing antioxidant enzyme that catalyzes the dismutation of superoxide ($O_2^{\bullet-}$) to oxygen and H_2O_2. GPx and CAT are responsible for the neutralization of H_2O_2. GPx catalyzes the reduction of H_2O_2 to water through GSH as an electron donor. CAT converts H_2O_2 to water and O_2 [45, 46]. Glutathione (GSH) is a tripeptide antioxidant which acts as a free radical scavenger and co-factor for antioxidant enzymes like GPx, glutathione reductase and glutathione transferase [47].

1.2.1.2 Increasing ROS production by chronic stress and chronic CORT treatment:

Chronic stress and chronic CORT treatment can increase ROS production in neurons. Mitochondria is a major source of ROS production. Under physiological conditions, it is estimated

that around 1-2% of oxygen can be partially reduced to ROS. In mitochondria, electrons flow through the electron transport chain (ETC) and are finally accepted by oxygen to produce water. ETC consists of complex I-IV, which facilitate the transfer of electrons [48]. Complex I and III are considered to be major source of mitochondrial superoxide production [49]. Both chronic unpredictable stress (CUS) for 40 days and CORT treatment for 40 days were found to decrease mitochondrial membrane potential, complex I, III and IV activities, and mitochondrial NADH levels in rat brains [50, 51]. Furthermore, both CUS and CORT treatment were found to increase mitochondrial ROS levels in rat brain [50-53]. *In vitro* studies have also shown that CORT treatment at 1 μM for 24 hours decreased mitochondrial membrane potential and increased intracellular ROS levels in primary cultured rat hippocampal neurons [54]. GR agonist dexamethasone treatment at 50 μM increased ROS levels in rat hippocampal slices [55]. Treatment with dexamethasone was also found to decrease mRNA levels of mitochondrial NADH dehydrogenase 3 (complex I subunit) and mitochondrial cytochrome B (complex III subunit) in rat embryonic neural stem cells [56]. These findings suggest that chronic stress and chronic or excessive CORT treatment may impair mitochondrial function and increase ROS production.

NADPH oxidase (NOX) is another important source of ROS. NOX catalyzes the transfer of electrons from NADPH to molecular oxygen, resulting in the production of ROS [57]. NOX enzyme complex consists of 6 subunits: 3 cytosolic subunits (p47phox, p67phox and p40phox), two membrane subunits (gp91phox and p22phox) and RhoGTPase. Under normal conditions, the p47phox, p40phox and p67phox subunits exist in the cytoplasm as complex. When activated, p47phox undergoes phosphorylation, and the entire complex translocate to the membrane and interacts with the complex of gp91phox and p22phox, resulting in the formation of the activated complex. The activated complex transfers electrons from NADPH to oxygen, resulting in the

formation of superoxide ($O_2^{\bullet}$) [58]. Mice exposed to chronic restraint stress at 2 hr daily for 14 days had increased p67 phox and p47 phox mRNA levels in the hippocampus and frontal cortex [59]. Chronic administration of CORT (35 µg/ml in drinking water) for 21 days increased NOX1 mRNA levels in the mouse ventral tegmental area [60]. In vitro studies have also shown that 1 µM cortisol treatment for 24 hrs increased p67phox and p47phox mRNA levels in SH-SY5Y human neuroblastoma cells [59]. 50 µM dexamethasone treatment increased p47phox mRNA levels in rat hippocampal slice culture [55]. These findings suggest that chronic stress and chronic CORT treatment may impair NADPH oxidase, increasing ROS production.

Chronic stress and chronic CORT treatment-increased ROS production may further induce oxidative damage to DNA, lipids, and protein. DNA and RNA oxidation is detected by measuring 8-hydroxy-2-deoxyguanosein (8-OHdG) and 8-oxo-7,8-dihydroguanosine (8-oxo-G) levels respectively. The study has shown that chronic unpredictable stress for 5 weeks increased the number of 8-OHdG/8-oxo-G positive neurons in mouse brain, indicating increased neuronal DNA and RNA oxidation [61]. MDA is an end product of lipid peroxidation. It has been found that CUS for 40 days and chronic CORT treatment for 40 days increased MDA levels in rat brain [50, 51], indicating chronic stress and chronic CORT treatment increase lipid peroxidation. CUS also increased the level of carbonylated proteins in the rat frontal cortex [52, 53]. Previously, our laboratory found that CUS increased protein sulfenylation in mouse prefrontal cortex and hippocampus [62]. We also found that CORT treatment at 1 µM in HT22 mouse hippocampal cells for 5 days increased protein sulfenylation [63]. These findings suggest that chronic stress or chronic CORT treatment, which increases the production of ROS, may further cause oxidative damage to nucleic acids, proteins and lipids.

1.2.1.3 Decreasing antioxidant capacity by chronic stress and chronic CORT treatment:

Chronic stress and chronic CORT treatment can inhibit antioxidant capacity. The chronic restraint stress for 21 days decreased the reduced glutathione levels in rat brain [64]. Chronic restraint stress decreased the number of GPx4 positive stained neurons in rat hippocampal CA1 region, and decreased total antioxidant capacity, SOD, CAT and GPx activities and total GSH content in rat hippocampus [34, 65]. Rats exposed to social defeat stress for 28 days have shown decreased protein levels of copper-zinc SOD, manganese SOD and glutathione reductase 1 in the hippocampus and amygdala [66]. The long-term administration of CORT also alters levels of antioxidant enzymes in the brain. It has been found that chronic corticosterone administration reduced levels of glutathione, copper/zinc SOD and GPx, and decreased activities of GPx, CAT and SOD in rat brain [67, 68]. Chronic CORT treatment was also found to decrease manganese SOD levels and reduced GSH/GSSG ratio in mitochondria of rat brain [50]. These findings suggest that chronic stress and chronic CORT treatment may increase ROS and oxidative damage by inhibiting antioxidant defense.

1.2.2 Chronic stress, chronic CORT treatment and neuroinflammation

Neuroinflammation is the inflammatory response in the nervous system mediated by pro-inflammatory cytokines, chemokines, ROS and others. Neuroinflammation acts as a defense mechanism to promote tissue repair and remove cell debris. However, sustained neuroinflammation can damage neurons, promote synaptic dysfunction, neuronal apoptosis and cognitive impairment, and inhibit neurogenesis. Microglia and astrocytes play an important role in neuroinflammation. Microglia and astrocytes can secrete proinflammatory cytokines and chemokines that can target neurons and induce neuronal damage. Neuroinflammation can be caused by various inducers. Sustained chronic inflammation causes neurotoxicity and promotes neurodegeneration.

Chronic stress and chronic CORT treatment can promote neuroinflammation. NOD-like receptor family pyrin domain containing 1 (NLRP1) or containing 3 (NLRP3) inflammasome consists of NLRP1 or NLRP3 protein, apoptosis-associated speck-like protein containing a caspase-activating recruitment domain (ASC), and pro-caspase-1. ASC connects NLRP1 or NLRP3 to pro-caspase-1, causing activation of caspase-1, which cleaves pro-IL-1β to mature IL-1β and cleaves pro-IL-18 to mature IL-18. Release of IL-1β and IL-18 promotes the amplification of inflammatory response and cell death signals, leading to neuronal damage [69-71]. It has been reported that CUS for 6 weeks increased NLRP1, ASC and caspase-1 protein as well as mRNA levels in mouse hippocampus [72]. CUS increased NLRP3 mRNA levels in rat hippocampus [73]. Treatment with GR agonist dexamethasone at 5 mg/kg s.c. for 28 days also increased NLRP1, caspase-1 and ASC protein and mRNA levels in rat hippocampus [71]. These findings suggest that chronic stress and chronic CORT treatment may activate NLRP1 and NLRP3 inflammasome.

Previously, it was found that CUS for 21 days increased pro-inflammatory cytokines like TNFα and IL-6 protein levels in rat hippocampus and frontal cortex [74]. CUS for 6 weeks was also reported to increase pro-inflammatory chemokines CXCL1 and CXCR2 mRNA levels in mouse hippocampus [72]. It has also been found that chronic social defeat stress for 10 days not only increased protein and mRNA levels of pro-inflammatory cytokines IL-6, IL-1β and TNFα but also decreased protein and mRNA levels of anti-inflammatory cytokines IL-4 and IL-10 in mouse hippocampus and frontal cortex [75]. Chronic treatment with CORT at 20 mg/kg/day, s.c. for 22 days increased protein levels of proinflammatory cytokines IL-2 and TNFα in mouse frontal cortex [76]. These findings suggest that chronic stress and chronic CORT treatment may activate pro-inflammatory signaling and inhibit anti-inflammatory signaling in rodent brain.

1.2.3 Chronic stress and psychiatric disorders:

Chronic stress is a major risk factor for psychiatric disorders like major depressive disorder (MDD), anxiety, bipolar disorder and others. In a recent cross-sectional clinical study, it was found that serum cortisol level was highly elevated in patients with MDD as compared to healthy controls [77]. It was found that long-term use of glucocorticoid medication resulted in the incidence of depression and anxiety in 16% and 11% of the patients respectively [78]. In another study, it was found that treatment with antidepressant selective serotonin reuptake inhibitors (SSRI) for 3 weeks decreased the level of salivary cortisol similar to the level of healthy subjects. In patients, the reduction of cortisol level significantly is correlated with the decrease in Hamilton Rating Scale for depression (HAMD) and improvement in cognitive test scores for trial making test A & B [79]. Similarly, long-term exposure to corticosterone can cause result in increased immobility in forced swim test and tail-suspension test indicating depression-like symptoms in rodents [80, 81]. The chronic stress can lead to HPA axis overactivation which can cause alteration in serotonin (5-HT) neurons and dopaminergic neurons, promote neuronal remodelling and neuroplasticity and neuronal damage which can lead to increased risk for depression [82]. In addition to this, a large cohort study revealed that patients with anxiety had higher awakening salivary cortisol levels as compared to healthy patients [83]. In another study with adolescents, it was found that girls with concurrent general and social anxiety had higher levels of serum cortisol as compared to healthy subjects [84]. Similarly, administration of CORT in mice for 2 weeks in drinking water resulted in repetitive anxiety like behavior in elevated maze test [85]. This evidence suggests that chronic stress is a risk factor for depression and anxiety.

1.3. Astrocytes:

1.3.1 Role of astrocytes in the central nervous system

Astrocytes are the major glial cells, which are around five times more numerous than neurons. They cover the entire CNS and are important in maintaining CNS function. Astrocytes play a critical role in neuroprotection, homeostatic maintenance, and metabolism regulation by releasing neurotrophic factors, removing ROS, maintaining BBB integrity, regulating ion and neurotransmitter concentrations, and supporting energy, respectively (Figure 4) [86].

1.3.1.1 Astrocytes and neuroprotection

Astrocytes exert neuroprotective effects by releasing neurotrophic factors, removing ROS, maintaining BBB integrity (Figure 4). Astrocytes can secrete various neurotrophic factors such as brain-derived neurotrophic factor (BDNF), glial-derived neurotrophic factor (GDNF) [87] and mesencephalic astrocyte-derived neurotrophic factor (MANF) [88]. These neurotrophic factors promote the survival, development and differentiation of neurons and protect neurons from neurological insults. BDNF has a high affinity for tyrosine kinase B (TrkB) receptor. The binding of BDNF to TrkB can activate MAP kinase, PI3-kinase and protein kinase C pathways, which phosphorylates cAMP response element binding protein (CREB) and increases expression of genes involved in neural plasticity, neurogenesis, stress resistance and neuronal survival [89]. GDNF can bind to GDNF-family receptor-α1 (GFRα1) and activate GFRα1 receptor. Activated GFRα1 receptor increases affinity to RET tyrosine receptor and promotes GFRα-RET binding, which induces phosphorylation of tyrosine residue in RET. The phosphorylated RET recruits various signaling proteins, including PLC-γ, PI3-kinase and MAP kinase. GDNF was found to promote the survival of dopaminergic neurons and motor neurons and the development and differentiation of parasympathetic and enteric neurons [90]. MANF is localized to the ER and is

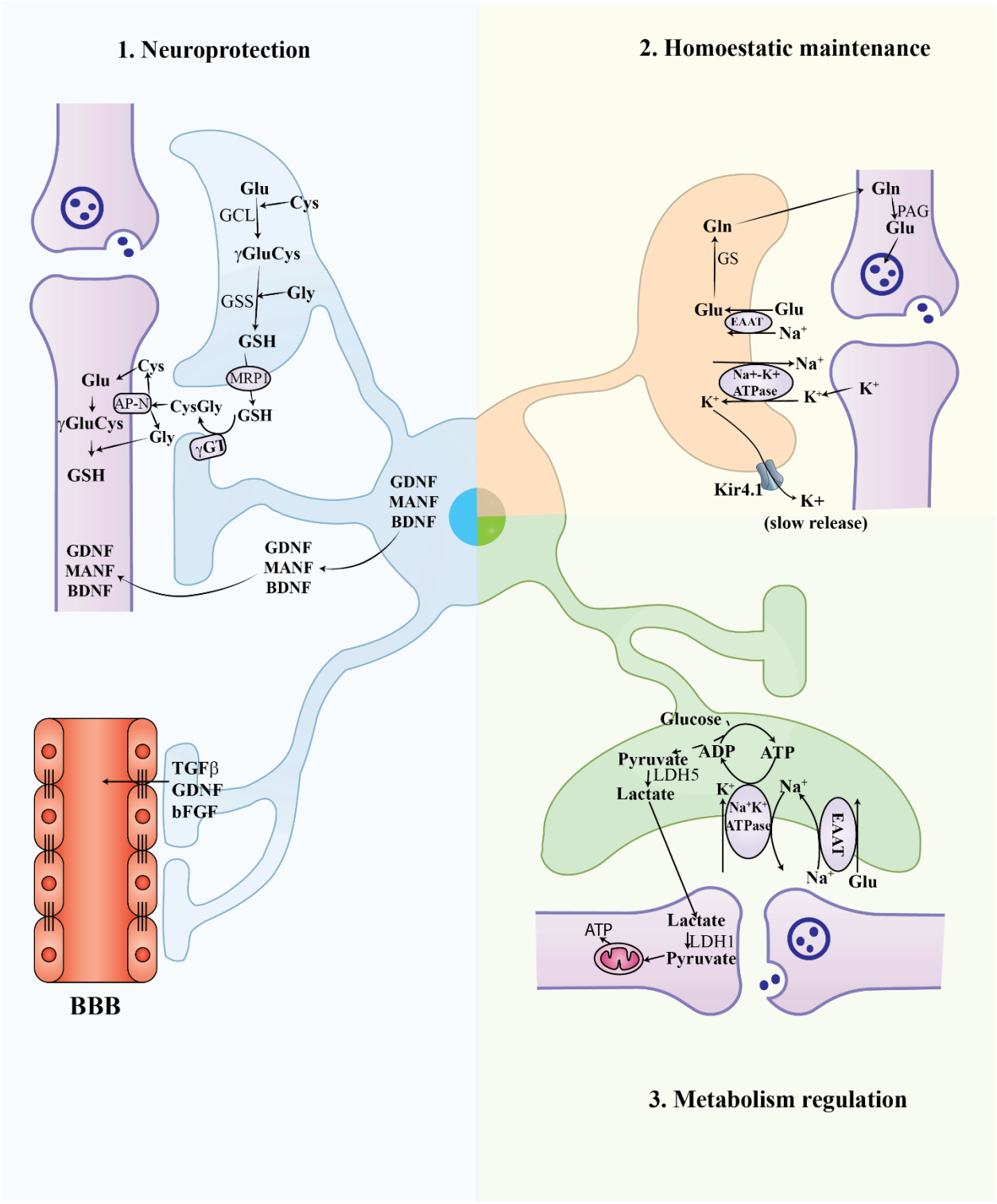

Figure 4. Physiological roles of astrocytes in central nervous system: 1. Neuroprotection; 2. Homeostatic maintenance; and 3. Metabolism regulation

secreted upon ER stress. MANF can interact with the luminal domain of ER IRE1α protein and inhibit ER stress-activated ER unfolded protein response. MANF plays an important role in the survival and maintenance of neurons by attenuating ER stress [91, 92].

Astrocytes can protect neurons against oxidative stress. Due to the high rate of oxidative metabolism and neuronal activity, ROS is produced at a higher rate in neurons. In addition, neurons have lesser antioxidative capacity than astrocytes, which leads to ROS accumulation. Increased ROS levels cause lipid peroxidation and protein oxidation, which can cause neuronal degeneration [93, 94]. Because the brain has a much lower amount of catalase than other body organs, glutathione (GSH) plays a major role against ROS-induced oxidative stress [95]. GSH is a tripeptide composed of cysteine, glycine and glutamate. First of all, glutamate-cysteine ligase (GCL) catalyzes ligation between glutamate (Glu) and cysteine (Cys) to form γ-glutamylcysteine dipeptide. Then, glutathione synthetase (GSS) catalyzes the reaction between γ-glutamylcysteine dipeptide and glycine (Gly) to form GSH. In neurons, Cys is a rate-limiting substrate for GSH synthesis and is imported through neuronal membrane excitatory amino acid transporter [96, 97]. Both neurons and astrocytes can synthesize GSH, but neurons depend on astrocytes for the maintenance of GSH level. Astrocytes contain higher levels of GSH as compared to neurons and are the main source of Cys for neuronal GSH synthesis [95]. Astrocytes release GSH through multidrug resistance protein 1 into the extracellular matrix. The released GSH is cleaved by γ-glutamyl transpeptidase into γ-glutamyl moiety and CysGly dipeptide. The dipeptide CysGly is hydrolyzed by aminopeptidase N into Cys and Gly. Neurons uptake Cys by excitatory amino acid transporter and utilize it for GSH synthesis [98-100].

Astrocytes also protect neurons by maintaining the integrity of the blood-brain barrier (BBB). BBB is a physical barrier formed between the neural interface and brain blood vessels.

BBB regulates the movement of ions, molecules, and cells between blood vessels and CNS, resulting in the formation of a brain microenvironment, which is essential for regulating ionic homeostasis, the pool of neurotransmitter and neuroactive agents, and transportation of nutrients in the brain [101, 102]. BBB is composed of endothelial cells, astrocytic endfeet and pericytes. Brain endothelial cells are connected by tight junctions that prevent the paracellular transport of molecules and ions between the cells. Pericytes are enwrapping cells between endothelial cells and astrocytic endfeet and neurons and are responsible for regeneration, angiogenesis, control of endothelial cell proliferation and neovascularization. Astrocytes establish close contact between blood vessels and neuroglials in the neurovascular unit. Astrocyte endfeet acts as an additional barrier to exclude blood-borne factors. Astrocytes are also responsible for the secretion of various growth factors like basic fibroblast growth factor (bFGF), GDNF and transforming growth factor β (TGFβ) to maintain endothelial cell tight junction and BBB integrity. Loss of astrocyte function caused by infection, neurodegenerative diseases, inflammation, and ischemia can make BBB more permeable [101-103].

1.3.1.2 Astrocytes and homeostatic maintenance

Astrocytes play a critical role in homeostatic maintenance by regulating ion and neurotransmitter concentrations (Figure 4). During an action potential, after Na^+ influx-induced depolarization, K^+ channels open and move K^+ to extracellular space, which increases extracellular K^+ concentration ($[K^+]_o$). In the brain, $[K^+]_o$ is maintained at a resting level of 3 mM, while neuronal activity can increase $[K^+]_o$ to 10-12 mM. The excess of K^+ is uptaken by Na^+/K^+-ATPase. Both neurons and astrocytes express Na^+/K^+-ATPase. However, neuronal Na^+/K^+-ATPase has a higher affinity for K^+ ions and is saturated at resting $[K^+]_o$, while astrocytic Na+/K+-ATPase has a lower affinity and is sensitive to elevated $[K^+]_o$ level. Therefore, elevated $[K^+]_o$ after

repolarization stimulates astrocytic Na^+/K^+-ATPase and is taken up by astrocytes. Uptaken K^+ ions are then transported to adjoining astrocytes through gap junction and released gradually to the extracellular matrix through inward rectifying K^+ (Kir) 4.1 channels. Astrocytes are important in buffering spatial K^+ [104-106].

Astrocytes play an important role in maintaining the level of both the excitatory neurotransmitter glutamate and the inhibitory neurotransmitter GABA. The perisynaptic astrocytic process contacts synapses through which astrocytes can interact and modulate neuronal activity and function. The combination of this perisynaptic astrocytic process with a presynaptic and postsynaptic membrane is known as a tripartite synapse [107]. Astrocytes express glutamate transporter-1 and glutamate aspartate transporter, which can uptake glutamate from the synaptic cleft. Glutamate is converted into glutamine by glutamine synthetase, and then glutamine is released by astrocytes to the extracellular matrix. Glutaminergic neurons can uptake glutamine and convert it to glutamate by phosphate-activated glutaminase. Astrocyte helps in glutamate-glutamine cycling and regulates the level of glutamate in the synaptic cleft [108-110]. Astrocyte-released glutamine can also be uptaken by GABAergic neuron. Uptaken glutamine can be converted to glutamate, which is converted to GABA by glutamate dehydrogenase. Therefore, astrocytes are also important in the biosynthesis of GABA in GABAergic neurons [108, 110-112].

1.3.1.3 Astrocytes and metabolism regulation

Astrocytes contribute to the regulation of CNS energy metabolism through the astrocyte-neuron lactate shuttle (Figure 4). Glucose from capillaries is transported to astrocytes by the Glucose transporter 1 (GLUT1). Transported glucose enters glycolysis to form pyruvate, which can either enter TCA cycle to produce ATP or form lactate catalyzed by lactate dehydrogenase. The astrocytes have high glycolytic activity, high levels of lactate dehydrogenase 5 and

NADH/NAD+ ratio, and a low rate of oxygen metabolism, which favours conversion of pyruvate to lactate over entry into the TCA cycle. When the neuronal activity increases, the release of glutamate from the axon terminal of glutaminergic neurons also increases. Astrocytes can uptake released glutamate by sodium-dependent glutamate transporters that also co-transport Na^+ into astrocytes. Increased astrocytal Na^+ levels activate Na^+/K^+ ATPase, which decreases ATP levels in astrocytes, consequently, increases glucose uptake and triggers glycolysis, which leads to increased lactate production and release in extracellular matrix. The released lactate is taken up by neurons and converted into pyruvate catalyzed by LDH1. Pyruvate acts as an energy substrate in neurons and enters into the TCA cycle to generate ATP [113-115].

1.3.2 Role of astrocyte in neuroinflammation

Although astrocytes are neuroprotective in nature, persistent noxious stimuli can induce the formation of reactive astrogliosis. Reactive astrocytes can release pro-inflammatory cytokines and ROS production, facilitating neuroinflammation and neuronal damage [116, 117].

Reactive astrocytes are associated with Alzheimer's disease, traumatic brain injury, multiple sclerosis, and other pathological conditions [117]. Astrocytes can recognize pathogen-associated molecular pattern (PAMP) and danger-associated molecular pattern (DAMP) which can trigger activation of astrocytes. Toll-like receptor (TLR) 2/3/4/7, NOD-like receptor protein 2 (NLRP2), NOD-like receptor protein 3 (NLRP3) and NOD-like receptor C4 (NLRC4) are expressed in astrocytes, and can induce activation of astrocyte in response to DAMP and PAMP [86, 118, 119]. TLR receptors can recognize PAMP and activate myeloid differentiation primary response 88-dependent signaling pathway and toll/interleukin-1 receptor-domain-containing adapter-inducing interferon-β dependent signaling pathway, which regulates the expression of pro-inflammatory cytokines and interferons [120]. NLRP receptors can recognize PAMP and DAMP

and form inflammasomes by recruitment of ASC and procaspase-1, leading to cleavage of procaspase-1 to active caspase-1, which subsequently releases proinflammatory cytokines like IL-18 and IL-1β [119, 121].

1.3.3 Glucocorticoid and astrocytes:

Astrocytes express both mineralocorticoid receptor (MR) and glucocorticoid receptor (GR). However, astrocytes contain more GR than MR [122]. Glucocorticoids can alter the morphology of astrocytes. Chronic restraint stress for 21 days and CUS for 21 days was found to decrease the length and the number of astrocyte branches in rat and mouse hippocampus. [123]. CUS also decreased the total surface area occupied by astrocytes in mouse hippocampal dentate gyrus [124]. Treatment with CORT at 100 nM in primary rat astrocytes for 6 days was found to reduce the length and abundance of cultured filopodia [125]. These findings indicate that chronic stress and chronic CORT treatment can impair astrocytes.

Glucocorticoids can also alter astrocyte-astrocyte communication. Gap junction coupling allows intercellular communication between two adjacent astrocytes to pass small molecules, ions, amino acids and second messenger up to 1 kDa. Connexin 43 (Cx43) is a major component of gap junctional protein, forms a hexamer on the plasma membrane and acts as hemichannels. Opposed Cx43 between two cells forms a complete gap junction channel. CUS for 21 days decreased the diffusion of the fluorescent dye Lucifer yellow and a number of coupled astrocytes in the rat prelimbic cortex. The ultrastructural examination of prelimbic cortex slices by electron microscopy showed the gap between two neighboring astrocytes in stressed rats was nearly 1.5 times wider than in control rats [126]. The treatment with 50 µM CORT for 24 hrs was also found to decrease the diffusion of Lucifer yellow in primary cultured rat astrocytes [127]. These results indicate that chronic stress and CORT treatment can impair gap junction intercellular

communication. Furthermore, it has been found that CUS for 3 weeks decreased Cx43 mRNA and protein levels in rat hippocampus [128]. Cx43 phosphorylation at S368 can decrease gap junction channel permeability. It has been found that treatment with CORT (35 μg/ml/day; p.o.) for 3 weeks increased Cx43 phosphorylation in rat hippocampus [129]. Treatment with CORT at 50 μM for 24 hrs was found to decrease total Cx43 protein levels and increase phosphorylation of Cx43 at S368 in primary cultured rat astrocytes [127]. These findings suggest that glucocorticoid may impair gap junction intercellular communication by phosphorylation of Cx43.

Glucocorticoids affect the glucose metabolism in astrocytes. It has been reported that CORT administration (40 mg/kg/day, sc) for 21 days decreased [^{18}F]-fluorodeoxyglucose uptake in astrocytes of rat frontal cortex [130]. Treatment with CORT at 0.1 μM for 72 hours or 1 μM for 24 hours was also found to inhibit the uptake of 2-deoxyglucose in primary cultured rat astrocytes [131]. Treatment with GR agonist dexamethasone 100 nM for 24 hrs also decreased 2-deoxyglucose uptake in primary cultured rat astrocytes [131]. It has been found that treatment with CORT at 0.1 μM for 24 hrs decreased GLUT1 transporter translocation to the plasma membrane and glycogen level and lactate production in primary rat astrocytes [130]. Dexamethasone treatment for 4 hrs was also found to decrease glycogen synthetase activity [132]. These findings suggest that glucocorticoids can decrease glucose uptake, glucose metabolism and glycogen synthesis in astrocytes.

Glucocorticoids can induce stress in the mitochondria of astrocytes. It has been found that treatment of 10 μM CORT for 24 hrs increased the level of MitoSOX fluorescence in primary cultured mouse astrocytes, indicating that CORT increased mitochondrial ROS production [133]. Uncoupling protein-2 (UCP-2) presents in mitochondrial inner-membrane protein, which is responsible for decreasing mitochondrial membrane potential, maintenance of respiration and

prevention of ROS accumulation in mitochondria [134]. It has been found that 100 µM CORT treatment for 24 hrs decreased UCP2 promoter activity and UCP-2 mRNA levels in primary cultured mouse astrocytes. Knockdown of the UCP2 gene using siRNA increased ROS production [135]. These findings suggest that glucocorticoid might induce mitochondrial damage.

1.4 Thioredoxin protein

Thioredoxin (Trx) is a 12 kDa oxidoreductase protein which is responsible for maintaining redox status in cells by catalyzing disulfide/dithiol protein conversion. It is ubiquitously expressed in all life forms, from bacteria to mammals. As shown in Figure 5, the Trx protein consists of a highly conserved protein motif -Cys-Gly-Pro-Cys- in its active site. The nucleophilic N-terminal cysteine in the active site can donate electrons to the disulfide of the oxidized protein, resulting in the formation of an intermediate with a disulfide bond between Trx and the target protein. This reaction forms one free thiol in the target protein. In the next step, Trx C-terminal thiol is converted to thiolate, which donates electrons to the disulfide bond in the mixed disulfide complex. Thus, it releases a reduced target protein with a dithiol group and oxidizes Trx with a disulfide bond. Trx can be reduced back to its active form by thioredoxin reductase (TrxR) with the help of NADPH. Trx protein, along with NADPH and TrxR, form a thioredoxin antioxidant system. In mammals, there are three Trx isoforms: cytosolic Trx1, mitochondrial Trx2 and spermatozoid specific Trx3. Mammalian Trx1 consists of additional cysteine residues, Cys62, Cys69 and Cys73, which are responsible for redox signaling regulation. The oxidation at Cys73 can lead to the formation of Trx1 dimer and loss of its catalytic activity [136, 137].

1.4.1 Thioredoxin function

Trx can reduce H_2O_2-induced protein cysteine oxidation, facilitating Prx-mediated scavenging of H_2O_2 and other peroxides and inhibiting the ASK1-activated apoptotic process.

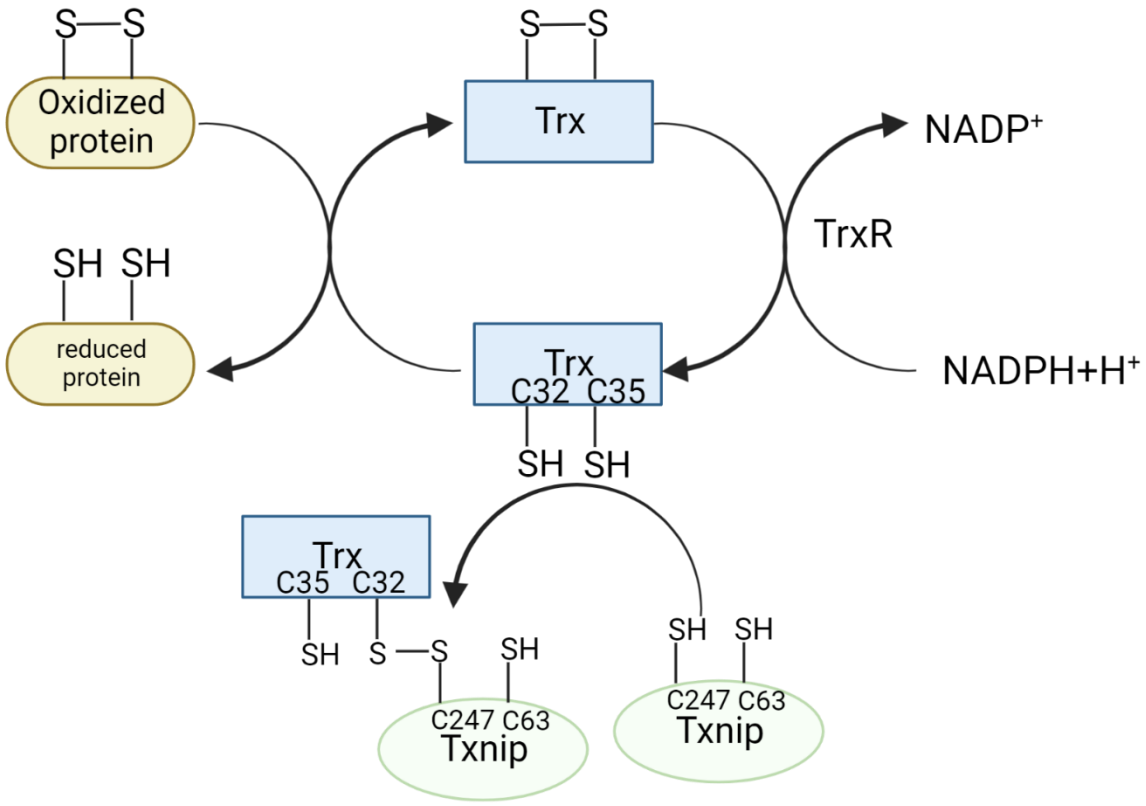

Figure 5. Thioredoxin antioxidant system: Under normal conditions, reduced thioredoxin (Trx) transfers the electron to oxidized disulfide protein by disulfide/dithiol exchange to form reduced dithiol protein and oxidized disulfide Trx. Trx reductase (TrxR) transfers the electron from NADPH to oxidized Trx to form reduced Trx. Trx-interacting protein (Txnip) forms covalent bond with Cys32 of Trx resulting in the inhibition of Trx activity. (Created using BioRender.com)

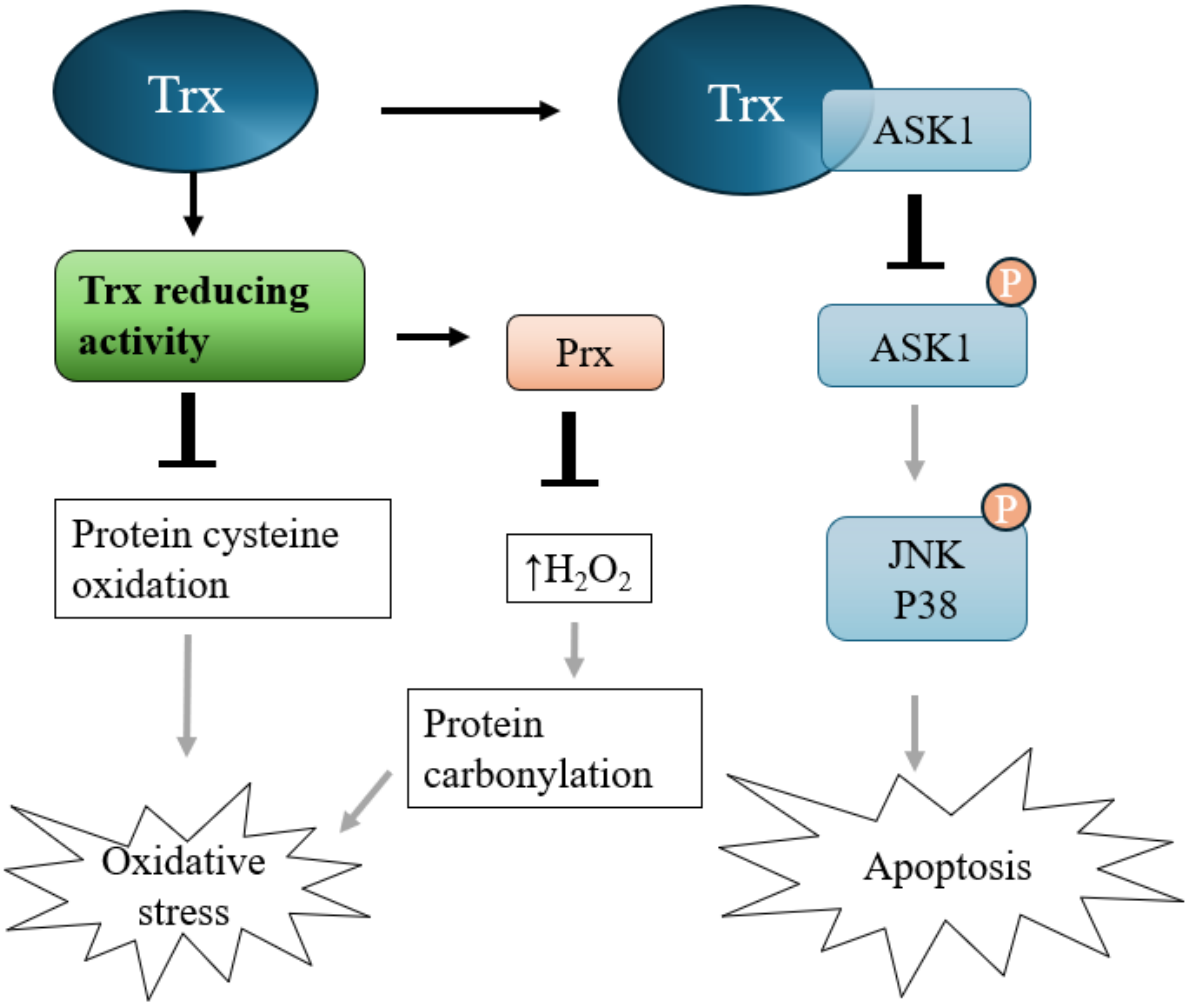

Figure 6. Antioxidative and Antiapoptotic role of Trx: Antioxidative and Antiapoptotic role of Trx: Trx reduces protein cysteine oxidation and peroxiredoxin (Prx) to its active reduced form. Reduced Prx can scavenge H2O2 and inhibit protein carbonylation. Trx binds to apoptosis signal-regulating kinase 1 (ASK1), which can inhibit phosphorylation of ASK1, JNK kinase and P38 kinase, ⊣ inhibit, → activate

Trx acts as an antioxidant directly by reducing protein cysteine oxidation, such as cysteine sulfenylation and disulfidation (figure 6). Cysteine residues is one of the conserved residues in protein and plays an important role in the structure of protein, metal binding, catalytic activity, redox reaction, regulation and post-translational modification of protein [138]. The cysteine residue is highly polarizable and nucleophilic due to the high electronegativity of the sulphur atom. As reviewed above, cysteine oxidation includes reversible sulfenylation and disulfidation, as well as irreversible sulfinylation and sulfonylation. Sulfenylation and disulfidation can alter protein activity, protein interaction and redox status of cells. These reversible cysteine oxidation can be reduced back to its thiol form by Trx [137]. Sulfinylation and sulfonylation can lead to protein degradation and permanent loss of protein activity.

Trx can also maintain peroxiredoxin (Prx), reducing activity (figure 6). Prx is a ubiquitous peroxidase enzyme responsible for neutralizing H_2O_2 and other peroxides. Prx consists of both perioxidatic Cys (C_p) and resolving Cys (C_R). Under physiological pH, C_p is present as thiolate due to the low pKa value of C_p. When the thiolate C_p donates electrons to H_2O_2 and reduces H_2O_2 to water, Cp is oxidized to C_p-sulfenic acid (C_p-SOH). Then C_p-SOH reacts with C_R of another Prx to form a dimer with an intermolecular disulfide bond between two Prxs, which makes Prx inactive [139-141]. Prx can be reduced by Trx with disulfide/dithiol mechanism to its active reduced Prx form [137]. Trx can maintain Prx reducing activity to facilitate Prx-mediated H_2O_2 scavenge. Because H_2O_2 can react with the oxidized form of transition metals like Fe^{3+} or Cu^{2+} to generate reactive $HO^{\bullet}$ radical through the Fenton reaction, while produced $HO^{\bullet}$ radicals can further attack protein threonine, lysine, proline and arginine residues to yield protein carbonylation [43, 142]. Therefore, Trx can maintain Prx reducing activity to indirectly prevent protein carbonylation by scavenging H_2O_2.

Trx can bind to apoptosis signal-regulating kinase 1 (ASK1) and inhibit ASK1 activity (figure 6). ASK1 belongs to the mitogen-activated protein kinase kinase kinase (MAP3K) family. ASK1 is activated by various stress conditions like ROS, ER stress and TNFα. Under the stress condition, ASK1 dissociates from Trx and recruits tumor necrosis factor receptor-associated factor 2 (TRAF2) and TRAF6, resulting in ASK1 oligomerization and autophosphorylation at Thr^{838}. The ASK1 phosphorylation further induces activation of p38 MAPK and c-Jun N-terminal kinase (JNK) [143-145]. Activated JNK can translocate to the nucleus, where it can transactivate c-Jun and other transcription factors to increase the expression of pro-apoptotic genes. Besides this, JNK can promote apoptosis by releasing cytochrome C and activating caspases [146, 147]. Under physiological conditions, Trx binds to the N-terminal region of ASK1 and thus negatively regulates its kinase activity [144, 148].

1.4.2 Regulation of thioredoxin by thioredoxin reductase:

Thioredoxin reductase (TrxR) is a homodimeric selenoprotein which helps to maintain the activity of Trx. It is a flavoprotein and consists of one tightly bound flavin adenine dinucleotide (FAD) per subunit. TrxR has 3 isoforms: TrxR1 (cytosol), TrxR2 (mitochondria) and TrxR3 (cytosol and mitochondria). The N-terminal consists of one active-site motif with sequence -Cys^{59}-Val-Asn-Val-Gly-Cys^{64}. C-terminal consists of another active site with sequence -Glyc-Cys^{497}-$SeCys^{498}$-Gly. The SeCys residue is important catalytic activity of TrxR, as removal of SeCys can cause inactivation. The Cys^{497}-$SeCys^{498}$ residue of one subunit is in proximity of Cys^{59}-XXXX-Cys^{64} of another subunit. This allows electrons to be transferred from the disulfide/dithol of one subunit to the Cys-SeCys of another subunit. Under the physiological pH, active TrxR selenothiol (-SeH) exists as selenolate ($-Se^-$) because of its low pKa. The reduction of Trx begins with the binding of -Se- anion with the disulfide of Trx to form Trx-TrxR selenenylsulfide (Trx-S-Se-TrxR)

intermediate. This intermediate is reduced by Cys^{497} to release reduced Trx and oxidized selenenylsulfide TrxR. Selenenylsulfide TrxR is reduced by N-terminal dithiol from another subunit. As a result, N-terminal dithiol maintains reduced selenothiol form in the C-terminal. Finally, NADPH transfers the electron to N-terminal disulfide via FAD to form reduced N-terminal dithiol [149, 150].

1.4.3 Regulation of thioredoxin by Thioredoxin interacting protein

Txnip (Txnip), also known as thioredoxin binding protein (TBP) or Vitamin-D3 upregulated protein 1(VDUP 1), belongs to the α-arrestin family. It has two arrestin-like domains: PxxP sequence (binding motif for SH3 domains) and PPxY (binding domain for WW domain) sequence. The human Txnip gene is present in chromosome 1q21.1 with a length of 4174 bp [142, 151-153]. Under normal conditions, Txnip is found to be localized predominantly in the nucleus. It is found to interact with arrestin-α_1 under basal conditions, which is responsible for its nuclear localization and exerts its transcriptional co-repressor activity [154, 155]. However, under stressful conditions, it can translocate to various intracellular structures like cytoplasm, mitochondria, cell surface and plasma membrane to exert diverse biological functions [142, 154]. Txnip is an endogenous inhibitor of Trx. Txnip binds at the active site of reduced Trx by the formation of disulfide linkage between Cys-32 of Trx and Cys-247 of Txnip, resulting in inhibiting of Trx activity (Figure 5) [142, 156]. Txnip promotes oxidative stress in cells by inhibiting Trx activity.

1.4.4 Chronic stress and thioredoxin

The effect of chronic stress on Trx is not very clear. It has been reported that CUS for 21 days decreased Trx immunostaining in CA1 region of rat hippocampus [157]. Chronic restraint stress (3 hrs daily) for 14 days was also reported to decrease Trx protein levels in mouse

hippocampus [158]. In contrast to this, chronic intermittent cold (6 hrs daily) for 14 days was reported to increase Trx protein levels in rat cortex, hippocampus and cerebellum [159].

Previously, our laboratory has found that chronic unpredictable stress for 28 days didn't produce any effect on Trx and TrxR protein levels but increased Txnip protein levels in mouse hippocampus and cortex [62]. Furthermore, our laboratory also found that although treatment with CORT for 5 days had no effect on Trx and TrxR protein levels, this treatment increased Txnip protein levels in primary cultured mouse cerebrocortical neurons and HT22 mouse hippocampal neurons. Knocking down Txnip prevented chronic CORT treatment-induced protein sulfenylation in cultured HT22 cells [160]. Since Txnip is an endogenous inhibitor, our findings suggest that CORT may upregulate Txnip, inhibiting Trx activity and subsequently causing oxidative damage.

1.5 Summary

Stress is an organism's response to environmental challenges. Acute stress is **beneficial, but** chronic stress has a harmful effect on health. Chronic **stress** is found to be a major risk factor for **depression**. Studies have shown that chronic stress and chronic treatment with stress hormone CORT can increase ROS production, decrease antioxidant levels, and promote protein oxidation in rodent brain. Chronic stress and chronic CORT treatment were also found to activate inflammatory signaling and release pro-inflammatory cytokines. These findings suggest that chronic stress and chronic CORT treatment can promote oxidative stress and neuroinflammation. Antioxidant Trx is an oxidoreductase that maintains redox balance and inhibits oxidative stress and inflammation in cells. The activity of Trx is negatively controlled by Txnip. Previous studies from our laboratory has revealed that chronic stress and chronic CORT treatment increased Txnip protein levels in mouse brain in vivo and in cultured mouse neurons in vitro. Our finding suggests that chronic stress and chronic CORT treatment may promote oxidative stress and inflammation

through the upregulation of Txnip. Astrocytes as an immune-competent cells, participate in immunological reactions and release cytokines, chemokines and ROS that promote neuroinflammation and facilitate oxidative damage. Our results may also indicate that astrocytes may play a role in chronic stress and chronic CORT treatment-induced oxidative damage and inflammation.

1.6 Hypothesis and Objectives

We hypothesize that chronic CORT treatment can increase Txnip expression in astrocytes. CORT-induced Txnip:

- may inhibit Trx activity and **increase protein oxidation**
- may also activate NLRP3 inflammasome and release pro-inflammatory cytokines

The objective of this project is:

1. To determine if CORT treatment upregulates Txnip and further causes protein oxidation in primary cultured mouse astrocytes.
2. To determine if CORT treatment activates NLRP3 inflammatory signaling and if Txnip mediates CORT-induced activation in primary cultured mouse astrocytes.

CHAPTER 2. MATERIALS AND METHODS

2.1 Cell culture:

Primary astrocytes were obtained from postnatal P1 to P3 CD1 mice pups. The brain was isolated, the cerebral cortex was dissected, and the meninges were peeled off. The cortex was minced and then 1 ml of 0.25% trypsin with 4 ml of phosphate buffer saline (PBS) was added. The tissue was incubated with trypsin for 10 min at 37 ºC with occasional stirring. Then, cortices were washed twice with Dulbecco's Modified Eagle's Medium (DMEM) (Life Technologies Inc, Burlington, ON, Canada) supplemented with 10% fetal bovine serum (FBS) and 1% streptomycin and penicillin. The cells were dissociated by pipetting up and down in 10 ml of DMEM with 10% FBS and 1% streptomycin and penicillin. The medium with cells was transferred to T-75 flask coated with collagen (100 µg/ml). The medium was changed every two days for seven days. When the mixed glial culture in T-75 gets confluent, microglia and oligodendrocytes were removed by shaking at 240 rpm overnight. Then, the T-75 flask was shaken vigorously the next day to remove any remaining microglia and oligodendrocytes. The astrocytes remaining in the T-75 flask were seeded in 6-well plates coated with collagen at a density of 3×10^5 cells/well, incubated at 37 ºC with 5% CO_2 for two days and then treated with CORT.

2.13 Protein extraction

Primary astrocytes were washed twice with PBS, and 75 µl of lysis buffer (containing 20 mM HEPES, 250 mM NaCl, 20% glycerol, 30 mM $MgCl_2$, 0.5 mM EDTA, 0.1 mM EGTA, 0.3 mM DTT, 1% NP40 and 1× protease inhibitor cocktail) was added to every wells. Then, the cells were scrapped off and kept on ice for 1 hour with occasional vortexing. After cells were centrifuged at 13,500 ×g at 4 ºC for 15 min, the supernatant was collected to obtain protein extract [160]. The concentration of protein was determined using Bradford assay [161].

2.3. Immunoblotting analysis

The protein sample was mixed with equal volume of 2× SDS gel-loading buffer (containing 100 mM Tris. HCl (pH 6.8), 20% glycerol, 4% SDS, 0.2% bromophenol blue, 200 mM DTT). The mixture was heated for 5 min at 95 ºC, and the sample was spin-down. The sample was loaded in 12% SDS- polyacrylamide gel and electrophoresis was performed at 120 V for 90 min. The proteins were transferred to a polyvinylidene fluoride (PVDF) (Millipore, Billerica, MA) membrane for 2 hours at 220 mA on ice. The membrane was blocked with 5% milk in Tris-buffered saline-tween (TBST) containing 10 mM Tris-HCl, pH 7.4 and 0.1% Tween-20. The membranes were incubated overnight at 4ºC including with a primary antibody like rabbit monoclonal Trx1 (1:1000 dilution, Cell Signaling Technology, Danvers, MA, USA), rabbit polyclonal anti-cysteine sulfenic acid antibody (1:3000 dilution, Millipore Canada Ltd, Etobicoke, ON, Canada), mouse monoclonal NLRP3 (1:1000 dilution, Adipogen, CA, USA) or rabbit monoclonal Txnip (1:2000 dilution, Abcam Inc., Toronto, ON, Canada). It was followed by 4 washes with TBST for 10 min each and then incubated with horseradish peroxidase (HRP)-conjugated secondary antibody for 1 hour at room temperature. The membrane was washed again 4 times with the same TBST for 10 min each. The enhanced chemiluminescence reagent was added to the membrane. The chemiluminescence detected immunoreactive bands and bands were imaged using ChemiDoc MP system (Bio-Rad). The band intensity was determined using image Lab software.

2.4 Determination of Trx activity

Thioredoxin activity was measured using eosin-labeled insulin kit (Cayman Chemical, Canada). The cells were lysed using Tris buffer (100 mM Tris-HCl pH 7.5, 1 mM EDTA and 1× protease inhibitor). Then the sonification was performed to increase protein extraction. 20 µl of sample, including 10g protein, 40 µl of 1× Assay buffer and 10 µl of 0.16 U TrxR was added to

the sample well while 20 µl of sample and 50 µl of 1×Assay buffer were added to the sample background well. 10 µl of 0.25 mM NADPH was added in each well and incubated at 37 ºC for half hour. Then, 20 µl of eosin-labeled insulin was added to all wells in the dark and incubated for 1 hr. The fluorescence intensity was measured at Excitation/Emission of 520/560 nm.

2.5 Reduced thiol level determination:

Ellman's assay was used to determine reduced thiol levels [162]. The free thiol group (-SH) reacts with 5,5'-dithiobis-(2-nitrobenzoic acid) (DTNB) to give mixed disulfide and yellow-colored product, 2-nitro-5-thiobenzoic acid (TNB). The TNB^{2-} anion concentration anion can be measured by detecting absorbance at 412 nm. 5 µl of Ellman's reagent (4 mg of DTNB in 1 ml of Reaction buffer (0.1 M sodium phosphate, pH 8.0 and 1 mM EDTA)), 150 µl of Reaction buffer and 50 µl of sample were added in every well and incubated for 15 min at room temperature. The absorbance intensity was measured at 412 nm.

2.6 Dimedone conjugation method for detection of protein sulfenylation

Protein sulfenylation was measured using dimedone conjugation [160]. Dimedone is a cell permeable nucleophile which can label cysteine sulfenic acid to form a stable thioether product. This modified protein can be analyzed using an immunoblotting assay with an anti-sulfenic acid antibody. The cells were washed with PBS and incubated with 0.25% trypsin for 3 min at 37 ºC. Then, the trypsinization was terminated with DMEM containing 10% FBS. Then, the cells were centrifuged at 800 ×g for 5 min, and the supernatant was removed. The cells were resuspended in DMEM and 5 mM dimedone (Sigma Aldrich, Canada) for 2 hours. In every 20-30 minutes, cells were suspended by pipetting up and down gently. After the incubation, the cells were centrifuged at 800 ×g for 5 min. The supernatant was removed, and cells were washed with PBS once. They were centrifuged again at 500 ×g for 5 min and lysed with 75 µl of lysis buffer (containing 2 mM

dimedone, 0.1% Triton-X, 12 mM sodium phosphate dibasic, 0.01% SDS, 10 mM N-ethylmaleimide (NEM), 10 mM EDTA, 3mM citric acid, 10 mM iodoacetamide (IAM) and 200 units/ml catalase. Dimedone, NEM and IAM were added just before the experiment.). The cells were incubated on ice for an hour and vortexed occasionally. Then, cells were centrifuged at 13,500 ×g for 15 min at 4 ºC. 15 µg of protein was mixed with 2× SDS-gel loading buffer and loaded in 12% SDS/PAGE gel and analyzed by immunoblotting assay using rabbit polyclonal anti-cysteine sulfenic acid antibody.

2.7 Biotin hydrazide conjugation method for detection of protein carbonylation:

Protein carbonylation was measured by biotin hydrazide conjugation method [163]. Protein carbonylation is a marker for protein oxidation. The protein carbonyl group reacts with biotin hydrazide to form a stable biotin-tagged derivative. The biotin-tagged carbonyl derivative can be analyzed using an immunoblotting assay using HRP-streptavidin. The cells were lysed using 20 mM N-Morpholino-ethane sulfonate (MES) buffer at pH 5.5. The cells were incubated in ice for 1 hour and centrifuged at 13,500 ×g for 15 min at 4 ºC. To 50 µl of the sample, 10% additional volume of 50 mM biotin hydrazide was added. The solution was incubated at 37ºC for 2 hrs with gentle agitation periodically. Then, the sample was mixed with an equal volume of 2 ×SDS loading buffer, heated for 5 min at 95ºC and loaded in 12% SDS/PAGE gel. Samples were transferred to a PVDF membrane as described above. The membrane was blocked at room temperature using 4% bovine serum albumin (BSA) in TBST. The membrane was incubated with HRP-streptavidin for 1 hour at room temperature followed by washed 3 times with TBST for 10 min each. Blots were developed using Enhanced Chemiluminescence reagent, and bands were analyzed using the ChemiDoc MP system (Biorad).

2.8 Co-immunoprecipitation:

Co-immunoprecipitation was used to study the interaction between Txnip and NLRP3. 80 µg of cell lysate was precleared first by mixing with 10 µl of protein A/G beads. The mixture was incubated at 4 ºC for an hour with rotation. The mixture was spin-down, and the supernatant was transferred to another tube. The protein in the supernatant was incubated with mouse monoclonal anti-NLRP3 overnight at 4 ºC with rotation. Then, 10 µl of protein A/G beads were added on and incubated for 4 hrs at 4 ºC with rotation. The mixture was spin-down, and the supernatant was removed. The bead was washed 3 times with cold lysis buffer. 15 µl of 2×SDS buffer was added to the sample. The sample was loaded into 12% SDS-PAGE gel and transferred to PVDF membrane as described above. The membrane was incubated with primary Txnip antibody overnight at 4ºC followed by incubation with HRP-conjugated secondary antibody for 1 hr at room temperature. The chemiluminescence was used to detect immunoreactive bands and imaged using ChemiDoc. The membrane was reprobed again with NLRP3 antibody as a loading control.

2.9 Caspase-1 activity assay:

Caspase-1 activity was measured by using fluorogenic substrate Z-YVAD-AFC [164, 165]. The caspase-1 in the sample cleaves the substrate to release 7-amino-4-trifluoromethylcoumarin (AFC). The fluorescence from released AFC can be used to quantify caspase-1 activity. The cells were lysed using caspase-1 lysis buffer (50 mM HEPES pH 7.4, 1 mM EDTA, 0.1% CHAPS, 10 mM DTT), incubated on ice for 1 hour and centrifuged at 13,500 ×g to obtain the protein. 50 µg of protein (1 µg/µl) was added to each well in 96 well plates containing 50 µl of 2× Reaction buffer (200 mM HEPES pH 7.4, 20% sucrose, 100 mM NaCl, 10 mM DTT 0.2% CHAPS, 1 mM EDTA). Then 5µl of 1 mM Z-YVAD-AFC (Cayman Chemical, CA) was added to every well and incubated

at 37 ºC for 2 hours. The fluorescence intensity of released AFC was detected at Excitation/Emission of 400nm/505 nm.

2.10 Enzyme-Linked Immunosorbent assay (ELISA)

The medium from cultured cells was taken and concentrated to around 180 µl using Amicon Ultra Centrifugal Filter (Sigma Aldrich, Canada) with molecular weight cut off of 3 kDa. The ELISA (Thermo Scientific, Canada) was performed to determine the IL-1β level in concentrated medium. First, all of the wells were washed with 1× wash buffer 4 times. 50 µl of the medium was added, and then 50 µl of sample diluent was also added in each well. Then, 50 µl of Biotin-conjugate was added to all wells. Wells were covered properly with a film and incubated for 2 hours at room temperature on a microplate shaker. Then all of the wells were emptied and washed 4 times with 1× wash buffer. After washing, 100 µl of Streptavidin-HRP was added in all wells and incubated at room temperature for 1 hr on microplate shaker. The wells were washed 4 times with 1× wash buffer. Then, 100 µl of Substrate solution was added to each well. The plate was incubated in the dark for 10 min at room temperature on a microplate shaker. After incubation, 100 µl of Stop Solution was added to each well. The absorbance was detected at 450 nm.

2.11 Knocking out Txnip using CRISPR/Cas9

Txnip was knocked out using CRISPR/Cas9 as described previously [165]. CRISPR/Cas9 All-in-One lentivector (pLenti-U6-sgRNA-SFFV-Cas9-2A-Puro) used in our experiment contains Txnip single guide RNA (sgRNA) and CRISPR/Cas9 (ABM Inc Richmond, BC, Canada). CRISPR/Cas9 lentivector containing scrambled sgRNA was used as a control. Lentivector was packaged with lentivirus by the Canadian Neurophotonics Platform Viral Vector Core Facility in Quebec. Primary cultured mouse astrocytes are grown in collagen-coated 6-well plates till 50% confluency. Then, lentivirus was added to each well containing 1 ml DMEM medium with 10%

FBS and 1% penicillin/streptomycin and incubated overnight at 37 ºC. 1 ml fresh DMEM was added to each well and incubated for an additional 24 hours. Then, a medium containing viral particles was removed and cultured with DMEM containing 1 μg/ml puromycin for 6 days. The Txnip knockout primary mouse astrocyte was used for further experiments.

2.12 Statistical analysis

We performed statistical analysis using IBM SPSS (IBM, Armonk, New York, USA). Results are presented as mean ± standard error of the mean (SEM). To evaluate the significant differences in means, we used one-way analysis of variance (ANOVA) with Tukey post hoc tests. Student's t-test was employed for comparison between two groups. Statistical significance was defined when a p-value was below 0.05.

CHAPTER 3. RESULTS

3.1 To determine if CORT treatment upregulates Txnip and further causes protein oxidation in primary cultured mouse astrocytes.

3.1.1 Effect of CORT on Txnip and Trx protein levels in primary cultured mouse astrocytes

Glial fibrillary acidic protein (GFAP) is a marker for astrocytes, while ionized calcium-binding adaptor molecule 1 (Iba1) is a marker for microglia. The purity of astrocytes in primary cultured mouse cerebrocortical astrocytes was determined by using immunocytochemistry with GFAP antibody and Iba1 antibody. Nucleus was stained by Hoechst33342. 84% of the cells were found to be GFAP-positive, while 2% of the cells were found to be Iba1 positive. Our findings suggest that our cell culture was enriched with astrocytes (figure 7).

To study the effect of CORT on Trx and Txnip protein levels, primary astrocytes were treated with CORT at 0.01, 0.1, 1 and 10 μM for 24 hrs. Immunoblotting showed that Trx band was obtained approximately at 12 kDa while Txnip band was obtained approximately at 50 kDa. We found that CORT treatment did not have any significant effect on Trx protein levels ($N = 4$, $p>0.05$) (figure 8A). We also found that although CORT treatment at 0.01 μM had no effect on Txnip protein levels, CORT treatment at 0.1, 1 and 10 μM significantly increased Txnip protein levels by 93.98± 5.5%, 128.84± 2.7% and 102.76± 5.86% respectively when compared to the control (CTL) ($N=4$, $p<0.05$) (figure 8B). The highest increase in Txnip level was obtained at 1 μM CORT treatment. 1 μM of CORT treatment was decided to be used for the following experiments.

To study if CORT treatment has a time-dependent effect on Txnip protein levels, cultured astrocytes were treated with CORT at 1μM for 1, 4, 8 and 24 hours. We found that CORT treatment for 1 and 4 hours significantly decreased Txnip protein levels, but CORT treatment for 8 and 24

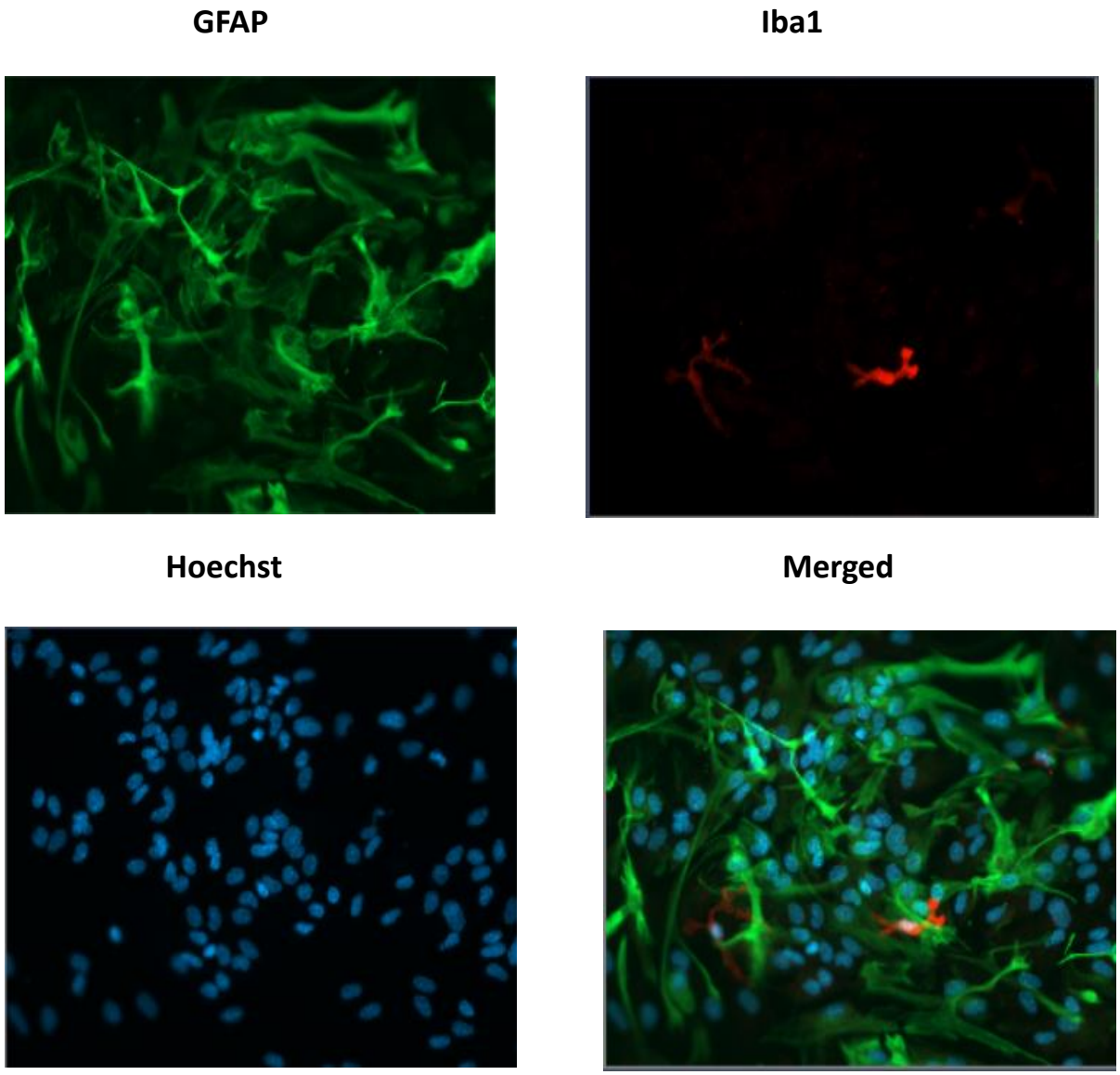

Figure 7. Primary mouse astrocytes were stained by GFAP, Iba1, and Hoechst33342. The images were used to count cells using the Cell Counter plugin in ImageJ. About 84% of cells were GFAP-positive cells and 2% of cells were Iba1-positive.

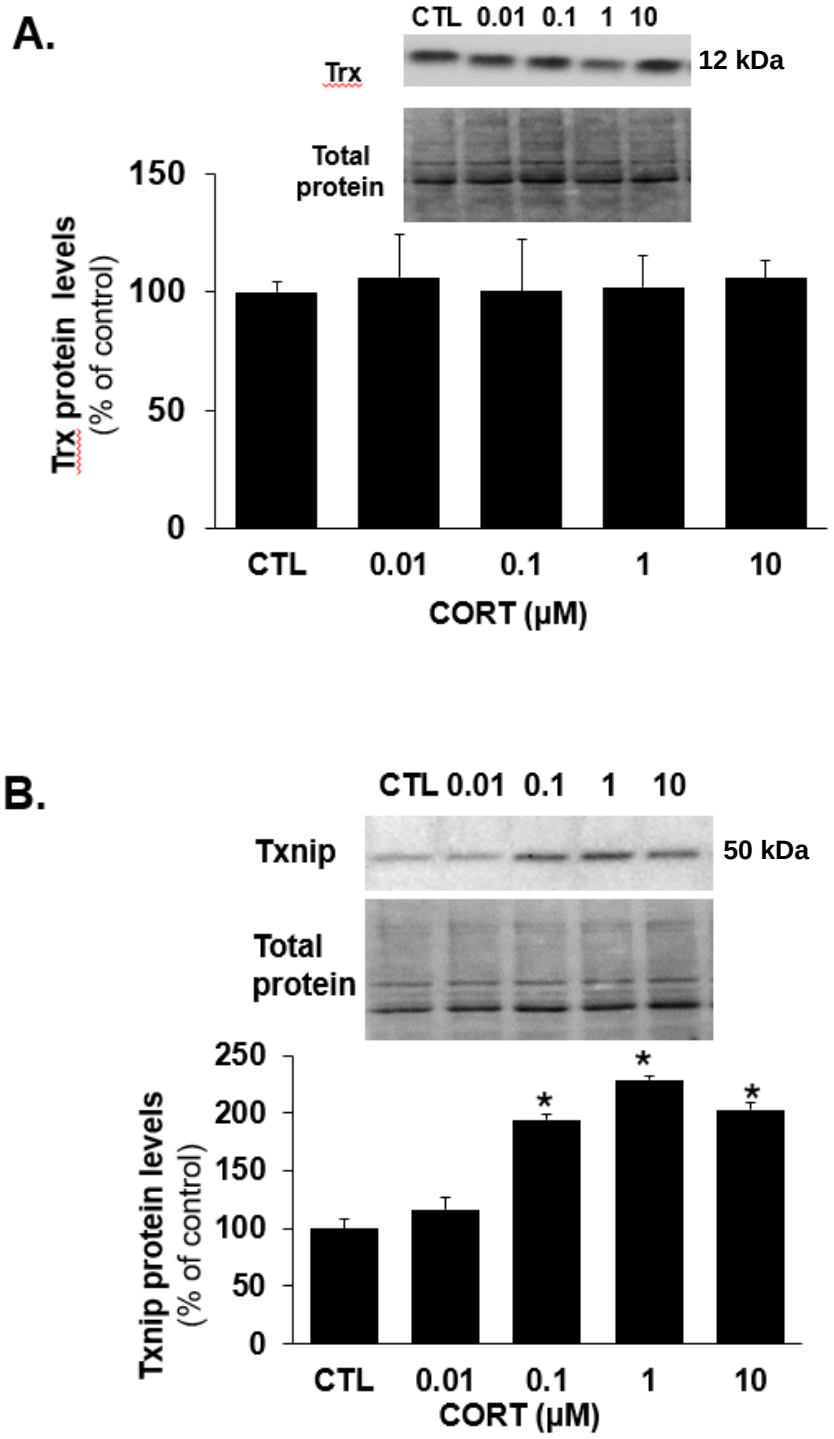

Figure 8. Effect of CORT on Trx (A) and Txnip (B) protein levels: Astrocytes were treated with corticosterone (CORT) at 0.01-10 μM for 24 hours. Protein levels of Trx and Txnip were measured using western blot. Stain free blot was used as loading control. Data are displayed as mean ± SEM (N = 4). * indicates $p<0.05$ when compared to controls (CTL) determined by one-way ANOVA followed by Tukey's post-hoc analysis.

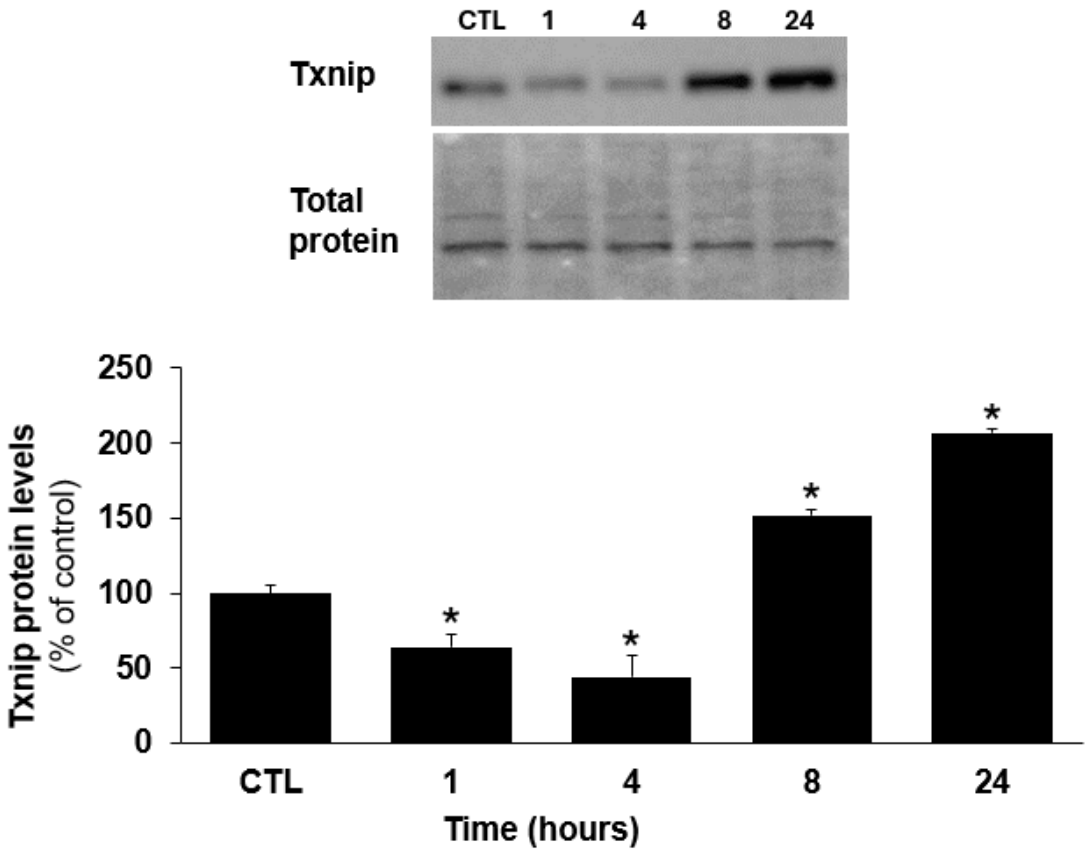

Figure 9. Effect of CORT on Txnip level at different time course: Astrocytes were treated with corticosterone (CORT) at 1 μM for 1, 4, 8 and 24 hrs. Protein levels of Txnip were measured using western blot. Stain free blot was used as loading control. Data are displayed as mean ± SEM (N = 4). * indicates $p<0.05$ when compared to controls (CTL) determined by one-way ANOVA followed by Tukey's post-hoc analysis.

hours significantly increased Txnip protein levels when compared to the CTL (N=4, $p<0.05$) (figure 9). This result suggests that only longer period of treatment, but not a shorter period of treatment can upregulate Txnip.

To determine if GR and MR mediate CORT-increased Txnip protein levels, cultured astrocytes were treated with GR antagonist RU486 at 1μM or MR antagonist spironolactone at 1 μM along with CORT treatment for 24 hrs. We found that treatment with RU486 had no effect on Txnip levels while treatment with spironolactone significantly decreased Txnip levels (N = 4, $p<0.05$). We further found that treatment with CORT alone significantly increased the Txnip protein levels (N = 4, $p<0.05$) as compared with CTL, but treatment with RU486 or spironolactone significantly reduced CORT-increased Txnip protein levels (N = 4, $p<0.05$) (figure 10). This result suggests that both GR antagonist and MR antagonist can inhibit CORT-upregulated Txnip.

3.1.2 Effect of CORT on Trx activity

Txnip can bind to Trx protein and inhibits Trx activity. Since CORT treatment upregulates Txnip, we determined the effect of CORT on Trx activity in primary cultured mouse astrocytes. PX12 is a Trx pharmacological inhibitor and was utilized as a positive control. Cultured astrocytes were treated with vehicle, 1 μM CORT or 15 μM PX12 for 24 hrs. We found that treatment with PX12 significantly decreased Trx activity by 18.24 ± 1.82% (N=5, $p<0.05$) and treatment with CORT significantly decreased Trx activity by 8.86 ± 1.86% (N=5, $p<0.05$) as compared to control (figure 11). This result suggests that CORT treatment modestly inhibit Trx activity in primary cultured mouse astrocytes.

3.1.3 Effect of CORT on reduced thiol levels

Trx can reduce thiol oxidation. So, we studied the effect of CORT treatment on total reduced thiol levels in primary cultured mouse astrocytes. H_2O_2 is an oxidizing agent and can

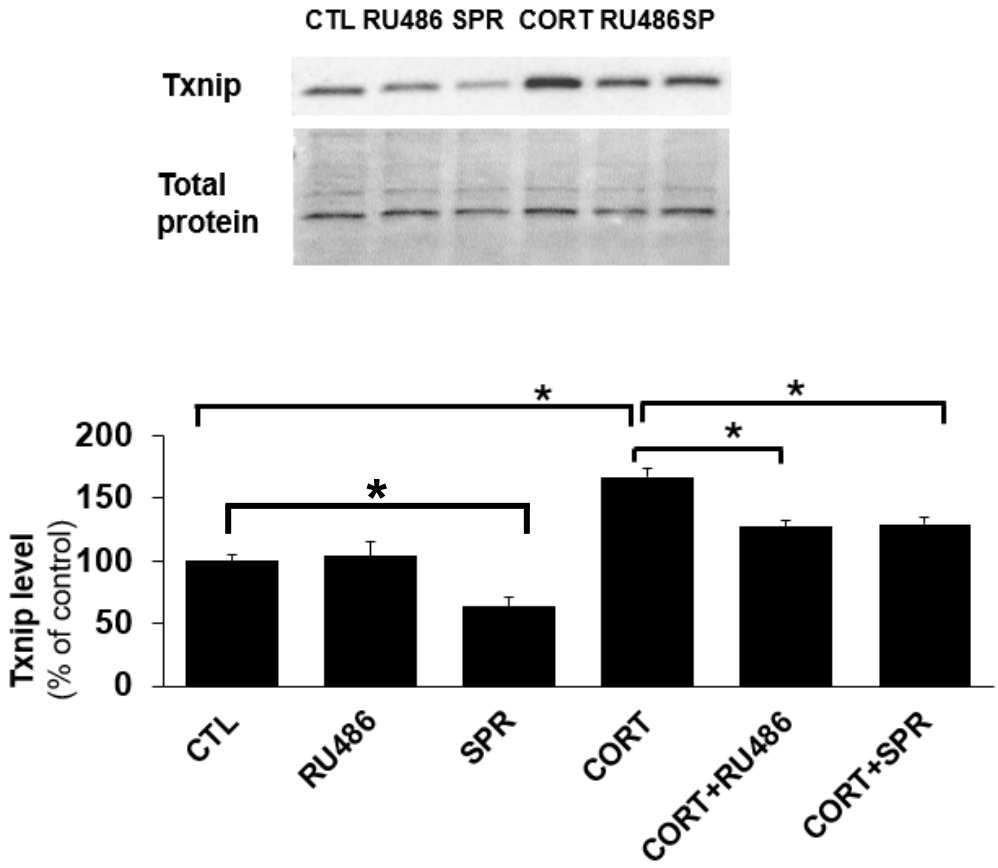

Figure 10. Effect of GR and MR antagonist on CORT-increased Txnip protein levels: Astrocytes were treated with corticosterone (CORT), MR antagonist Spironolactone (SPR), and GR antagonist RU486 for 24 hours. Protein levels of Txnip were measured using a western blot. Stain-free blot was used as a loading control. Data are displayed as mean ± SEM (N = 4). * indicates $p<0.05$ when compared to controls (CTL) determined by one-way ANOVA followed by Tukey's post-hoc analysis.

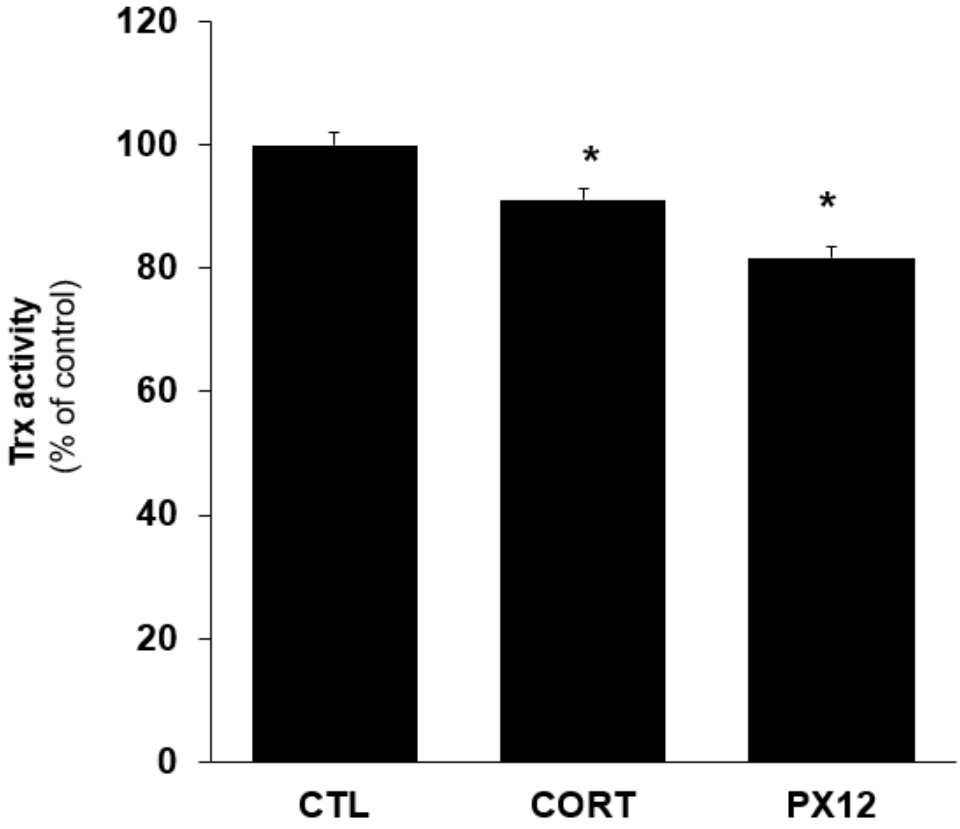

Figure 11. Effect of CORT on Trx activity: Astrocytes were treated with corticosterone (CORT) at 1µM, and PX12 at 15µM for 24 hours. The Trx activity was measured using a Cayman Trx activity kit. Data are displayed as mean ± SEM (N = 5). * indicates $p<0.05$ when compared to controls (CTL) determined by one-way ANOVA followed by Tukey's post-hoc analysis.

induce thiol oxidation, resulting in decrease of total reduced thiol levels. H_2O_2 was utilized as a positive control. Initially, to determine the H_2O_2 concentration that would decrease the level of reduced thiol levels, we treated C6 glioma with 1, 2 and 4 mM H_2O_2 for 1.5 hours. We found that H_2O_2 treatment significantly decreased total reduced thiol levels in C6 glioma as compared to CTL ($N=4$, $p<0.05$) (figure 12A). Next, we treated primary cultured astrocytes with 1 μM CORT for 24 hrs and with 2 mM H_2O_2 for 1.5 hrs. We found that H_2O_2 treatment significantly decreased total reduced thiol level as compared to CTL ($N=4$, $p<0.05$), CORT treatment didn't have any effect on total reduced thiol levels ($N=4$) (figure 12B).

3.1.4 Effect of CORT on protein sulfenylation and carbonylation

Inhibition of Trx activity may promote protein sulfenylation. Next, we determined whether CORT treatment induces protein-sulfenylation. H_2O_2 can oxidize protein cysteine thiols and form sulfenylated proteins. H_2O_2 was utilized as a positive control. First, C6 glioma was treated with H_2O_2 to determine the concentration that would cause sulfenylation. C6 glioma cells were treated with H_2O_2 at the concentration of 0.5, 1 and 2 mM for 2 hours. Although 0.5 mM H_2O_2 treatment didn't increase sulfenylated protein levels, 1 mM and 2 mM H_2O_2 treatment significantly increased sulfenylated protein levels as compared to CTL ($N = 4$, $p<0.05$) (figure 13A). Then, we treated primary cultured mouse astrocytes with 1 μM CORT for 24 hrs or 2 mM H_2O_2 for 2 hrs. We found that H_2O_2 treatment significantly increased sulfenylated protein levels ($N=4$, $p< 0.05$), but CORT treatment didn't have any significant effect on sulfenylated protein levels ($N=4$, $p> 0.05$) (figure 13B). This result suggests that CORT treatment cannot cause protein cysteine sulfenylation in primary cultured mouse astrocytes.

Inhibition of Trx activity may also promote protein carbonylation. Next, we determined whether CORT treatment induces protein carbonylation. H_2O_2 was utilized as a positive control.

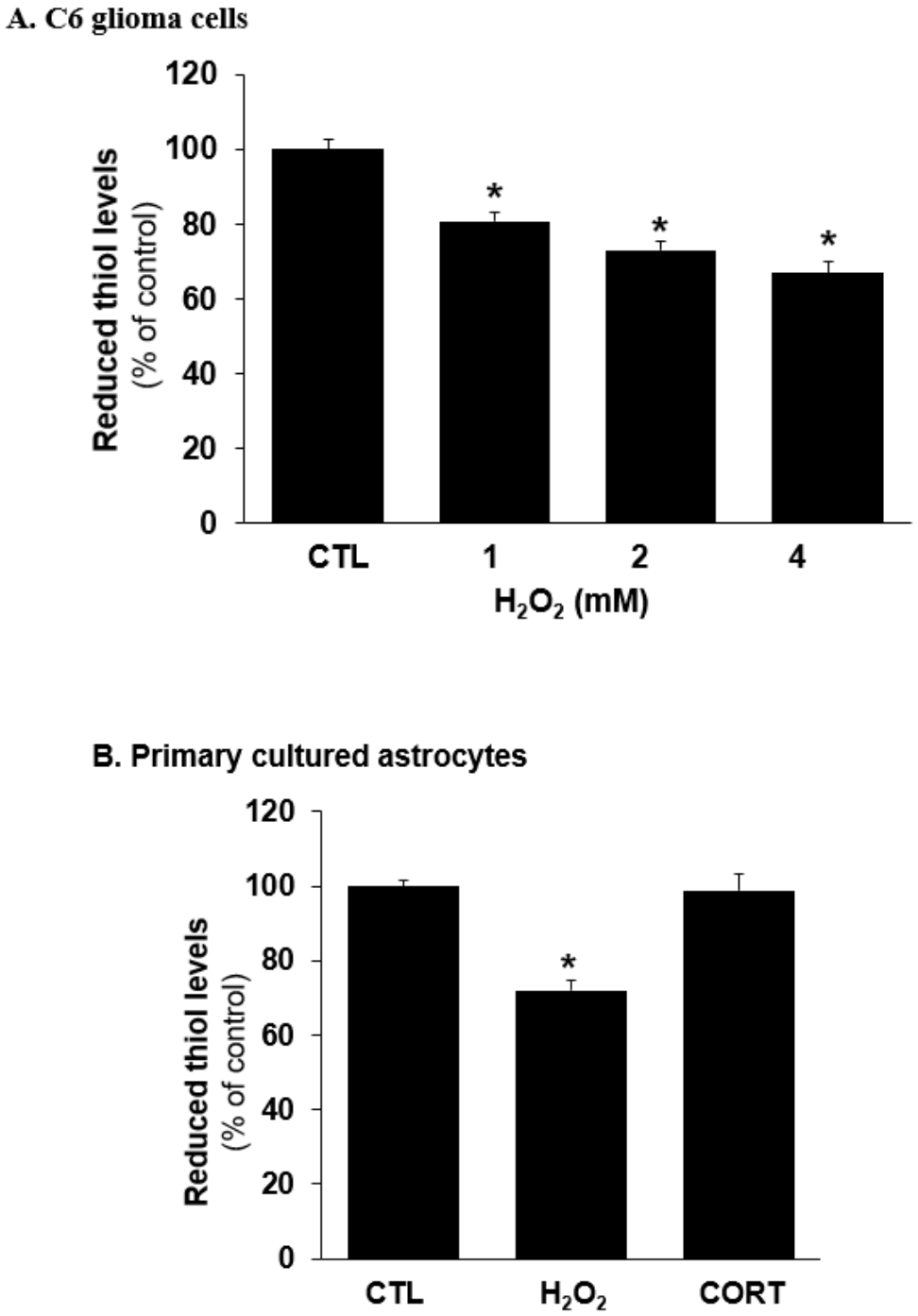

Figure 12. Effect of H_2O_2 and CORT on reduced thiol levels: (A) C6 glioma cells were treated with H_2O_2 at 1 mM, 2 mM, and 4 mM for 1.5 hours. Reduced thiol level was determined by using Ellman's assay. (B) Primary astrocytes were treated with 2 mM H_2O_2 for 1.5 hours as positive control and 1 uM CORT for 24 hours. Data are displayed as mean ± SEM (N = 4). * indicates $p<0.05$ when compared to controls (CTL) determined by one-way ANOVA followed by Tukey's post-hoc analysis.

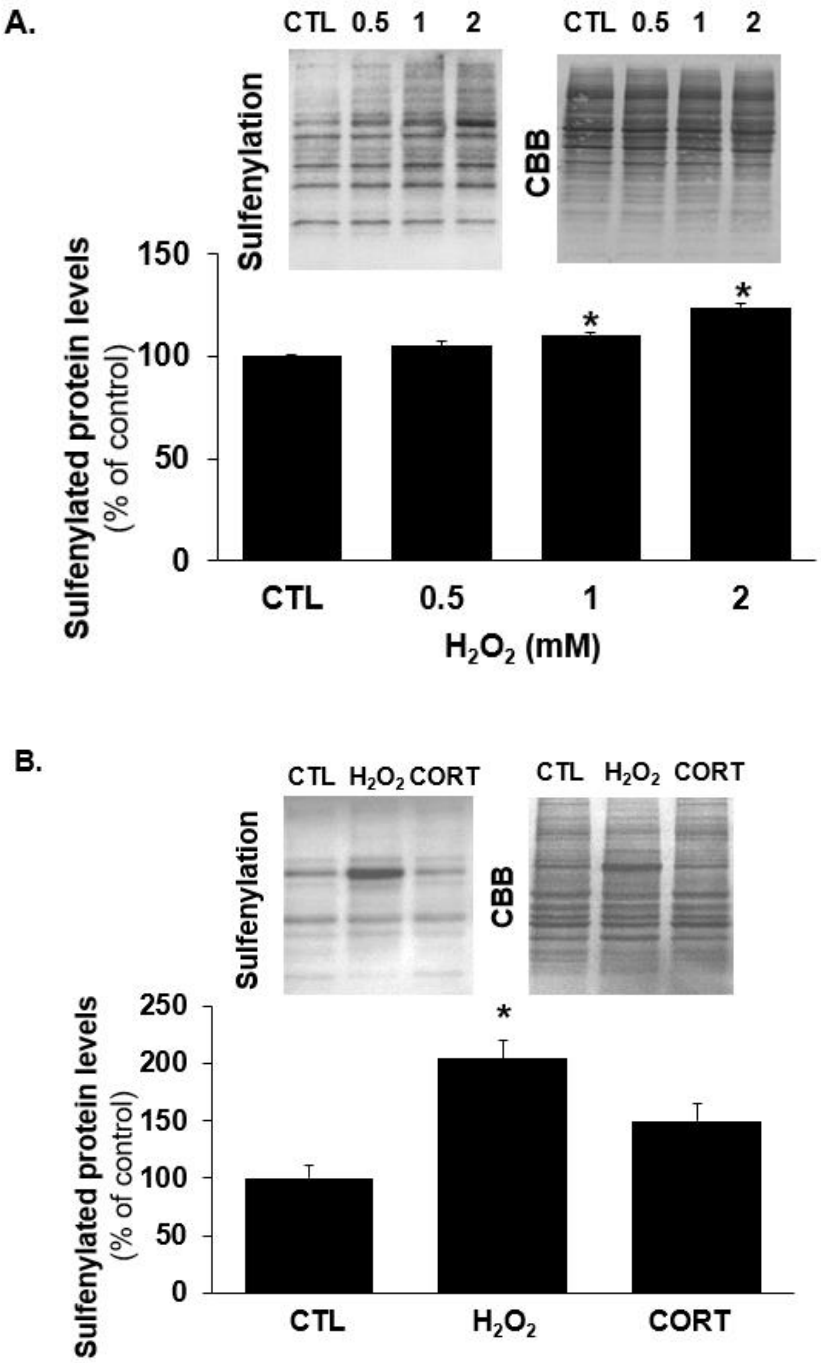

Figure 13. Effect of H_2O_2 and CORT on sulfenylated protein levels: (A) C6 glioma cells were treated with H_2O_2 at 0.5, 1 and 2 mM for 2 hours (B) Primary mice astrocytes were treated with H_2O_2 at 2 mM for 2 hours or CORT at 1 μM for 24 hours. Sulfenylated protein levels were measured using dimedone conjugation followed by western blot. Coomassie brilliant blue (CBB) was used as a loading control. Data are displayed as mean ± SEM (N = 4). * indicates $p<0.05$ when compared to controls (CTL) determined by one-way ANOVA followed by Tukey's post-hoc analysis.

First, C6 glioma was treated with H_2O_2 to determine the concentration that would cause protein carbonylation. C6 glioma cells were treated with H_2O_2 at of 0.5, 1 and 2 mM for 2 hrs. We found that H_2O_2 treatment at 0.5 and 1 mM didn't have any significant effect on carbonylated protein level but H_2O_2 treatment at 2 mM significantly increased carbonylated protein levels as compared to CTL ($N = 4$, $p<0.05$) (figure 14A). Next, we treated primary cultured astrocytes with CORT at 1 μM for 24 hrs or H_2O_2 at 2 mM for 2 hours. We found that H_2O_2 treatment significantly increased carbonylated protein levels as compared to CTL ($N = 4$, $p<0.05$), but CORT treatment didn't have any significant effect on carbonylated protein levels ($N = 4$, $p>0.05$) (figure 14B). This result suggests that CORT treatment cannot cause protein carbonylation in primary cultured mouse astrocytes.

3.2 To determine if CORT treatment activates NLRP3 inflammatory signaling and if Txnip mediate CORT-induced activation in primary cultured mouse astrocytes.

3.2.1 Effect of CORT on NLRP3 protein levels and Txnip/NLRP3 binding activity

Txnip can interact with NLRP3 protein and promote the formation of NLRP3 inflammasome. Next, we studied whether the CORT treatment have any effect on NLRP3 protein levels and Txnip/NLRP3 binding activity. LPS is a major endotoxin that can activate innate immune system and can prime NLRP3 inflammasome by increasing the expression of NLRP3 protein. ATP can directly activate NLRP3 inflammasome. LPS and ATP were used as positive control. First, primary cultured mouse astrocytes were treated with 1 μM CORT for 24 hrs or 500 ng/ml of LPS for 4 hrs followed by 5 mM of ATP for half hour. We found that LPS+ATP significantly increased NLRP3 protein levels ($N = 3$, $p<0.05$), but CORT treatment didn't show any significant effect on NLRP3 protein levels as compared to CTL ($N = 3$, $p>0.05$) (figure 15). Second, we determined if CORT treatment increased the interaction between Txnip and NLRP3.

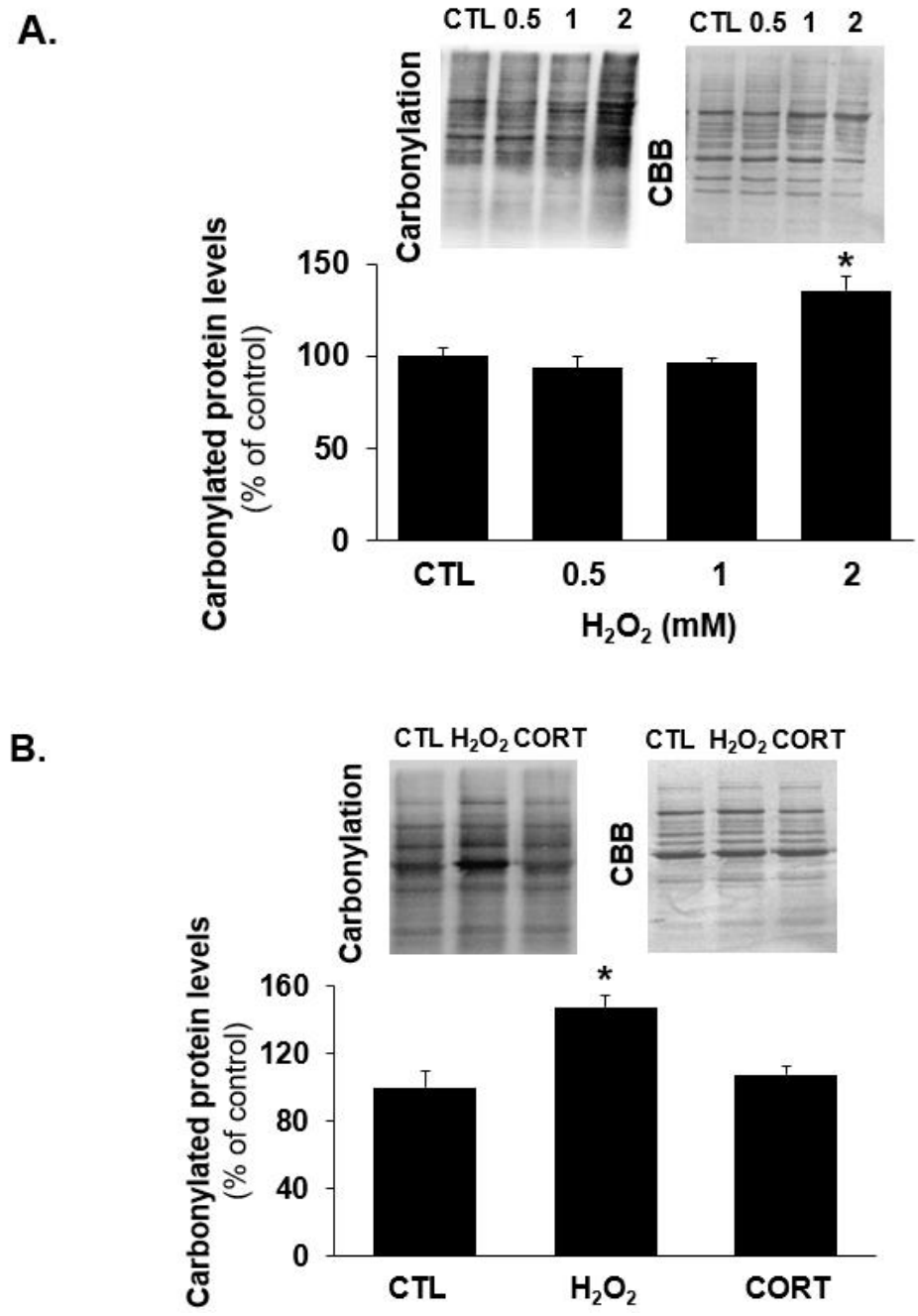

Figure 14. Effect of H_2O_2 and CORT on carbonylated protein levels: (A) C6 glioma cells were treated with H_2O_2 at 0.5, 1 and 2 mM for 2 hours. followed by western blot. (B) Primary mice astrocytes were treated with H_2O_2 at 2 mM for 2 hours or CORT at 1 μM for 24 hours. Carbonylated protein levels were measured using biotin-hydrazide conjugation. Coomassie brilliant blue (CBB) was used as a loading control. Data are displayed as mean ± SEM (N = 4). * indicates $p<0.05$ when compared to controls (CTL) determined by one-way ANOVA followed by Tukey's post-hoc analysis.

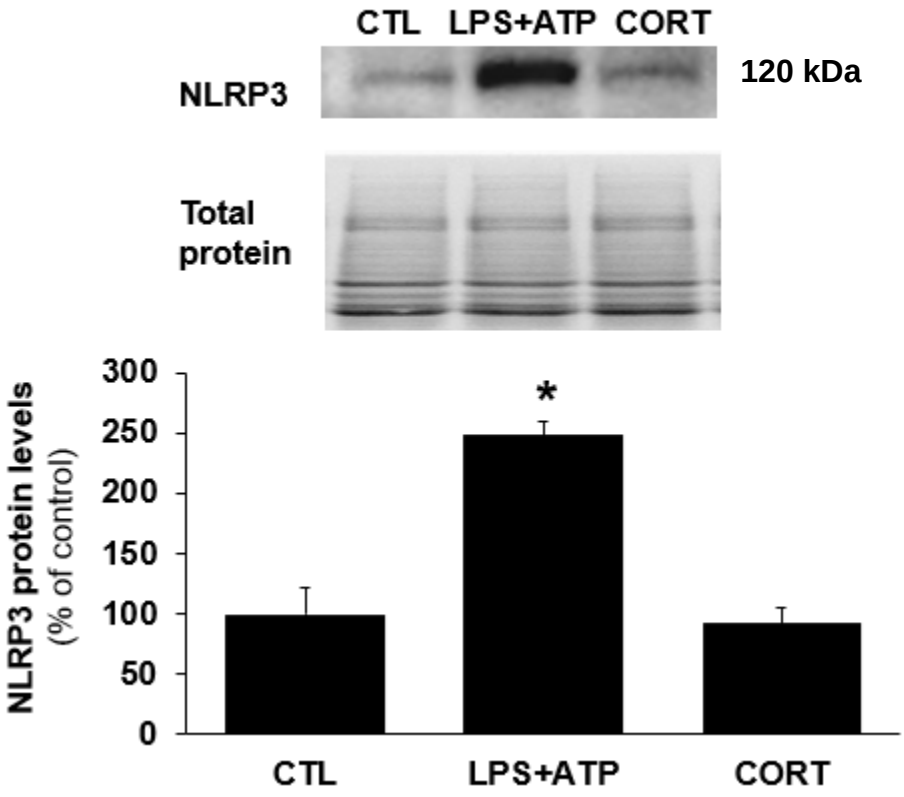

Figure 15. Effect of CORT on NLRP3 protein levels in primary astrocytes: Astrocytes were treated with corticosterone (CORT) at 1 μM for 24 hours or 500 ng/ml LPS for 4 hours followed by 5 mM ATP for 30 min. Protein levels of NLRP3 were measured by western blot. The stain-free blot was used as a loading control. Data are displayed as mean ± SEM (N = 3). * indicates $p<0.05$ when compared to controls (CTL) determined by one-way ANOVA followed by Tukey's post-hoc analysis.

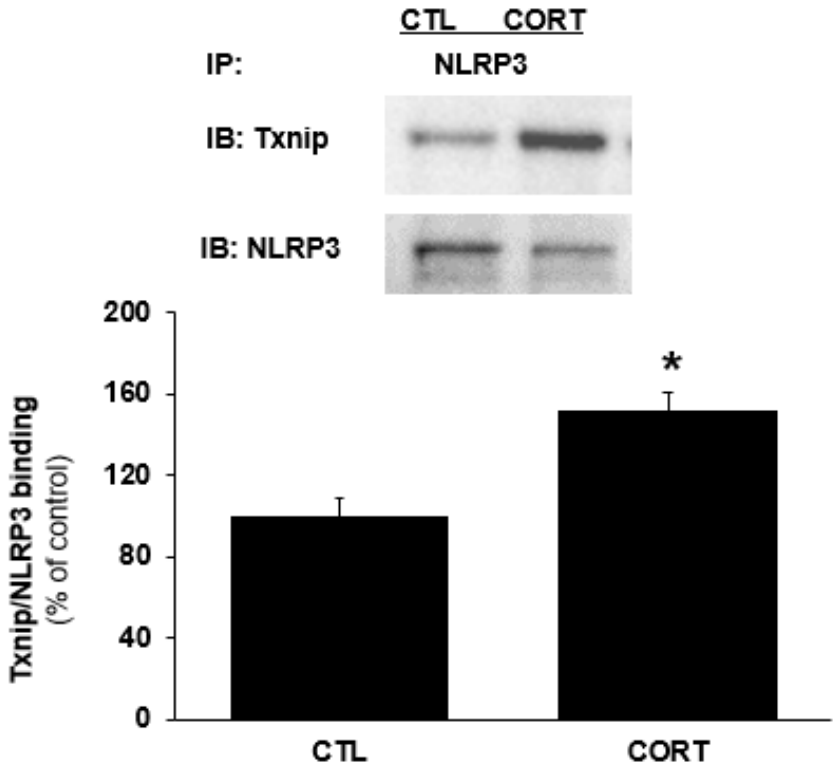

Figure 16. Effect of CORT on Txnip/NLRP3 binding activity in primary astrocytes: Astrocytes were treated with corticosterone (CORT) at 1 μM for 24 hours. Cell lysate was immunoprecipitated (IP) by NLRP3 antibody overnight. Protein levels of Txnip and NLRP3 in immunoprecipitated proteins were measured using immunoblotting (IB) analysis. The ratio of Txnip band intensity/NLRP3 band intensity was used to determine Txnip/NLRP3 binding activity. Data are displayed as mean ± SEM (N = 4). * indicates $p<0.05$ when compared to controls (CTL) determined by t-test.

We treated primary cultured astrocytes with CORT at 1 μM for 24 hrs. As shown in Figure 16, the protein sample was immunoprecipitated using a mouse monoclonal NLRP3 antibody. Then, it was analyzed with Txnip antibody by immunoblotting analysis, and then the same blot was re-probed with NLRP3 antibody for measuring loading control. The ratio of Txnip band intensity/NLRP3 band intensity was used to determine Txnip/NLRP3 binding activity. We found that CORT treatment significantly increased Txnip/NLRP3 binding activity as compared to the CTL ($N = 4$, $p<0.05$).

3.2.2 Effect of CORT on caspase-1 activity

The NLRP3 inflammasome can promote cleavage of pro-caspase-1 to active caspase-1. Next, we determined if CORT treatment increased caspase-1 activity. Treatment with LPS and ATP was used as a positive control. Primary cultured mouse astrocytes were treated with 500 ng/ml LPS for 4 hrs and then followed by treatment with 5 mM ATP for a half-hour or treated with 1 μM CORT for 24 hrs. The protein extract was incubated with Z-YVAD-AFC for 2 hrs at 37 ºC and fluorescence intensity was measured. As expected, LPS/ATP treatment significantly increased caspase-1 activity by 57.91 ± 3.02% as compared to CTL ($N = 4$, $p<0.05$). We also found that CORT treatment significantly increased caspase-1 activity by 34.27 ± 2.5 % as compared to the CTL ($N = 4$, $p<0.05$) (figure 17).

3.2.3 Effect of CORT on IL-1β release

Active caspase-1 can convert inactive pro-IL-1β to active IL-1β which is then released by the cells. Next, we determined whether CORT treatment increases IL-1β release. We treated primary cultured mouse astrocytes with 1 μM CORT for 24 hrs. LPS/ATP was used as a positive control. After the treatment, medium was collected and concentrated using Amicon ultracentrifuge filter with molecular weight cut off of 3 kDa. Then, ELISA was performed to determine IL-1β

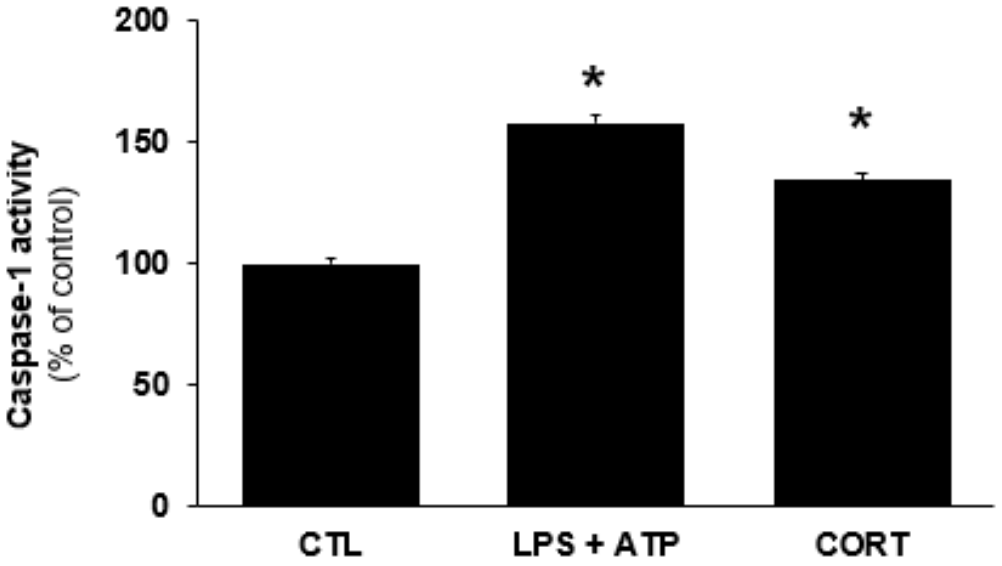

Figure 17. Effect of CORT and LPS+ATP on caspase-1 activity: Astrocytes were treated with corticosterone (CORT) at 1 μM for 24 hours or 500 ng/ml LPS for 4 hours followed by 5 mM ATP for 30 min. Caspase-1 activity was measured using Z-YVAD-AFC. Data are displayed as mean ± SEM (N = 4). * indicates $p<0.05$ when compared to controls (CTL) determined by one-way ANOVA followed by Tukey's post-hoc analysis.

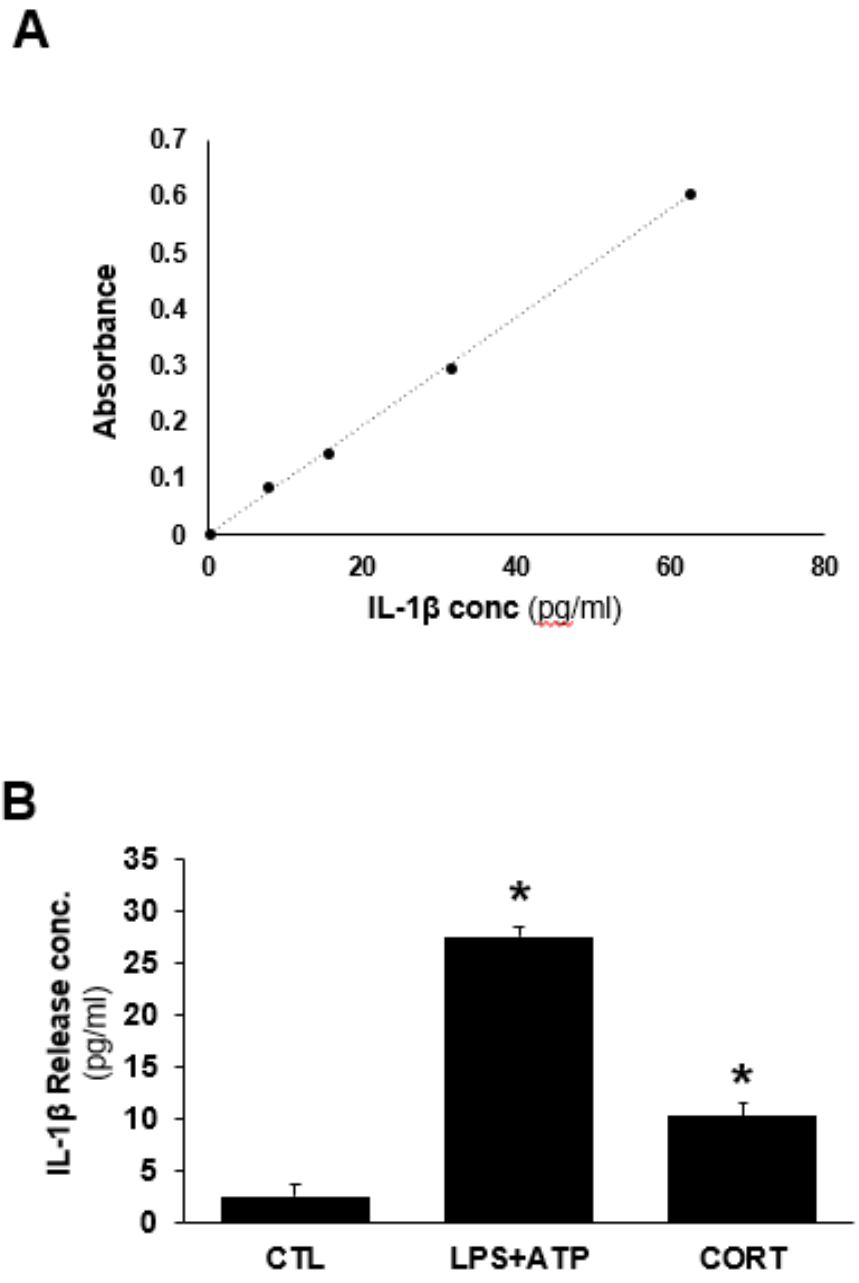

Figure 18. Effect of CORT and LPS+ATP on IL-1β release: A. Standard curve for IL-1β B. Astrocytes were treated with corticosterone (CORT) at 1 μM for 24 hours or 500 ng/ml LPS for 4 hours followed by 5 mM ATP for 30 min. Released IL-1β was determined by using ELISA. Data are displayed as mean ± SEM (N = 4). * indicates $p<0.05$ when compared to controls (CTL) determined by one-way ANOVA followed by Tukey's post-hoc analysis.

release from astrocytes. Figure 18A is a standard curve for IL-1β, showing that IL-1β concentration is positively proportional to absorbance OD value. As shown in figure 18B, LPS/ATP treatment released 27.59 ± 1.02 pg/ml of IL-1β from astrocytes, CORT treatment released 10.32 ± 1.3 pg/ml of IL-1β from astrocytes, and vehicle treatment released only 2.6 ± 1.07 pg/ml of IL-1β (N = 4). Statistical analysis indicated that both LPS/ATP treatment and CORT treatment significantly increased IL-1β release (N=4, $p < 0.05$).

3.2.4 Effect of Txnip knockout on CORT-induced caspase-1 activation and IL-1β release:

To evaluate whether Txnip contributes to CORT-induced caspase-1 activation and IL-1β release, Txnip was knocked out in primary astrocytes using CRISPR/Cas9, and then we measured the effect of CORT on caspase-1 activity and IL-1β release in primary cultured mouse astrocytes. Lentivirus containing CRISPR/Cas9/Txnip sgRNA and CRISPR/Cas9/scrambled sgRNA vectors were transduced to cultured astrocytes. As shown in Figure 19, scrambled sgRNA transduced astrocytes didn't have any significant change in Txnip protein levels as compared to wild-type astrocytes (N=4, $p<0.05$). Txnip sgRNAs transduced astrocytes had significantly lower Txnip protein levels than scrambled sgRNAs transduced astrocytes ($p<0.05$, N=4). After cultured astrocytes were treated with CORT at 1 μM CORT for 24 hrs, we found that CORT treatment significantly increased caspase-1 activity in scrambled sgRNAs transduced astrocytes (N=3, $p<0.05$), but had no effect on caspase-1 activity in Txnip sgRNAs transduced astrocytes (N=3, $p>0.05$) (figure 20A). Although CORT treatment significantly increased IL-1β release in scrambled sgRNAs transduced astrocytes (N=3, $p<0.05$), CORT-treatment had no effect on IL-1β release in Txnip sgRNAs transduced astrocytes (N=3, $p>0.05$) (figure 20B). This result suggests that knocking out Txnip gene can inhibit CORT-treatment-increased caspase 1 activity and IL-1β release in primary cultured mouse astrocytes.

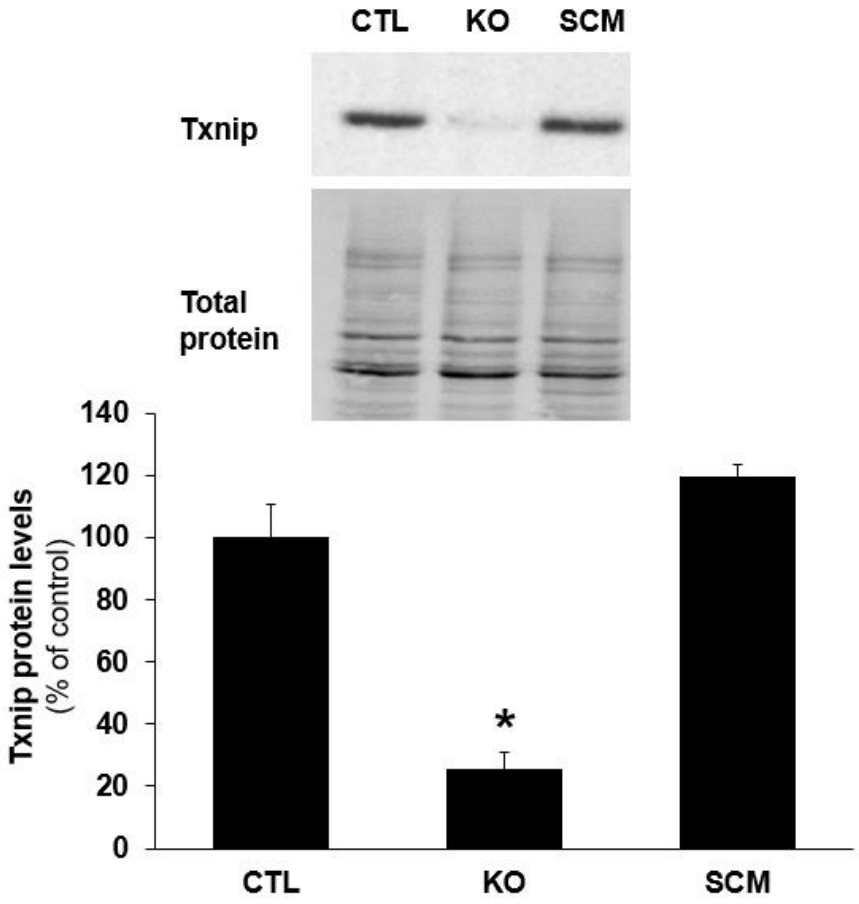

Figure 19 Knocking out Txnip gene expression by CRISPR/Cas9/Txnip sgRNA: Lentivirus containing CRISPR/Cas9/Txnip sgRNA (KO) and CRISPR/Cas9/scrambled sgRNA (SCM) vectors were transduced to cultured astrocytes. Protein levels of Txnip was measured using western blot. Stain free blot was used as loading control. Data are displayed as mean ± SEM (N = 4). * indicates $p<0.05$ when compared to controls (CTL) determined by one-way ANOVA followed by Tukey's post-hoc analysis

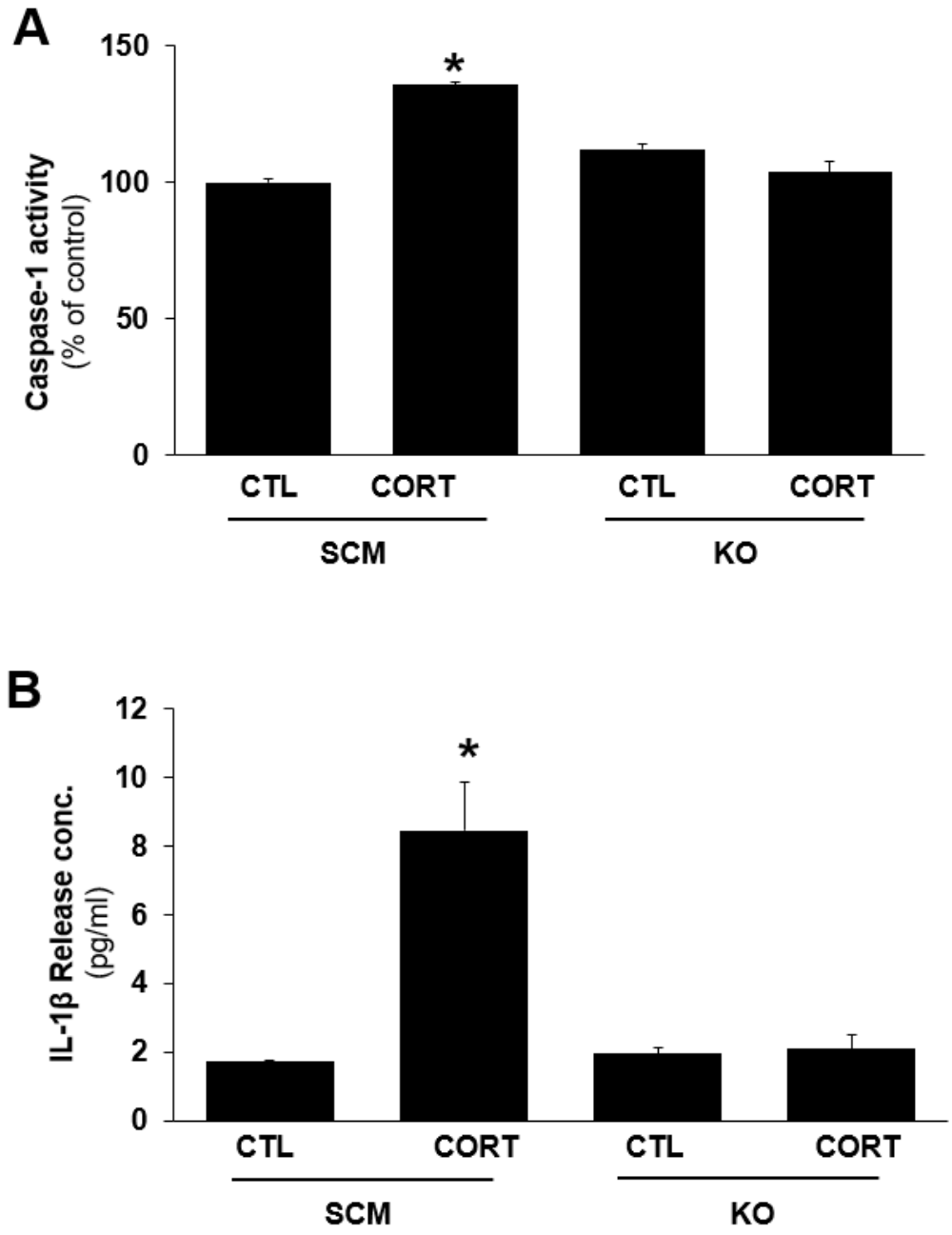

Figure 20. Effect of CRISPR/cas9 knockout on CORT-induced caspase-1 activation and IL-1β release. Lentivirus containing CRISPR/Cas9/Txnip sgRNA (KO) and CRISPR/Cas9/scrambled sgRNA (SCM) vectors were transduced to cultured astrocytes. Astrocytes were treated with vehicle (CTL) or 1 μM CORT for 24 hrs. A) Caspase-1 activity was measured using Z-YVAD-AFC substrate B) Released IL-1β was measured using ELISA. Data are displayed as mean ± SEM (N = 3). * indicates $p<0.05$ when compared to controls (CTL) determined by one-way ANOVA followed by Tukey's post-hoc analysis.

CHAPTER 4. DISCUSSION

4.1 CORT treatment upregulates Txnip in astrocytes

Astrocytes contribute a significant role to the regulation of neuroinflammation. Once astrocytes are activated, astrocytes release pro-inflammatory cytokines and increase ROS production, which facilitates neuroinflammation and causes neuronal damage. In this present study, although treatment with corticosterone (CORT) for 24 hours had no effect on Trx protein levels, this treatment increased Txnip protein levels in primary cultured mouse astrocytes. We also found that Txnip protein levels were increased by treatment with CORT for 24 hours, but not for 1 and 4 hours, suggesting that longer time treatment is required for CORT to upregulate Txnip. Previously, our laboratory found that CORT treatment increased Txnip protein levels in primary cultured mouse cerebrocortical neurons and primary cultured mouse microglia [160, 165]. **Our results together suggest that Txnip protein levels can be increased by CORT treatment not only in neurons and microglia, but also in astrocytes.** Our laboratory has also found that CUS for 28 days in mice not only induced depressive-like behaviours, but also increased Txnip protein levels in the frontal cortex and hippocampus [62]. Since chronic unpredictable stress can increase serum CORT levels in mice, our findings also suggest that chronic stress may increase CORT levels, upregulating Txnip and causing depressive-like behaviours.

CORT can bind to both MR and GR. When CORT binds to either MR or GR, CORT/receptor complexes translocate to the nucleus. Then MR and GR can form homodimer or heterodimer and bind to glucocorticoid response elements (GRE) in the promoter region of target genes and increase transcription of these genes [166]. In our study, CORT-increased Txnip protein levels were reversed by both GR antagonist RU486 and MR antagonist spironolactone in cultured mouse astrocytes. This result suggests that CORT treatment can activate both MR and GR, causing

MR and GR homodimer or heterodimer and further regulating Txnip expression.

It is interesting that Txnip gene contains a putative GRE site from -940 to -764 in its promoter region. When WEHI7.2 murine T-cells were transfected by pGL3B vector containing a luciferase report under control of Txnip promoter region from -1081 to the transcription start site, it has been found that treatment with 1μM dexamethasone increased luciferase activity by 6-fold. Deletion and mutation of this putative GRE sequence was found to suppress dexamethasone-increased luciferase activity [167]. Furthermore, it was also found in WEHI7.2 murine T-cells using Northern blotting analysis that treatment with dexamethasone for 24 hours increased Txnip mRNA levels, and GR antagonist RU486 can reverse dexamethasone-increased Txnip mRNA levels [167]. It has also been found in mouse erythroid progenitor cells that treated with dexamethasone increased Txnip mRNA levels, while GR mutation in the dimerization domain reduced dexamethasone-increased Txnip mRNA levels [168]. This evidence suggest that the Txnip promoter region contains a functional GRE site and that ligand-activated GR can translocate into the nucleus, bind to the GRE in the Txnip promoter region, and induce Txnip gene expression.

CORT may also regulate Txnip expression through antioxidant response element (ARE). Txnip promoter region contains a putative ARE from -1286 to -1276. It has been found that deletion of ARE sequence increased Txnip promoter-luciferase reporter activity [169]. Nuclear factor erythroid 2-related factor (Nrf2) is a transcription factor that interacts with ARE. ChIP analysis revealed that Nrf2 can interact with ARE site in Txnip promoter region. Overexpression of Nrf2 in H9C2 cells was found to decrease Txnip mRNA levels, while knocking down Nrf2 using siRNA increased Txnip mRNA levels [169]. This evidence suggests that Nrf2 can act on ARE in Txnip promoter region and negatively regulate Txnip expression. Previously, it has been found that CUS for 4 weeks decreased Nrf2 protein levels in rat brain [170]. CORT administration

(20 mg/kg/day, s.c.) for 3 weeks decreased Nrf2 protein levels in mouse frontal cortex and hippocampus [171]. Treatment of human SK-N-SH neuroblastoma cells with CORT (200 μM) for 24 hrs also decreased Nrf2 protein levels [172]. These findings suggest that CORT treatment can down-regulate Nrf2/ARE transcription activity, increasing Txnip gene expression.

CORT may also regulate Txnip expression through Forkhead box class O (FOXO) binding sites. It has been found that Txnip promoter region has a FOXO binding site [173-175]. ChIP assay indicated that FOXO was associated with Txnip promoter [173]. Overexpression of FOXO was found to increase Txnip protein levels, while knockdown of FOXO3a using shRNA decreased Txnip protein levels in SH-SY5Y cells [176]. The phosphorylation of FOXO promotes its translocation from nucleus to cytoplasm, inhibiting FOXO activity [177]. It has been found that CUS for 3 weeks decreased phosphorylated- FOXO levels in rat brain [177]. The treatment of PC12 with 400 μM CORT for 24 hrs increased nuclear FOXO protein levels [178]. These findings suggest that CORT treatment may upregulate FOXO transcription activity, increasing Txnip gene expression.

In summary, we found that CORT treatment for 24 hrs increased Txnip protein levels in primary cultured mouse astrocytes. We also found that inhibition of MR and GR by spironolactone and RU486 respectively decreased CORT-increased Txnip protein levels. Since the Txnip promoter region contains a GRE site, CORT treatment may activate MR and GR and increase GRE-driven Txnip gene expression. Because Txnip promoter region also contains Nrf2/ARE binding site and FOXO binding site, CORT treatment may also regulate Txnip expression by these DNA binding sites.

4.2 CORT-upregulated Txnip does not cause oxidative damage in astrocytes

Txnip plays an important role in maintaining redox status, mitochondrial function, induction of apoptosis, regulation of glucose metabolism and inflammatory signaling. Txnip is an endogenous inhibitor of Trx [142, 151]. Trx can reduce cysteine thiol oxidation such as sulfenylation. Binding Txnip to Trx can inhibit Trx-reducing capability, resulting in a decrease of total free thiol levels and an increase of protein cysteine sulfenylation. Trx can reduce oxidized peroxiredoxin, which facilitates peroxiredoxin-mediated neutralization of peroxides including H_2O_2 [137]. H_2O_2 can react with the oxidized form of transition metals to produce hydroxyl radicals that induce protein carbonylation [43, 179]. The binding of Txnip to Trx can cause H_2O_2 accumulation and promotes protein carbonylation. In this study, we found that although CORT treatment didn't have any effect on Trx protein levels, this treatment not only increased Txnip protein levels but also modestly inhibited Trx reducing activity in primary cultured mouse astrocytes. Our finding suggests that CORT-upregulated Txnip can further inhibit Trx activity in astrocytes. However, in the present study, we also found that CORT treatment had no effects on total free thiol levels, protein sulfenylation and protein carbonylation in cultured astrocytes. This result suggests that CORT-decreased Trx activity was not sufficient to reduce thiol levels and not sufficient to promote protein sulfenylation and carbonylation in cultured astrocytes.

Astrocytes have more resistance to oxidative damage when compared to neurons. For example, the incubation of primary cultured mouse neurons with 100 μM of H_2O_2 for 30 min was found to result in the death of more than 50% of neurons in the culture. However, treatment of primary cultured mouse astrocytes with H_2O_2 up to 1 mM for 1 hr didn't have any effect on cell viability [180]. It was also found that when the same number of primary astrocytes and neurons were incubated with 100 μM H_2O_2, the concentration of H_2O_2 was found to be nearly 7 times lower in astrocytes as compared to neurons after 15 minutes of incubation [180, 181]. This suggests that

astrocytes may be more protective against ROS-induced oxidative damage when compared to neurons.

Astrocytes have high level of antioxidants as compared to neurons. Enriched levels of antioxidants may help astrocytes to resist oxidative damage. GSH plays an important role in the brain against oxidative damage. Astrocytes contain high amounts of GSH levels. Previously, total glutathione levels was found to be 35.4% higher in primary cultured rat cortical astrocytes than in primary cultured rat cortical neurons [45, 181]. Tert-butylhydroquinone (tBHQ) is a major metabolic product of butylated hydroxyanisole and can activate Nrf2 which upregulates expression of various antioxidant proteins like GSH, GST, quinone oxidoreductase and GCL [182, 183]. It has been found that treatment with tert-butylhydroquinone for 24 hrs increased GSH levels higher in primary cultured mouse astrocytes than in primary cultured mouse cortical neurons [184]. GCL catalyzes the binding of cysteine to glutamate, resulting in the formation of γ-glutamyl cysteine, which then reacts with glycine in the presence of glutathione synthetase to form glutathione (GSH). It has been reported that GCL catalytic subunit mRNA levels were 8 times higher in primary cultured mouse astrocytes than in primary cultured mouse cortical neurons [185]. The activity of GCL was also found to be 7 times higher in primary cultured chick astrocytes than in primary cultured chick forebrain neurons [186].

GSH is a prominent low-molecular-weight thiol antioxidant in cells. First, GSH can convert H_2O_2 to water catalyzed by glutathione peroxidase, which prevents H_2O_2-induced protein cysteine sulfenylation. High levels of GSH in astrocytes may prevent CORT-increased Txnip from further increasing oxidized thiol levels and protein cysteine sulfenylation. Because protein carbonylation is caused by hydroxyl radicals that is generated by reaction of H_2O_2 with oxidized transition metals, GSH-induced H_2O_2 scavenging may also prevent CORT from inducing protein

carbonylation. Second, under oxidative stress, GSH can react with protein sulfenic acid (PS-OH) to form protein-mixed disulfide with GSH (PS-SG) and induce protein cysteine glutathionylation. Glutathionylation makes the protein unavailable for further oxidation by ROS and protects it from irreversible loss of protein activity. Glutathionylation is reversible process and important in maintaining redox status [187-189].

In addition to the glutathione system, the activity of both catalase and glutathione peroxidase in primary striatal mouse astrocytes was found to be nearly 4.5 times higher than in primary cultured mouse striatal neurons [180]. Glutathione peroxidase (GPx) and catalase play important roles in maintaining the redox status of cells. They are responsible for the neutralization of H_2O_2. GPx catalyzes the reduction of H_2O_2 to water in presence of GSH as an electron donor. It also catalyzes the reduction of organic hydroperoxides to their corresponding alcohols. Catalase converts H_2O_2 to water and O_2 [45]. These findings suggest that higher expression of antioxidants like GSH, GPx and catalase could make astrocytes more resistant to oxidative stress than neurons.

In summary, we found that although CORT treatment inhibited Trx activity, this treatment didn't affect total reduced thiol levels, protein sulfenylation, and protein carbonylation in primary cultured mouse astrocytes. Since astrocytes enrich with antioxidants such as glutathione, catalase, glutathione peroxidase, and others, CORT-increased Txnip may not be sufficient to cause further oxidative damage in astrocytes.

4.3 CORT-upregulated Txnip activates NLRP3 inflammatory signaling in astrocytes.

NLPR3 inflammasome consists of sensor NLRP3 protein, apoptosis-associated speck-like protein containing a caspase recruitment domain (ASC) and procaspase-1. The activation of NLRP3 inflammasome has two steps: priming and activation. First of all, priming is stimulated by PAMPs, or DAMPs, which increases the expression of NLRP3, pro-IL-1β and pro-IL-18 protein

levels. The second activation step induces the forming of NLRP3 inflammasome complex among NLRP3, ASC and pro-caspase 1. The activation of NLRP3 inflammasome results in cleavage of pro-caspase-1 into the active caspase 1, which subsequently converts pro-interleukin (IL)-1**β** and pro-IL 18 into active IL-1**β** and IL-18. Then cell can secrete IL-1**β** and IL-18 [151, 190].

Txnip can bind with NLRP3 protein and promote NLRP3 inflammasome formation, which accelerates proinflammatory responses. NLRP3 protein has three major domains from N-terminal to C-terminal including pyrin domain (PYD), ATPase-containing nucleotide binding and oligomerization domain (NACHT) and leucine-rich repeat domain (LRR). PYD can bind to ASC, which recruits procaspase 1; NACHT assists in the formation of NLRP3 inflammasome, while LRR can interact with other proteins. In order to determine the specific NLRP3 domain that interacts with Txnip, individual PYD, NACHT or LRR flagged construct of NLRP3 was prepared and transfected to human embryonic kidney HEK293 cells. When the extracts were immunoprecipitated with anti-flag agarose beads and analyzed by immunoblotting analysis using Txnip antibody, it was found that the Txnip band signal was strong in the LRR construct, weak in the NACHT construct but not observed in the PYD construct [191]. This result suggests that LRR domain of NLRP3 is the major binding site for Txnip. Studies using co-ip have shown that Txnip and NLRP3 can directly interact with each other. When flagged NLRP3 was immunoprecipitated using an anti-flag agarose bead and analyzed by immunoblotting analysis using Txnip antibody, the Txnip signal was obtained, indicating Txnip directly binds to NLRP3 [191]. It has also been found that Txnip co-localized with NLRP3 in immortalized mouse podocyte cell line and human promonocytic leukemia cell line [192]. Co-localization between ASC and NLRP3 was also observed in the podocyte cell line. After Txnip was knockdown using Txnip siRNA, the colocalization between NLRP3 and ASC was significantly attenuated, indicating the role of Txnip

in formation of NLRP3 inflammasome assembly [192]. These findings suggest that the interaction of Txnip with NLRP3 could be essential for NLRP3 inflammasome assembly.

Chronic stress and CORT treatment can regulate NLRP3 inflammasome. In CNS, NLPR3 protein is highly expressed in astrocytes and microglia [193]. In this study, we found that although CORT treatment didn't have any effects on NLRP3 protein level, this treatment increased Txnip/NLRP3 binding activity in primary cultured mouse cerebrocortical astrocytes. Previously, our laboratory had reported that CORT treatment in cultured N9 mouse microglia cells increased Txnip/NLRP3 binding [165]. These studies suggest that CORT-treatment may increase Txnip expression, resulting in increased Txnip/NLRP3 binding in glial cells. Previously, it has been found that CUS for 4 weeks increased NLRP3 and ASC protein levels in rat hippocampus [194]. Oral administration of CORT at 20 mg/kg daily for 35 days increased NLRP3 and ASC protein levels in mouse hippocampus and frontal cortex [195]. It has also been found that rats exposed to CUS showed increased NLRP3/ASC binding activity and ASC/pro-caspase-1 binding activity in the hippocampus and frontal cortex [196]. These findings suggest that chronic stress or CORT treatment may increase the binding of Txnip to NLRP3 and promote the assembly of the NLRP3 inflammasome.

Activation of NLRP3 inflammasome cleaves pro-caspase-1 into active caspase-1. Pro-caspase-1 consists of N-terminal caspase activation and recruitment domain (CARD), p20 subunits, interdomain linker and p10 subunits. Pro-caspase-1 can be cleaved by NLRP3 inflammasome and release p10 and p20 subunits. The large p20 subunit has a catalytic site, while the smaller p10 subunit has a dimer interface. These subunits interact with each other to form an active caspase-1 enzyme. Active caspase-1 promotes maturation of pro-IL-1β and pro-IL-18 to active IL-1β and IL-18 [197, 198]. Previously, it has been found that the high glucose treatment

not only increased Txnip protein levels but also increased ASC and IL-1β protein levels in the HLEC cell line, while the knockdown of Txnip using Txnip siRNA attenuated high glucose-induced increased IL-1β protein levels [199]. Similarly, high glucose treatment was also found to increase Txnip protein levels, cleaved caspase-1 p20 levels and IL-1β protein levels in U937 monocytes, while the knockdown of Txnip decreased glucose-increased caspase-1 p20 subunit and IL-1β levels [200]. This evidence suggests that binding of Txnip to NLRP3 can stimulate NLRP3 inflammasome, further activating caspase-1 and cleaving pro-IL-1β to active IL-1β.

Chronic stress and CORT treatment regulate NLRP3 inflammasome, caspase-1 and IL-1β. CUS for 4 weeks increased cleaved caspase-1 p10 subunit protein levels and caspase-1 catalytic activity, decreased pro-IL-1β protein levels, and increased mature IL-1β protein levels in mouse hippocampus and frontal cortex [201]. Chronic restraint stress (4 hrs/day) for 9 days was also found to increase caspase-1 p20 subunit protein levels and IL-1β protein levels in mouse hippocampus [202]. Mice subjected to repeated forced swim stress (10 min twice daily) for 14 days showed an increase in mature IL-1β protein levels. Repeated forced swim stress was also found to increase co-localization of NLRP3 and IL-1β in frontal cortex. Repeated forced swim stress-induced IL-1β protein levels were inhibited in NLRP3 knockout mice [203]. CORT administration (20 mg/kg/day, s.c.) for 21 days was increased IL-1β levels and caspase-1 levels in mouse hippocampus [204]. These results suggest that chronic stress/CORT treatment can activate NLRP3, increasing caspase-1 activity and IL-1β production.

In the present study, we found that CORT treatment in primary cultured mouse astrocytes increased caspase-1 activity. CORT treatment increased the release of IL-1β from astrocytes. Our result suggests that CORT-increased Txnip in astrocytes may activate NLRP3 inflammasome, which subsequently increases caspase-1 activity and promotes the release of IL-1β. Previous

studies from our laboratory also showed that the CORT treatment increased caspase-1 activity and IL-1β release from mouse N9 microglia cells [165]. The treatment of HAPI rat microglial cells with 0.5 μM dexamethasone for 24 hrs was also found to increase cleaved caspase-1 p20 protein level and IL-1β levels [205]. This evidence suggests that CORT treatment may facilitate NLRP3 inflammasome-activated pro-inflammatory process through both astrocytes and microglia.

To understand the function of Txnip in CORT treatment-activated NLRP3 inflammasome, in the present study, we determined whether knocking out Txnip inhibits CORT treatment-induced caspase-1 activation and IL-1β release. Txnip gene was knocked out using CRISPR/Cas9/Txnip sgRNA in primary cultured mouse cerebrocortical astrocytes. We found that Txnip sgRNA can knock out Txnip gene expression in cultured astrocytes. We further found that although CORT treatment for 24 hours increased caspase-1 activity and IL-1β release in CRISPR/Cas9/ scrambled sgRNA transduced astrocytes, there was no effect of CORT treatment on caspase-1 activity and IL-1β release in CRISPR/Cas9/ Txnip sgRNA transduced astrocytes. This evidence suggests that Txnip gene knockout can prevent CORT treatment- increased caspase-1 activation and IL-1β release. Our findings together suggest that CORT-upregulated Txnip in astrocytes may bind to NLRP3 protein, inducing NLRP3 inflammasome formation and activation, which activates caspase-1 activation and releases IL-1β. These findings also suggest that Txnip mediates CORT-induced NLRP3 inflammasome activation and might play an important role in the CORT treatment-activated inflammatory process.

In summary, we found that although treatment with CORT for 24 hours had no effect on NLRP3 protein levels, this treatment increased NLRP3/Txnip binding activity, caspase-1 activity and IL-1β release in primary cultured mouse astrocytes. The knockout of Txnip using CRISPR/Cas9/Txnip sgRNA attenuated CORT-induced caspase-1 activity and IL-1β release. Our

finding suggests that CORT treatment upregulates Txnip, subsequently activating NLRP3 inflammasome, which can activate caspase-1 and release IL-1β in astrocytes.

CHAPTER 5. CONCLUSION, LIMITATION AND FUTURE STUDIES

5.1 Conclusion

We found that CORT treatment for 24 hrs had no effect on Trx protein levels but increased Txnip protein levels in primary cultured mouse astrocytes. Treatment with either GR antagonist RU486 or MR antagonist spironolactone decreased CORT treatment-induced Txnip protein levels. Since Txnip can inhibit Trx activity, promoting oxidative stress and Txnip can also bind to NLRP3 and activate NLRP3 inflammasome, facilitating NLRP3-mediated pro-inflammatory pathway, we determined whether CORT-upregulated Txnip further cause oxidative stress and inflammation. First, we found that although CORT-treatment decreased Trx activity, this treatment had no effects on total reduced thiol levels, sulfenylated protein levels and carbonylated protein levels in primary cultured mouse astrocytes. Because astrocytes are enriched with high levels of antioxidants, CORT-increased Txnip may further inhibit Trx activity, but not be sufficient to exert thiol oxidation, protein sulfenylation and protein carbonylation in these cells. Second, we found that CORT treatment had no effect on NLRP3 protein levels, but this treatment increased Txnip-NLRP3 binding activity, caspase-1 enzyme activity and IL-1β release in primary cultured mouse astrocytes. Knocking out Txnip using CRISPR/Cas9/Txnip sgRNA attenuated CORT treatment-increased caspase-1 activity and IL-1β release in cultured astrocytes. As shown in Figure 21, our results suggest that CORT upregulates Txnip by MR and GR receptors in astrocytes. Upregulated Txnip may bind to NLRP3 and stimulate NLRP3 inflammasome forming, which activates caspase-1 activity and releases IL-1β, facilitating the neuroinflammatory process. Since chronic stress is a risk factor for depression and other psychiatric disorders, our findings also suggest that Txnip has a therapeutic potential for the treatment of depression.

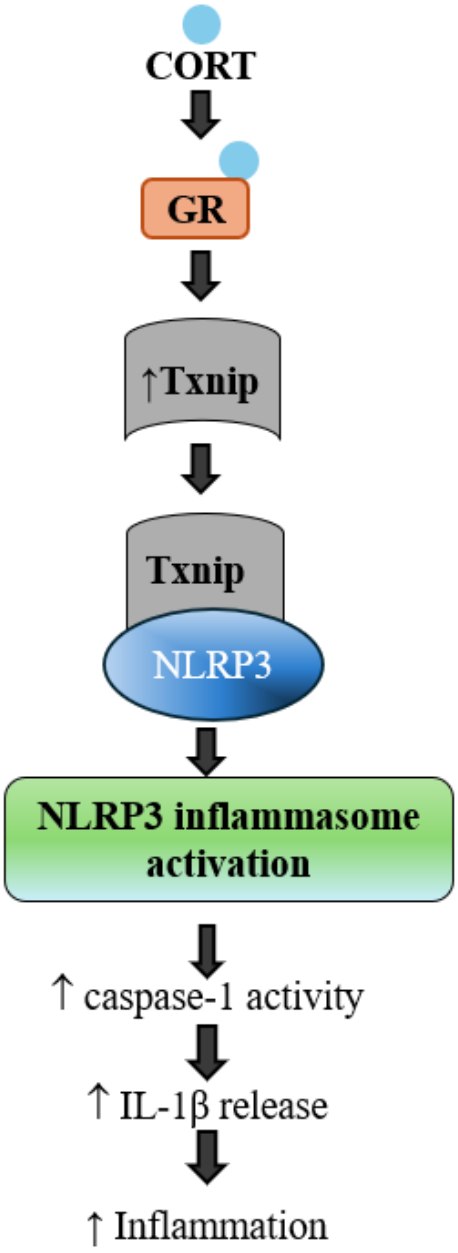

Figure 21. Possible role of CORT Txnip in CORT-induced inflammation in astrocytes: CORT may bind to GR, which can increase Txnip levels. Txnip can bind to NLRP3, which activates NLRP3 inflammasome formation. This results in increased caspase-1 activity and release of IL-1β from astrocytes which promotes inflammation. CORT- Corticosterone, GR- Glucocorticoid Receptor, NLRP3- NOD-like receptor protein 3, IL-1β- Interleukin 1-β, Txnip- Thioredoxin interacting protein

5.2 Limitations and future studies

There are some limitations in this study. First, we found that CORT treatment increased Txnip/NLRP3 binding activity, caspase-1 activity and IL-1β release in cultured astrocytes. Our results suggest that CORT treatment may upregulate Txnip and stimulate NLRP3 inflammasome forming. However, we do not have any direct evidence showing that CORT treatment stimulates NLRP3 inflammasome forming. In future, we will measure the effect of CORT treatment NLRP3/ASC/procaspase-1 binding activity by co-immunoprecipitation and determine whether knocking out Txnip has any effect on NLRP3/ASC/procaspase-1 binding in cultured astrocytes.

Second, in this study, we only determined the role of Txnip in the CORT-activated NLRP3 inflammatory pathway in cultured astrocytes *in vitro*. In vitro cultured astrocytes do not have any communication between astrocytes and neurons and are physiologically limited. In future, we will analyze the effect of CORT on astrocytal Txnip and NLRP3 inflammatory signaling in animal in vivo. We can analyze the effect of CORT on astrocytal Txnip, NLRP3, caspase-1 and IL-1β in animals using immunohistochemistry. To further understand the role of Txnip in CORT-activated NLRP3 inflammatory signaling, we can knockdown Txnip in astrocytes using Cre-Lox mice and determine whether Txnip-knockdown in astrocytes has any effect on CORT-induced inflammation, oxidative stress and depression-like behaviours.

Third, in this study, our results suggest that CORT treatment may upregulate Txnip and stimulate NLRP inflammatory signaling, which causes neuroinflammation. However, we do not have any direct evidence showing that CORT treatment can cause neuronal damage by targeting astrocytal Txnip and NLRP3 inflammasome. To determine if CORT treatment in astrocytes release cytokines can further damage neurons, in future we can analyze the effect of CORT-treated

astrocyte-conditioned medium on cultured neurons and determine whether this medium has any effects on neuronal toxicity.

Fourth, in this study, CRISPR/Cas9 was used to knockout Txnip in primary astrocytes. CRISPR/Cas9 may cleave other DNA targets, which results in undesired effects. In this study, we didn't determine whether CRISPR/Cas9/Txnip sgRNA had any off targets. CRISPR/Cas9/Txnip sgRNA lentivector was purchased from ABM Inc. ABM Inc. has stated that CRISPResso Software was used to ensure that the Txnip sgRNA has no predicted off-target binding sites. However, we think that it may still have some off-targets. In the future, we will use GUIDE-seq, CIRCLE-seq, DISCOVER-seq, ChIP-seq or other methods to identify off-target sites, and determine if these deletions contribute to CORT-stimulated NLRP3 inflammatory signaling in astrocytes.

REFERENCES

1. Vitellius, G., et al. *Pathophysiology of glucocorticoid signaling*. in *Annales d'endocrinologie*. 2018. Elsevier.
2. Walker, J.J., et al., *The origin of glucocorticoid hormone oscillations.* 2012. **10**(6): p. e1001341.
3. Sacta, M.A., Y. Chinenov, and I.J.A.r.o.p. Rogatsky, *Glucocorticoid signaling: an update from a genomic perspective.* 2016. **78**: p. 155-180.
4. Niraula, A., et al., *Corticosterone production during repeated social defeat causes monocyte mobilization from the bone marrow, glucocorticoid resistance, and neurovascular adhesion molecule expression.* 2018. **38**(9): p. 2328-2340.
5. Koning, A.-S.C., et al., *Glucocorticoid and mineralocorticoid receptors in the brain: a transcriptional perspective.* 2019. **3**(10): p. 1917-1930.
6. van Steensel, B., et al., *Partial colocalization of glucocorticoid and mineralocorticoid receptors in discrete compartments in nuclei of rat hippocampus neurons.* 1996. **109**(4): p. 787-792.
7. Gomez-Sanchez, E. and C.E. Gomez-Sanchez, *The multifaceted mineralocorticoid receptor.* Compr Physiol, 2014. **4**(3): p. 965-94.
8. de Kloet, E.R., *Brain mineralocorticoid and glucocorticoid receptor balance in neuroendocrine regulation and stress-related psychiatric etiopathologies.* Curr Opin Endocr Metab Res, 2022. **24**: p. 100352.
9. Weikum, E.R., et al., *Glucocorticoid receptor control of transcription: precision and plasticity via allostery.* 2017. **18**(3): p. 159-174.
10. Wright, A.P., et al., *Structure and function of the glucocorticoid receptor.* 1993. **47**(1-6): p. 11-19.
11. Bledsoe, R.K., et al., *Crystal structure of the glucocorticoid receptor ligand binding domain reveals a novel mode of receptor dimerization and coactivator recognition.* Cell, 2002. **110**(1): p. 93-105.
12. Desmet, S.J. and K.J.T.J.o.c.i. De Bosscher, *Glucocorticoid receptors: finding the middle ground.* 2017. **127**(4): p. 1136-1145.
13. Lu, N.Z. and J.A.J.A.o.t.N.Y.A.o.S. Cidlowski, *The origin and functions of multiple human glucocorticoid receptor isoforms.* 2004. **1024**(1): p. 102-123.
14. Vandevyver, S., L. Dejager, and C.J.E.r. Libert, *Comprehensive overview of the structure and regulation of the glucocorticoid receptor.* 2014. **35**(4): p. 671-693.
15. Silverstein, A.M., et al., *Protein phosphatase 5 is a major component of glucocorticoid receptor· hsp90 complexes with properties of an FK506-binding immunophilin.* 1997. **272**(26): p. 16224-16230.
16. Johnson, J.L. and D.O.J.J.o.B.C. Toft, *A novel chaperone complex for steroid receptors involving heat shock proteins, immunophilins, and p23.* 1994. **269**(40): p. 24989-24993.
17. Nicolaides, N.C., G. Chrousos, and T. Kino, *Glucocorticoid receptor*, in *Endotext [Internet]*. 2020, MDText. com, Inc.
18. Owens-Grillo, J.K., et al., *The Cyclosporin A-binding Immunophilin CyP-40 and the FK506-binding Immunophilin hsp56 Bind to a Common Site on hsp90 and Exist in Independent Cytosolic Heterocomplexes with the Untransformed Glucocorticoid Receptor (∗).* 1995. **270**(35): p. 20479-20484.
19. Schoneveld, O.J., et al., *Mechanisms of glucocorticoid signalling.* 2004. **1680**(2): p. 114-128.
20. Guo, D.F., et al., *Identification of a cis-acting glucocorticoid responsive element in the rat angiotensin II type 1A promoter.* Circ Res, 1995. **77**(2): p. 249-57.
21. Hoeppner, M.A., J.C. Mordacq, and D.I. Linzer, *Role of the composite glucocorticoid response element in proliferin gene expression.* Gene Expr, 1995. **5**(2): p. 133-41.

22. Diamond, M.I., et al., *Transcription factor interactions: selectors of positive or negative regulation from a single DNA element.* Science, 1990. **249**(4974): p. 1266-72.
23. Hwang, J., et al., *The structural basis for the negative regulation of thioredoxin by thioredoxin-interacting protein.* Nat Commun, 2014. **5**(1): p. 2958.
24. Xavier, A.M., et al., *Gene Expression Control by Glucocorticoid Receptors during Innate Immune Responses.* Front Endocrinol (Lausanne), 2016. **7**: p. 31.
25. Surjit, M., et al., *Widespread negative response elements mediate direct repression by agonist-liganded glucocorticoid receptor.* Cell, 2011. **145**(2): p. 224-41.
26. Hudson, W.H., C. Youn, and E.A. Ortlund, *The structural basis of direct glucocorticoid-mediated transrepression.* Nat Struct Mol Biol, 2013. **20**(1): p. 53-8.
27. Nissen, R.M., K.R.J.G. Yamamoto, and development, *The glucocorticoid receptor inhibits NFκB by interfering with serine-2 phosphorylation of the RNA polymerase II carboxy-terminal domain.* 2000. **14**(18): p. 2314-2329.
28. Schoenfeld, T.J., et al., *Stress and Loss of Adult Neurogenesis Differentially Reduce Hippocampal Volume.* Biol Psychiatry, 2017. **82**(12): p. 914-923.
29. Galea, L.A., et al., *Sex differences in dendritic atrophy of CA3 pyramidal neurons in response to chronic restraint stress.* Neuroscience, 1997. **81**(3): p. 689-97.
30. Zach, P., et al., *Delayed effects of elevated corticosterone level on volume of hippocampal formation in laboratory rat.* Physiol Res, 2010. **59**(6): p. 985-996.
31. Woolley, C.S., E. Gould, and B.S. McEwen, *Exposure to excess glucocorticoids alters dendritic morphology of adult hippocampal pyramidal neurons.* Brain Res, 1990. **531**(1-2): p. 225-31.
32. Sapolsky, R.M., et al., *Hippocampal damage associated with prolonged glucocorticoid exposure in primates.* J Neurosci, 1990. **10**(9): p. 2897-902.
33. Wang, S., et al., *Mechanism of Chronic Stress-Induced Glutamatergic Neuronal Damage in the Basolateral Amygdaloid Nucleus.* Anal Cell Pathol (Amst), 2021. **2021**: p. 8388527.
34. Zhang, H., et al., *Combined exposure of alumina nanoparticles and chronic stress exacerbates hippocampal neuronal ferroptosis via activating IFN-gamma/ASK1/JNK signaling pathway in rats.* J Hazard Mater, 2021. **411**: p. 125179.
35. Donoso, F., et al., *Naturally Derived Polyphenols Protect Against Corticosterone-Induced Changes in Primary Cortical Neurons.* Int J Neuropsychopharmacol, 2019. **22**(12): p. 765-777.
36. Latt, H.M., et al., *Oxytocin Inhibits Corticosterone-induced Apoptosis in Primary Hippocampal Neurons.* Neuroscience, 2018. **379**: p. 383-389.
37. Olescowicz, G., et al., *Protective Effects of Agmatine Against Corticosterone-Induced Impairment on Hippocampal mTOR Signaling and Cell Death.* Neurotox Res, 2020. **38**(2): p. 319-329.
38. Zhang, M., et al., *Sinisan Protects Primary Hippocampal Neurons Against Corticosterone by Inhibiting Autophagy via the PI3K/Akt/mTOR Pathway.* Front Psychiatry, 2021. **12**: p. 627056.
39. Singh, A., et al., *Oxidative Stress: A Key Modulator in Neurodegenerative Diseases.* Molecules, 2019. **24**(8): p. 1583.
40. Stadtman, E.R. and R.L. Levine, *Protein oxidation.* Ann N Y Acad Sci, 2000. **899**(1): p. 191-208.
41. Reddie, K.G. and K.S.J.C.o.i.c.b. Carroll, *Expanding the functional diversity of proteins through cysteine oxidation.* 2008. **12**(6): p. 746-754.
42. Lo Conte, M. and K.S. Carroll, *The redox biochemistry of protein sulfenylation and sulfinylation.* J Biol Chem, 2013. **288**(37): p. 26480-8.
43. Akagawa, M., *Protein carbonylation: molecular mechanisms, biological implications, and analytical approaches.* Free Radic Res, 2021. **55**(4): p. 307-320.
44. He, L., et al., *Antioxidants Maintain Cellular Redox Homeostasis by Elimination of Reactive Oxygen Species.* Cell Physiol Biochem, 2017. **44**(2): p. 532-553.

45. Dringen, R., P.G. Pawlowski, and J. Hirrlinger, *Peroxide detoxification by brain cells.* J Neurosci Res, 2005. **79**(1-2): p. 157-65.
46. Aziz, M.A., A.S. Diab, and A.A.J.A. Mohammed, *Antioxidant categories and mode of action.* 2019. **2019**: p. 3-22.
47. Nimse, S.B. and D.J.R.a. Pal, *Free radicals, natural antioxidants, and their reaction mechanisms.* 2015. **5**(35): p. 27986-28006.
48. Palma, F.R., et al., *ROS production by mitochondria: function or dysfunction?* Oncogene, 2024. **43**(5): p. 295-303.
49. Murphy, M.P.J.B.j., *How mitochondria produce reactive oxygen species.* 2009. **417**(1): p. 1-13.
50. Liu, W. and C. Zhou, *Corticosterone reduces brain mitochondrial function and expression of mitofusin, BDNF in depression-like rodents regardless of exercise preconditioning.* Psychoneuroendocrinology, 2012. **37**(7): p. 1057-70.
51. Rezin, G.T., et al., *Inhibition of mitochondrial respiratory chain in brain of rats subjected to an experimental model of depression.* Neurochem Int, 2008. **53**(6-8): p. 395-400.
52. Lucca, G., et al., *Increased oxidative stress in submitochondrial particles into the brain of rats submitted to the chronic mild stress paradigm.* 2009. **43**(9): p. 864-869.
53. Arent, C.O., et al., *Synergist effects of n-acetylcysteine and deferoxamine treatment on behavioral and oxidative parameters induced by chronic mild stress in rats.* Neurochem Int, 2012. **61**(7): p. 1072-80.
54. Liu, B., et al., *Neuroprotective effects of icariin on corticosterone-induced apoptosis in primary cultured rat hippocampal neurons.* Brain Res, 2011. **1375**: p. 59-67.
55. You, J.M., et al., *Mechanism of glucocorticoid-induced oxidative stress in rat hippocampal slice cultures.* Can J Physiol Pharmacol, 2009. **87**(6): p. 440-7.
56. Bose, R., et al., *Glucocorticoids induce long-lasting effects in neural stem cells resulting in senescence-related alterations.* Cell Death Dis, 2010. **1**(11): p. e92.
57. Sedeek, M., et al., *NADPH oxidases, reactive oxygen species, and the kidney: friend and foe.* J Am Soc Nephrol, 2013. **24**(10): p. 1512-8.
58. Panday, A., et al., *NADPH oxidases: an overview from structure to innate immunity-associated pathologies.* 2015. **12**(1): p. 5-23.
59. Seo, J.S., et al., *NADPH oxidase mediates depressive behavior induced by chronic stress in mice.* J Neurosci, 2012. **32**(28): p. 9690-9.
60. Ibi, M., et al., *Depressive-Like Behaviors Are Regulated by NOX1/NADPH Oxidase by Redox Modification of NMDA Receptor 1.* J Neurosci, 2017. **37**(15): p. 4200-4212.
61. Maluach, A.M., et al., *Increased Neuronal DNA/RNA Oxidation in the Frontal Cortex of Mice Subjected to Unpredictable Chronic Mild Stress.* Chronic Stress (Thousand Oaks), 2017. **1**: p. 2470547017724744.
62. Zhou, H., et al., *Increased thioredoxin-interacting protein in brain of mice exposed to chronic stress.* Prog Neuropsychopharmacol Biol Psychiatry, 2019. **88**: p. 320-326.
63. Bharti, V., et al., *Upregulation of antioxidant thioredoxin by antidepressants fluoxetine and venlafaxine.* Psychopharmacology (Berl), 2020. **237**(1): p. 127-136.
64. Madrigal, J.L., et al., *Glutathione depletion, lipid peroxidation and mitochondrial dysfunction are induced by chronic stress in rat brain.* Neuropsychopharmacology, 2001. **24**(4): p. 420-9.
65. Zhang, H., et al., *Lycopene ameliorates chronic stress-induced hippocampal injury and subsequent learning and memory dysfunction through inhibiting ROS/JNK signaling pathway in rats.* 2020. **145**: p. 111688.
66. Solanki, N., et al., *Modulating Oxidative Stress Relieves Stress-Induced Behavioral and Cognitive Impairments in Rats.* Int J Neuropsychopharmacol, 2017. **20**(7): p. 550-561.

67. McIntosh, L.J., K.E. Hong, and R.M. Sapolsky, *Glucocorticoids may alter antioxidant enzyme capacity in the brain: baseline studies.* Brain Res, 1998. **791**(1-2): p. 209-14.
68. Samad, N., M. Rafeeque, and I.J.M.B.D. Imran, *Free–L-Cysteine improves corticosterone-induced behavioral deficits, oxidative stress and neurotransmission in rats.* 2023. **38**(3): p. 983-997.
69. Yang, L., et al., *Stress level of glucocorticoid exacerbates neuronal damage and Aβ production through activating NLRP1 inflammasome in primary cultured hippocampal neurons of APP-PS1 mice.* 2022. **110**: p. 108972.
70. Sun, L., et al., *Inhibition of NOX2-NLRP1 signaling pathway protects against chronic glucocorticoids exposure-induced hippocampal neuronal damage.* Int Immunopharmacol, 2019. **74**: p. 105721.
71. Zhang, B., et al., *Chronic glucocorticoid exposure activates BK-NLRP1 signal involving in hippocampal neuron damage.* J Neuroinflammation, 2017. **14**(1): p. 139.
72. Song, A.Q., et al., *NLRP1 inflammasome contributes to chronic stress-induced depressive-like behaviors in mice.* J Neuroinflammation, 2020. **17**(1): p. 178.
73. Sahin Ozkartal, C., et al., *Chronic mild stress-induced anhedonia in rats is coupled with the upregulation of inflammasome sensors: a possible involvement of NLRP1.* 2018. **28**(3): p. 236-244.
74. Sedaghat, K., et al., *Regulatory effect of vitamin D on pro-inflammatory cytokines and anti-oxidative enzymes dysregulations due to chronic mild stress in the rat hippocampus and prefrontal cortical area.* 2021. **48**: p. 7865-7873.
75. Pan, S., et al., *Indole-3-Carbinol Selectively Prevents Chronic Stress-Induced Depression-but not Anxiety-Like Behaviors via Suppressing Pro-Inflammatory Cytokine Production and Oxido-Nitrosative Stress in the Brain.* Front Pharmacol, 2022. **13**: p. 829966.
76. de Castro Chaves, R., et al., *The neuroprotective effect of Riparin IV on oxidative stress and neuroinflammation related to chronic stress-induced cognitive impairment.* 2020. **122**: p. 104758.
77. Bertollo, A.G., et al., *Stress and serum cortisol levels in major depressive disorder: a cross-sectional study.* 2020. **7**(4): p. 459.
78. Barrimi, M., et al., *Prolonged corticosteroid-therapy and anxiety-depressive disorders, longitudinal study over 12 months.* 2012. **39**(1): p. 59-65.
79. Hinkelmann, K., et al., *Changes in cortisol secretion during antidepressive treatment and cognitive improvement in patients with major depression: a longitudinal study.* 2012. **37**(5): p. 685-692.
80. Zhao, Y., et al., *A mouse model of depression induced by repeated corticosterone injections.* Eur J Pharmacol, 2008. **581**(1-2): p. 113-20.
81. Ding, H., et al., *Depression-like behaviors induced by chronic corticosterone exposure via drinking water: time-course analysis.* 2018. **687**: p. 202-206.
82. Fuchs, E. and G.J.D.i.c.n. Flügge, *Cellular consequences of stress and depression.* 2004. **6**(2): p. 171-183.
83. Vreeburg, S.A., et al., *Salivary cortisol levels in persons with and without different anxiety disorders.* 2010. **72**(4): p. 340-347.
84. Schiefelbein, V.L. and E.J.J.T.J.o.E.A. Susman, *Cortisol levels and longitudinal cortisol change as predictors of anxiety in adolescents.* 2006. **26**(4): p. 397-413.
85. Odland, A.U., R. Sandahl, and J.T.J.B.B.R. Andreasen, *Chronic corticosterone improves perseverative behavior in mice during sequential reversal learning.* 2023. **450**: p. 114479.
86. Sofroniew, M.V., *Astrocyte Reactivity: Subtypes, States, and Functions in CNS Innate Immunity.* Trends Immunol, 2020. **41**(9): p. 758-770.

87. Yan, M., et al., *Effects of dexmedetomidine on the release of glial cell line-derived neurotrophic factor from rat astrocyte cells.* Neurochem Int, 2011. **58**(5): p. 549-57.
88. Zhao, H., et al., *Mesencephalic astrocyte-derived neurotrophic factor inhibits oxygen-glucose deprivation-induced cell damage and inflammation by suppressing endoplasmic reticulum stress in rat primary astrocytes.* J Mol Neurosci, 2013. **51**(3): p. 671-8.
89. Bathina, S. and U.N. Das, *Brain-derived neurotrophic factor and its clinical implications.* Arch Med Sci, 2015. **11**(6): p. 1164-78.
90. Airaksinen, M.S. and M. Saarma, *The GDNF family: signalling, biological functions and therapeutic value.* Nat Rev Neurosci, 2002. **3**(5): p. 383-94.
91. Lindholm, P. and M. Saarma, *Cerebral dopamine neurotrophic factor protects and repairs dopamine neurons by novel mechanism.* Mol Psychiatry, 2022. **27**(3): p. 1310-1321.
92. Liu, Y.Y., et al., *Mesencephalic astrocyte-derived neurotrophic factor (MANF): Structure, functions and therapeutic potential.* Ageing Res Rev, 2022. **82**: p. 101763.
93. Kirchhoff, F., R. Dringen, and C. Giaume, *Pathways of neuron-astrocyte interactions and their possible role in neuroprotection.* Eur Arch Psychiatry Clin Neurosci, 2001. **251**(4): p. 159-69.
94. Watts, L.T., et al., *Astrocytes protect neurons from ethanol-induced oxidative stress and apoptotic death.* J Neurosci Res, 2005. **80**(5): p. 655-66.
95. Drukarch, B., et al., *Astrocyte-enhanced neuronal survival is mediated by scavenging of extracellular reactive oxygen species.* Free Radic Biol Med, 1998. **25**(2): p. 217-20.
96. Pérez-Sala, D. and M.A.J.I.J.o.M.S. Pajares, *Appraising the role of astrocytes as suppliers of neuronal glutathione precursors.* 2023. **24**(9): p. 8059.
97. Aoyama, K., M. Watabe, and T. Nakaki, *Regulation of neuronal glutathione synthesis.* J Pharmacol Sci, 2008. **108**(3): p. 227-38.
98. Raciti, M., et al., *Glucocorticoids alter neuronal differentiation of human neuroepithelial-like cells by inducing long-lasting changes in the reactive oxygen species balance.* Neuropharmacology, 2016. **107**: p. 422-431.
99. Dringen, R., B. Pfeiffer, and B.J.J.o.N. Hamprecht, *Synthesis of the antioxidant glutathione in neurons: supply by astrocytes of CysGly as precursor for neuronal glutathione.* 1999. **19**(2): p. 562-569.
100. McBean, G.J., *Cysteine, Glutathione, and Thiol Redox Balance in Astrocytes.* Antioxidants (Basel), 2017. **6**(3): p. 62.
101. Abbott, N.J., L. Ronnback, and E. Hansson, *Astrocyte-endothelial interactions at the blood-brain barrier.* Nat Rev Neurosci, 2006. **7**(1): p. 41-53.
102. Cabezas, R., et al., *Astrocytic modulation of blood brain barrier: perspectives on Parkinson's disease.* Front Cell Neurosci, 2014. **8**: p. 211.
103. Kadry, H., et al., *A blood–brain barrier overview on structure, function, impairment, and biomarkers of integrity.* 2020. **17**: p. 1-24.
104. Hertz, L. and Y. Chen, *Importance of astrocytes for potassium ion (K(+)) homeostasis in brain and glial effects of K(+) and its transporters on learning.* Neurosci Biobehav Rev, 2016. **71**: p. 484-505.
105. Hertz, L., et al., *Role of the Astrocytic Na(+), K(+)-ATPase in K(+) Homeostasis in Brain: K(+) Uptake, Signaling Pathways and Substrate Utilization.* Neurochem Res, 2015. **40**(12): p. 2505-16.
106. Larsen, B.R., et al., *Contributions of the Na(+)/K(+)-ATPase, NKCC1, and Kir4.1 to hippocampal K(+) clearance and volume responses.* Glia, 2014. **62**(4): p. 608-22.
107. Heller, J.P. and D.A. Rusakov, *The Nanoworld of the Tripartite Synapse: Insights from Super-Resolution Microscopy.* Front Cell Neurosci, 2017. **11**: p. 374.
108. Liu, B., A.G. Teschemacher, and S. Kasparov, *Neuroprotective potential of astroglia.* J Neurosci Res, 2017. **95**(11): p. 2126-2139.

109. Blanco‐Suárez, E., A.L. Caldwell, and N.J.J.T.J.o.p. Allen, *Role of astrocyte‐synapse interactions in CNS disorders.* 2017. **595**(6): p. 1903-1916.
110. Schousboe, A., H.S.J.A.i.M. Waagepetersen, and C. Biology, *Role of astrocytes in homeostasis of glutamate and GABA during physiological and pathophysiological conditions.* 2003. **31**: p. 461-474.
111. Schousboe, A., et al., *Regulatory role of astrocytes for neuronal biosynthesis and homeostasis of glutamate and GABA.* Prog Brain Res, 1992. **94**: p. 199-211.
112. Andersen, J.V., A. Schousboe, and A.J.P.i.n. Verkhratsky, *Astrocyte energy and neurotransmitter metabolism in Alzheimer's disease: integration of the glutamate/GABA-glutamine cycle.* 2022. **217**: p. 102331.
113. Bélanger, M., I. Allaman, and P.J.J.C.m. Magistretti, *Brain energy metabolism: focus on astrocyte-neuron metabolic cooperation.* 2011. **14**(6): p. 724-738.
114. Falkowska, A., et al., *Energy metabolism of the brain, including the cooperation between astrocytes and neurons, especially in the context of glycogen metabolism.* 2015. **16**(11): p. 25959-25981.
115. Beard, E., et al., *Astrocytes as key regulators of brain energy metabolism: new therapeutic perspectives.* 2022. **12**: p. 825816.
116. Giovannoni, F. and F.J. Quintana, *The Role of Astrocytes in CNS Inflammation.* Trends Immunol, 2020. **41**(9): p. 805-819.
117. Sofroniew, M.V.J.C.S.H.p.i.b., *Astrogliosis.* 2015. **7**(2): p. a020420.
118. Freeman, L., et al., *NLR members NLRC4 and NLRP3 mediate sterile inflammasome activation in microglia and astrocytes.* J Exp Med, 2017. **214**(5): p. 1351-1370.
119. Mamik, M.K. and C. Power, *Inflammasomes in neurological diseases: emerging pathogenic and therapeutic concepts.* Brain, 2017. **140**(9): p. 2273-2285.
120. Li, L., et al., *Role of astroglial toll-like receptors (TLRs) in central nervous system infections, injury and neurodegenerative diseases.* Brain Behav Immun, 2021. **91**: p. 740-755.
121. Voet, S., et al., *Inflammasomes in neuroinflammatory and neurodegenerative diseases.* EMBO Mol Med, 2019. **11**(6): p. e10248.
122. Bohn, M.C., et al., *Glial cells express both mineralocorticoid and glucocorticoid receptors.* 1991. **40**(1-3): p. 105-111.
123. Tynan, R.J., et al., *Chronic stress-induced disruption of the astrocyte network is driven by structural atrophy and not loss of astrocytes.* 2013. **126**(1): p. 75-91.
124. Virmani, G., et al., *Subfield-specific effects of chronic mild unpredictable stress on hippocampal astrocytes.* Eur J Neurosci, 2021. **54**(5): p. 5730-5746.
125. Champeil-Potokar, G., et al., *Docosahexaenoic acid (DHA) prevents corticosterone-induced changes in astrocyte morphology and function.* J Neurochem, 2016. **136**(6): p. 1155-1167.
126. Sun, J.D., et al., *Gap junction dysfunction in the prefrontal cortex induces depressive-like behaviors in rats.* Neuropsychopharmacology, 2012. **37**(5): p. 1305-20.
127. Xia, C.Y., et al., *Ginsenoside Rg1 alleviates corticosterone-induced dysfunction of gap junctions in astrocytes.* J Ethnopharmacol, 2017. **208**: p. 207-213.
128. Li, D.Q., et al., *Wuling Capsule promotes hippocampal neurogenesis by improving expression of connexin 43 in rats exposed to chronic unpredictable mild stress.* Zhong Xi Yi Jie He Xue Bao, 2010. **8**(7): p. 662-9.
129. Quesseveur, G., et al., *Attenuated Levels of Hippocampal Connexin 43 and its Phosphorylation Correlate with Antidepressant- and Anxiolytic-Like Activities in Mice.* Front Cell Neurosci, 2015. **9**: p. 490.
130. Pan, S.M., et al., *Thioredoxin interacting protein drives astrocytic glucose hypometabolism in corticosterone-induced depressive state.* J Neurochem, 2022. **161**(1): p. 84-100.

131. Virgin, C.E., Jr., et al., *Glucocorticoids inhibit glucose transport and glutamate uptake in hippocampal astrocytes: implications for glucocorticoid neurotoxicity.* J Neurochem, 1991. **57**(4): p. 1422-8.
132. Allaman, I., L. Pellerin, and P.J. Magistretti, *Glucocorticoids modulate neurotransmitter-induced glycogen metabolism in cultured cortical astrocytes.* J Neurochem, 2004. **88**(4): p. 900-8.
133. Shu, X., et al., *The effect of fluoxetine on astrocyte autophagy flux and injured mitochondria clearance in a mouse model of depression.* Cell Death Dis, 2019. **10**(8): p. 577.
134. Pierelli, G., et al., *Uncoupling Protein 2: A Key Player and a Potential Therapeutic Target in Vascular Diseases.* Oxid Med Cell Longev, 2017. **2017**: p. 7348372.
135. Ji, J., et al., *Activating PPARβ/δ Protects against Endoplasmic Reticulum Stress-Induced Astrocytic Apoptosis via UCP2-Dependent Mitophagy in Depressive Model.* 2022. **23**(18): p. 10822.
136. Collet, J.F. and J. Messens, *Structure, function, and mechanism of thioredoxin proteins.* Antioxid Redox Signal, 2010. **13**(8): p. 1205-16.
137. Lu, J. and A. Holmgren, *The thioredoxin antioxidant system.* Free Radic Biol Med, 2014. **66**: p. 75-87.
138. Fomenko, D.E., S.M. Marino, and V.N. Gladyshev, *Functional diversity of cysteine residues in proteins and unique features of catalytic redox-active cysteines in thiol oxidoreductases.* Mol Cells, 2008. **26**(3): p. 228-35.
139. Stancill, J.S. and J.A. Corbett, *The Role of Thioredoxin/Peroxiredoxin in the beta-Cell Defense Against Oxidative Damage.* Front Endocrinol (Lausanne), 2021. **12**: p. 718235.
140. Perkins, A., et al., *Peroxiredoxins: guardians against oxidative stress and modulators of peroxide signaling.* Trends Biochem Sci, 2015. **40**(8): p. 435-45.
141. Rhee, S.G. and H.A. Woo, *Multiple functions of peroxiredoxins: peroxidases, sensors and regulators of the intracellular messenger H(2)O(2), and protein chaperones.* Antioxid Redox Signal, 2011. **15**(3): p. 781-94.
142. Choi, E.H. and S.J. Park, *TXNIP: A key protein in the cellular stress response pathway and a potential therapeutic target.* Exp Mol Med, 2023. **55**(7): p. 1348-1356.
143. Shiizaki, S., I. Naguro, and H.J.A.i.b.r. Ichijo, *Activation mechanisms of ASK1 in response to various stresses and its significance in intracellular signaling.* 2013. **53**(1): p. 135-144.
144. Kylarova, S., et al., *Cysteine residues mediate high‐affinity binding of thioredoxin to ASK 1.* 2016. **283**(20): p. 3821-3838.
145. Obsilova, V., K. Honzejkova, and T. Obsil, *Structural Insights Support Targeting ASK1 Kinase for Therapeutic Interventions.* Int J Mol Sci, 2021. **22**(24): p. 13395.
146. Dhanasekaran, D.N. and E.P. Reddy, *JNK signaling in apoptosis.* Oncogene, 2008. **27**(48): p. 6245-51.
147. Elmore, S., *Apoptosis: a review of programmed cell death.* Toxicol Pathol, 2007. **35**(4): p. 495-516.
148. Fujino, G., et al. *Thioredoxin and protein kinases in redox signaling*. in *Seminars in cancer biology*. 2006. Elsevier.
149. Zhong, L., E.S. Arnér, and A.J.P.o.t.N.A.o.S. Holmgren, *Structure and mechanism of mammalian thioredoxin reductase: the active site is a redox-active selenolthiol/selenenylsulfide formed from the conserved cysteine-selenocysteine sequence.* 2000. **97**(11): p. 5854-5859.
150. Bjørklund, G., et al., *Thioredoxin reductase as a pharmacological target.* 2021. **174**: p. 105854.
151. Pan, M., et al., *TXNIP: A Double-Edged Sword in Disease and Therapeutic Outlook.* Oxid Med Cell Longev, 2022. **2022**: p. 7805115.
152. Yoshihara, E., et al., *Thioredoxin/Txnip: redoxisome, as a redox switch for the pathogenesis of diseases.* Front Immunol, 2014. **4**: p. 514.

153. Tsubaki, H., I. Tooyama, and D.G. Walker, *Thioredoxin-Interacting Protein (TXNIP) with Focus on Brain and Neurodegenerative Diseases.* Int J Mol Sci, 2020. **21**(24): p. 9357.
154. Saxena, G., J. Chen, and A. Shalev, *Intracellular shuttling and mitochondrial function of thioredoxin-interacting protein.* J Biol Chem, 2010. **285**(6): p. 3997-4005.
155. Nishinaka, Y., et al., *Importin α1 (Rch1) mediates nuclear translocation of thioredoxin-binding protein-2/vitamin D3-up-regulated protein 1.* 2004. **279**(36): p. 37559-37565.
156. Junn, E., et al., *Vitamin D3 up-regulated protein 1 mediates oxidative stress via suppressing the thioredoxin function.* J Immunol, 2000. **164**(12): p. 6287-95.
157. Song, Y., et al., *Perilla aldehyde attenuates CUMS-induced depressive-like behaviors via regulating TXNIP/TRX/NLRP3 pathway in rats.* Life Sci, 2018. **206**: p. 117-124.
158. Kim, M.-H., Y.-H.J.J.o.E.N. Leem, and Biochemistry, *Neurogenic effect of exercise via the thioredoxin-1/extracellular regulated kinase/β-catenin signaling pathway mediated by β2-adrenergic receptors in chronically stressed dentate gyrus.* 2019. **23**(3): p. 13.
159. Wang, X., et al., *Effects of Mild Chronic Intermittent Cold Exposure on Rat Organs.* Int J Biol Sci, 2015. **11**(10): p. 1171-80.
160. Bharti, V., et al., *Glucocorticoid Upregulates Thioredoxin-interacting Protein in Cultured Neuronal Cells.* Neuroscience, 2018. **384**: p. 375-383.
161. Kielkopf, C.L., W. Bauer, and I.L.J.C.S.H.P. Urbatsch, *Bradford assay for determining protein concentration.* 2020. **2020**(4): p. pdb. prot102269.
162. Riddles, P.W., R.L. Blakeley, and B.J.A.b. Zerner, *Ellman's reagent: 5, 5′-dithiobis (2-nitrobenzoic acid)—a reexamination.* 1979. **94**(1): p. 75-81.
163. Hensley, K.J.P.B., D. Methods, and Protocols, *Detection of protein carbonyls by means of biotin hydrazide-streptavidin affinity methods.* 2009: p. 457-462.
164. Guo, H., et al., *Caspase-1 activation of caspase-6 in human apoptotic neurons.* 2006. **13**(2): p. 285-292.
165. Bharti, V., et al., *Txnip mediates glucocorticoid-activated NLRP3 inflammatory signaling in mouse microglia.* Neurochem Int, 2019. **131**: p. 104564.
166. Meijer, O.C., J.C. Buurstede, and M.J.M. Schaaf, *Corticosteroid Receptors in the Brain: Transcriptional Mechanisms for Specificity and Context-Dependent Effects.* Cell Mol Neurobiol, 2019. **39**(4): p. 539-549.
167. Wang, Z., et al., *Thioredoxin-interacting protein (txnip) is a glucocorticoid-regulated primary response gene involved in mediating glucocorticoid-induced apoptosis.* Oncogene, 2006. **25**(13): p. 1903-13.
168. Kolbus, A., et al., *Cooperative signaling between cytokine receptors and the glucocorticoid receptor in the expansion of erythroid progenitors: molecular analysis by expression profiling.* 2003. **102**(9): p. 3136-3146.
169. He, X. and Q. Ma, *Redox regulation by nuclear factor erythroid 2-related factor 2: gatekeeping for the basal and diabetes-induced expression of thioredoxin-interacting protein.* Mol Pharmacol, 2012. **82**(5): p. 887-97.
170. Liao, D., et al., *Curcumin Attenuates Chronic Unpredictable Mild Stress-Induced Depressive-Like Behaviors via Restoring Changes in Oxidative Stress and the Activation of Nrf2 Signaling Pathway in Rats.* Oxid Med Cell Longev, 2020. **2020**: p. 9268083.
171. Song, L., et al., *Antidepressant effect of catalpol on corticosterone-induced depressive-like behavior involves the inhibition of HPA axis hyperactivity, central inflammation and oxidative damage probably via dual regulation of NF-κB and Nrf2.* 2021. **177**: p. 81-91.
172. Sun, Q., et al., *Nrf2 Signaling Pathway Mediates the Antioxidative Effects of Taurine Against Corticosterone-Induced Cell Death in HUMAN SK-N-SH Cells.* Neurochem Res, 2018. **43**(2): p. 276-286.

173. García-Hernández, B. and J.J.F.i.M.N. Morán, *Txnip expression promotes JNK-mediated neuronal death in response to reactive oxygen species.* 2023. **16**.
174. Yamaguchi, F., et al., *FOXO/TXNIP pathway is involved in the suppression of hepatocellular carcinoma growth by glutamate antagonist MK-801.* 2013. **13**: p. 1-11.
175. Papadia, S., et al., *Synaptic NMDA receptor activity boosts intrinsic antioxidant defenses.* Nat Neurosci, 2008. **11**(4): p. 476-87.
176. Pan, Q., J. Ma, and K. Guo, *miR-223 Enhances the Neuroprotection of Estradiol Against Oxidative Stress Injury by Inhibiting the FOXO3/TXNIP Axis.* Neurochem Res, 2022. **47**(7): p. 1865-1877.
177. Kuang, W.-H., et al., *IGF-1 defends against chronic-stress induced depression in rat models of chronic unpredictable mild stress through the PI3K/Akt/FoxO3a pathway.* 2018. **34**(7): p. 370-376.
178. Chang, P.-R., et al., *The neuroprotective effects of flavonoid fisetin against corticosterone-induced cell death through modulation of ERK, p38, and PI3K/Akt/FOXO3a-dependent pathways in PC12 cells.* 2023. **15**(10): p. 2376.
179. Fedorova, M., R.C. Bollineni, and R.J.M.s.r. Hoffmann, *Protein carbonylation as a major hallmark of oxidative damage: update of analytical strategies.* 2014. **33**(2): p. 79-97.
180. Desagher, S., J. Glowinski, and J. Premont, *Astrocytes protect neurons from hydrogen peroxide toxicity.* J Neurosci, 1996. **16**(8): p. 2553-62.
181. Dringen, R., et al., *The glutathione system of peroxide detoxification is less efficient in neurons than in astroglial cells.* 1999. **72**(6): p. 2523-2530.
182. Zhao, Y.-L., et al., *Tbhq ‐ overview of multiple mechanisms against oxidative stress for attenuating methamphetamine ‐ induced neurotoxicity.* 2020. **2020**(1): p. 8874304.
183. Imhoff, B.R., J.M.J.C.b. Hansen, and toxicology, *Tert-butylhydroquinone induces mitochondrial oxidative stress causing Nrf2 activation.* 2010. **26**: p. 541-551.
184. Eftekharpour, E., A. Holmgren, and B.H.J.G. Juurlink, *Thioredoxin reductase and glutathione synthesis is upregulated by t ‐ butylhydroquinone in cortical astrocytes but not in cortical neurons.* 2000. **31**(3): p. 241-248.
185. Bell, K.F., et al., *Neuronal development is promoted by weakened intrinsic antioxidant defences due to epigenetic repression of Nrf2.* 2015. **6**(1): p. 7066.
186. Makar, T.K., et al., *Vitamin E, ascorbate, glutathione, glutathicne disulfide, and enzymes of glutathione metabolism in cultures of chick astrocytes and neurons: evidence that astrocytes play an important role in antioxidative processes in the brain.* 1994. **62**(1): p. 45-53.
187. Ren, X., et al., *Redox Signaling Mediated by Thioredoxin and Glutathione Systems in the Central Nervous System.* Antioxid Redox Signal, 2017. **27**(13): p. 989-1010.
188. Iversen, R., et al., *Thiol− disulfide exchange between glutaredoxin and glutathione.* 2010. **49**(4): p. 810-820.
189. Musaogullari, A. and Y.C. Chai, *Redox Regulation by Protein S-Glutathionylation: From Molecular Mechanisms to Implications in Health and Disease.* Int J Mol Sci, 2020. **21**(21): p. 8113.
190. Blevins, H.M., et al., *The NLRP3 Inflammasome Pathway: A Review of Mechanisms and Inhibitors for the Treatment of Inflammatory Diseases.* Front Aging Neurosci, 2022. **14**: p. 879021.
191. Zhou, R., et al., *Thioredoxin-interacting protein links oxidative stress to inflammasome activation.* Nat Immunol, 2010. **11**(2): p. 136-40.
192. Abais, J.M., et al., *Nod-like receptor protein 3 (NLRP3) inflammasome activation and podocyte injury via thioredoxin-interacting protein (TXNIP) during hyperhomocysteinemia.* J Biol Chem, 2014. **289**(39): p. 27159-27168.
193. Heneka, M.T., R.M. McManus, and E. Latz, *Inflammasome signalling in brain function and neurodegenerative disease.* Nat Rev Neurosci, 2018. **19**(10): p. 610-621.

194. Zhang, W.Y., et al., *Curcumin relieves depressive-like behaviors via inhibition of the NLRP3 inflammasome and kynurenine pathway in rats suffering from chronic unpredictable mild stress.* Int Immunopharmacol, 2019. **67**: p. 138-144.
195. Qin, Z., et al., *Berberine ameliorates depression-like behaviors in mice via inhibiting NLRP3 inflammasome-mediated neuroinflammation and preventing neuroplasticity disruption.* J Neuroinflammation, 2023. **20**(1): p. 54.
196. Yue, N., et al., *Activation of P2X7 receptor and NLRP3 inflammasome assembly in hippocampal glial cells mediates chronic stress-induced depressive-like behaviors.* J Neuroinflammation, 2017. **14**(1): p. 102.
197. Makoni, N.J. and M.R. Nichols, *The intricate biophysical puzzle of caspase-1 activation.* Arch Biochem Biophys, 2021. **699**: p. 108753.
198. Exconde, P.M., et al., *The tetrapeptide sequence of IL-18 and IL-1β regulates their recruitment and activation by inflammatory caspases.* 2023. **42**(12).
199. Lian, L., et al., *SIRT1 Inhibits High Glucose–Induced TXNIP/NLRP3 Inflammasome Activation and Cataract Formation.* 2023. **64**(3): p. 16-16.
200. Tseng, H.H., et al., *TRPM2 regulates TXNIP-mediated NLRP3 inflammasome activation via interaction with p47 phox under high glucose in human monocytic cells.* Sci Rep, 2016. **6**(1): p. 35016.
201. Geng, J., et al., *Andrographolide triggers autophagy-mediated inflammation inhibition and attenuates chronic unpredictable mild stress (CUMS)-induced depressive-like behavior in mice.* Toxicol Appl Pharmacol, 2019. **379**: p. 114688.
202. Song, M.-t., et al., *Astragaloside IV ameliorates neuroinflammation-induced depressive-like behaviors in mice via the PPARγ/NF-κB/NLRP3 inflammasome axis.* 2018. **39**(10): p. 1559-1570.
203. Zhang, Z., et al., *NLRP3 inflammasome activation mediates fatigue-like behaviors in mice via neuroinflammation.* Neuroscience, 2017. **358**: p. 115-123.
204. Camargo, A., et al., *Low doses of ketamine and guanosine abrogate corticosterone-induced anxiety-related behavior, but not disturbances in the hippocampal NLRP3 inflammasome pathway.* Psychopharmacology (Berl), 2021. **238**(9): p. 2555-2568.
205. Feng, X., et al., *Glucocorticoid-Driven NLRP3 Inflammasome Activation in Hippocampal Microglia Mediates Chronic Stress-Induced Depressive-Like Behaviors.* Front Mol Neurosci, 2019. **12**: p. 210.